THE RHINOVIRUS C: CAPSID STABILITY, VIRION PURIFICATION, AND IDENTIFICATION OF CELLULAR AND TISSUE TROPISM

By

Theodor Frank Griggs

A dissertation submitted in partial fulfillment of the requirements for the degree

DOCTOR OF PHILOSOPHY

(Cellular and Molecular Pathology)

at the

UNIVERSITY OF WISCONSIN—MADISON

2015

Date of final oral examination: 6/24/15

The dissertation is approved by the following members of the Final Oral Committee:

James E. Gern, Professor, Pediatrics

Ann C. Palmenberg, Professor, Biochemistry

Caitlin S. Pepperell, Assistant Professor, Medicine

Nathan M. Sherer, Assistant Professor, Oncology

John Yin, Professor, Chemical and Biological Engineering

THE RHINOVIRUS C: CAPSID STABILITY, VIRION PURIFICATION, AND IDENTIFICATION OF CELLULAR AND TISSUE TROPISM

Theodor F. Griggs

Under the supervision of Professor James E. Gern at the

University of Wisconsin—Madison

The common cold is the most prevalent infectious disease in humans, and the rhinovirus (RV) is the main pathogen responsible. While most RV infections result in mild illness, young and old patients and those with chronic airway inflammatory diseases, cystic fibrosis (CF), and immunodeficiencies are predisposed to higher symptom burdens and respiratory distress. Many studies have demonstrated an increased disease severity with the RV-C species in all of these populations, however there is still very little known about RV-C molecular biology and the mechanism by which they are able to cause more severe respiratory disease. Our knowledge of RV-C structure and biology is further limited by the lack of a robust culture system and purification method for their study. Furthermore, there are no data in the literature on the cellular tropism of the RV-C, an important consideration to fully understand the mechanism of RV-C entry and interactions with the host. Thus, there were two primary goals of this dissertation: the first was to develop a more robust growth and purification protocol for all RV-C clones; and the second was to identify the cellular and tissue targets of the RV-C in respiratory epithelium, and additionally determine the relationship of CDHR3 expression with RV-C tropism.

In this dissertation, we address the need for an improved purification protocol for multiple isolates of the RV-C, refute the hypothesis that RV-C capsids are intrinsically less stable than those of other species, and present a revised purification protocol that results in high levels of purified virus materials. We also

identified an increased sensitivity to low pH in all RV-C genotypes examined, and demonstrated an increased capacity for virion production in Wis.L cells (embryonic fibroblasts). We further identify the ciliated respiratory epithelial cell as the primary target of the RV-C by multiple methods and demonstrate that the majority and highest levels of CDHR3 expression occurs in the ciliated cell population. Our data also indicate that RV-C infection results in cell shedding, diminished CDHR3+ populations, and decreased CDHR3 expression in individually infected cells. We then present preliminary evidence that the RV-C target pharyngeal but not palatine tonsillar epithelium. The work presented in this thesis demonstrates foundational experiments that answered multiple important questions regarding basic RV-C capsid biology and tissue tropism and will serve as a springboard for future studies into RV-C structure, biochemistry, and interactions with the human host.

ACKNOWLEDGEMENTS

First and foremost, the work presented in this dissertation would not have been possible without the strong guidance from my thesis adviser, Dr. James Gern, whom accepted me into his lab without question and allowed me the freedom to pursue my research interests while maintaining a pleasant work and mentor-mentee environment though both high- and low- stress periods. All other members of the Gern lab have played a substantial role in my development as a scientist in one way or another. In particular, I would like to thank Dr. Yury Bochkov for teaching me everything I know about RV-C molecular biology, and always being available for scientific advice.

I would like to thank my committee members: Dr. Ann Palmenberg, Dr. Nathan Sherer, Dr. Caitlin Pepperell, and Dr. John Yin for their willingness to give advice and encouragement throughout this process. In particular, I would like to thank Dr. Palmenberg and Dr. Sherer for providing one-on-one experimental advice and aid that allowed me to overcome multiple roadblocks in this dissertation.

None of this work would have been possible without the valuable collaborations fostered here at the University of Wisconsin. Purification and live cell imaging advice from Marchel Hill (Palmenberg Lab) and Jordan Becker (Sherer Lab) proved to be valuable assets for the completion of this work. Members of the UW Pathology department, Dr. Erin Brooks, Dr. Tom Warner, and Dr. Richard Yang all provided advice that helped me burst through scientific blocks in completing morphological and interpretive studies for Chapter 3. Renee Szakaly (Sorkness Lab), Alyssa Leystra and Chelsie Sievers (Halberg Lab), and Kelli Pointer (Kuo Lab) provided valuable advice and resources needed to determine infected cell morphology. Lastly, the members of the UW-Carbone Cancer Center Flow Lab Core, Chris Erickson, Dagna Sheerar, and Rachael Sheridan provided not only flow cytometry training but also experimental and interpretive advice that proved invaluable for the completion of the work in Chapter 3.

Finally, I would like to thank my friends and family for going above and beyond in providing support throughout this process.

TABLE OF CONTENTS

LIST OF FIGURES

CHAPTER ONE

Clinical and Molecular Perspectives of the Rhinovirus and an Overview of Airway Biology

This introductory chapter is divided into six sections to address the known clinical and molecular perspectives of the rhinovirus (RV) and how they interact with the human host. The first section includes clinical concepts relating RV to viral upper respiratory tract infections (URTIs) and the common cold, and brings attention to multiple patient populations that are predisposed to more severe respiratory illnesses caused by RV infection as well as viral factors that contribute to disease variability. In addition, the first section reviews current and past efforts to develop antiviral pharmaceuticals and homeopathic remedies. As the bulk of my dissertation focuses on the RV-C species, Section II reviews their discovery, unique culture methods, and cell entry receptor elucidation. The third section reviews the taxonomy, structure, and molecular biology of the RV, while Section IV summarizes the research methods employed to study RV. Section V provides background information about the anatomy, physiology, and immunology of the airways with respect to RV infection, and the final section serves as a summary of this information and how it relates to my dissertation.

RHINOVIRUS CLINICAL REVIEW

The Common Cold

The common cold is a self-limiting infection of the upper respiratory tract (URTI) that has been recently defined as an acute viral rhinosinusitis with symptoms lasting less than ten days[1]. While these viral infections normally produce only cold symptoms, children, the elderly, the immunosuppressed, and those with asthma, COPD, or cystic fibrosis are predisposed to lower respiratory illnesses including wheezing, asthma exacerbations, respiratory distress, and secondary bacterial pneumonia that can result in hospitalization[2–10]. URTIs affect adults 1-3 times per year on average, while children are affected more frequently (6-8) making the common cold the most frequent acute infectious illness[11–13]. There is a long list of viruses that are known to cause the common cold, including respiratory syncytial virus (RSV), influenza virus, parainfluenza virus (PIV), coronaviruses, adenoviruses, Coxsackieviruses, echoviruses,

human bocavirus (HBoV), Epstein-Barr virus (EBV), and human metapnumovirus (hMPV)[14]. However, the rhinovirus (RV), which is composed of three species (A-C), is by far the most common cause, and has been detected in up to 80% of cases in epidemiologic studies[15,16].

In the US, the common cold stretches from early fall to spring, with peak RV infection incidence in the fall and spring, and a smaller peak in the summer months[17]. The reasons for these peaks are multifactorial, and likely related to close contact of school-age children in the fall and spring. While many other viruses (coronavirus, influenza virus, RSV, adenovirus, and HBoV) are more common in the winter, the increased cold incidence relative to the summer months is likely due to increased time spent indoors allowing for increased contact with sick individuals and dry indoor climate, increasing the environmental half-life of most viral capsids[18].

RV and High Risk-Populations

Some patient populations are at risk for more severe illness following a RV infection. These populations include young children, the elderly, those with asthma, COPD, or cystic fibrosis, and the immunocompromised.

RV infection is known to produce a range of symptoms in children from asymptomatic infections to lower respiratory illnesses, the latter being more frequent in children with chronic respiratory and immunological disorders[19]. One out of every ten school-age children is diagnosed with asthma in the US, and 80% of 9-11 year-olds presenting to the emergency department for asthma exacerbations or wheezing tested positive for a respiratory virus in one study[2,20]. The study further determined that 65% of these children had detectable RV infection. RV is a well-established cause of acute exacerbations of asthma in all age groups. While it is important to note that there are no asthma-related differences in susceptibility to RV or frequency of URTI, asthma is associated with a higher frequency of RV LRTIs[7,21].

Birth cohort studies suggest that RV may also contribute to the initiation of asthma. One study that followed children prospectively from birth to six years of age found that children who wheeze in the

first few years of life have an increased likelihood of asthma development when they are older, and further identified RV-induced wheeze to be the strongest predictor for asthma development later in life when compared to other viral causes of wheeze[22]. The strong correlation between early RV infections and the development of asthma later in life suggests a causal link between the two. It is unclear exactly why RV produces much more severe illness in children than adults, but it is likely multifactorial. One possibility is that infants and young children have relatively weak interferon responses, and may be biased towards type-2 cytokine responses that are linked to the development of atopy and allergic diseases[23,24]. The weaker interferon responses in blood or airway cells have been related to more severe RV illnesses in some translational studies. Other factors likely include the lack of immunologic memory to multiple genotypes of RV in babies, and contact with many sick children in day care or school.

Multiple studies have demonstrated the influence of respiratory viral infection on acute exacerbations of COPD (AECOPD) and cystic fibrosis[25–30]. Analysis of nasal lavage fluid, nasopharyngeal swab, and induced sputum specimens indicated that respiratory viruses are the most common cause of AECOPD, with RV being the most common inciting pathogen. While RV is the commonly associated virus in virus-induced respiratory exacerbations of CF patients, it was not associated with decreased pulmonary function as observed with other respiratory viruses[29,30]. However, a recent study identified an association with RV-C and respiratory exacerbations in Brazilian children with CF, that was not observed with the RV-A or B species[31].

RV can also cause lower respiratory symptoms in immunocompromised patients. As an example, one retrospective chart review of patients on immunosuppressive therapy for malignancy, HIV infection, or rheumatologic conditions or who were recipients of solid organ or hematopoietic stem cell transplants found that RV infection produces symptoms equivalent to pandemic H1N1 influenza[32]. In this study, symptoms were severe, including fever (50%), diarrhea (10%), and vomiting (8%), increased chest x-ray abnormalities (50%), and elevated liver function tests. Furthermore, more than one out of every ten RV-infected patients were admitted to the ICU, and four out of ten were hospitalized.

In summary, while RV usually causes a mild and self-limiting illness in the general population, infections can have severe and even life-threatening consequences for multiple at-risk populations.

Species Effects on Severity of Illness

The advent of molecular methods to detect and differentiate RV species in clinical samples made it clear that RV species plays a critical role in determining illness severity[33–40]. In support of this concept, a study of 259 Wisconsin infants predisposed to allergic sensitization or asthma revealed that the severity of illness during the first year of life was much higher for those infected with RV species A and C than for B, with the most severe symptoms having been experienced with the C species[41]. A more recent study involving children presenting to the Emergency and Urgent Care Departments at Seattle Children's Hospital for both mild upper respiratory tract and more severe lower tract illnesses showed that RV-A and C were detected in 63% and 34% of nasal swabs, respectively, while RV-B was only detected in 3%[42]. This study also demonstrated that lower respiratory tract infection (LRTI) was found more commonly in children infected with RV-C than the other species, and that RV genotype influences LRTI severity. Another study that analyzed children presenting with acute respiratory diseases (ARDs) noted that RV-C was significantly associated with wheezing, signifying involvement of the lower airways[43]. RV caused LRTIs in 80% of premature infants in another study, and RV-C was the most commonly implicated and associated with the highest cost of respiratory care[44]. In 2-16 year-olds with asthma, RV-C was the most frequently detected respiratory virus during acute asthma exacerbations, and was also associated with more severe asthma[45]. Furthermore, the RV-A and C appear to instigate the most severe upper and lower respiratory tract symptoms in infants and children under 5 years of age[8,41].

Thus, it is generally understood that the RV-A and C species cause much more severe infections and asthma symptoms than RV-B. The mechanisms for these differences in virulence are likely to be multifactorial, and may relate to differences in how RV species interact with the host, environment, and other pathogens. For example, an *in vitro* study of RV infection of airway epithelial cells (AECs)

demonstrated the highest cytotoxicity, release of inflammatory cytokines, and viral replication following inoculation with isolates of the RV-A and C species, indicating that these viruses cause more direct cellular damage than isolates from the RV-B[46]. The RV 2A protease ($2A^{pro}$) has been implicated in the destruction of a number of host cell processes, and is highly divergent in sequence, molecular target, and kinetics[47–52]. Analysis of $2A^{pro}$s from multiple isolates of the three RV species revealed a slower cleavage rate of eIF4G from the RV-B $2A^{pro}$s compared to those from the RV-A or C. Because the RV $2A^{pro}$ is responsible for shutoff of host transcript translation and inhibition of nuclear export, the slower RV-B proteases may inhibit translation in infected cells less efficiently, thus allowing for quicker clearance and less profoundly infected tissues.

Furthermore, receptor specificity differences between different RV types may play a role in infection severity. For example, inflammation can lead to the upregulation of ICAM-1, which is the major group RV receptor, thus there may be a heightened likelihood of major group RV binding and entry in chronically inflamed airways[53]. Because the cellular receptor for the RV-C was only recently discovered, similar studies into RV-C receptor regulation are lacking[54]. That being said, in Chapter 3, we describe the first evidence that the RV-C may have a slightly altered set of target tissues, likely due to restriction of cell-entry receptor expression, which may play a role in species-specific severity. Further study is needed to determine what controls the presentation of RV-C cell entry factors, the downstream consequences of RV-C binding to its receptor, and how it affects illness severity.

RV Transmission

RV transmission has been documented through direct contact between people or with fomites, as well as through the aerosol route[55,56]. Viral deposition on the hands and fingers can inoculate the eyes (conjunctival epithelium) or the nose (intranasal epithelium)[57]. Viral shedding typically initiates around 12-24 hours-post-inoculation (hpi), peaks at 48-72hpi, and can last for 3-7 days in adults, or longer in

young children or immunocompromised individuals[58–60]. Peak viral prevalence in the fall and spring are likely a result of close contact between infected children returning to school.

Antivirals

Vaccine therapy has remained elusive for the RV due to vast immunogenic diversity between the >160 genotypes of known isolates[61,62]. Therefore, research has focused on the development of antivirals that bind the viral capsid, inhibit viral proteases, or modulate the inflammatory response. Other approaches include nutritional compounds such as zinc and vitamin C, and treatment with intranasal or inhaled interferons.

Capsid-binding agents slip in through a pore in the RV capsid, displacing a putative lipid pocket factor, and prevent the virion from undergoing important conformational changes required for cell binding, entry and genome delivery. An example of this class of antivirals is pleconaril, which in two phase III clinical trials produced a one-day reduction in RV illness duration as well as a significant decrease in symptom burden, but it was not approved for safe use by the FDA due to interactions with hormonal contraception and HIV antivirals[63–66]. Another capsid-binding agent, vapendavir, has a similar mechanism of action and significantly reduced the incidence of RV and peak viral load in a phase IIa clinical trial[19,67]. Pirodavir, used as an intranasal spray, showed promising reduction in viral replication and shedding, but did not reduce the duration or severity of symptoms in phase III clinical trials and was thus discontinued[68–70]. No clinical data testing the efficacy of capsid-binding agents on the RV-C have been published, however, molecular modeling studies and *in vitro* data suggest that efficacy against RV-C is unlikely[71–74].

The 3C protease inhibitor, Rupintrivir, inhibits 3C proteases from a wide range of RVs and enteroviruses (EVs)[75,76]. In a phase II clinical trial, Rupintrivir was well tolerated and reduced viral loads and respiratory symptom burdens, but did not reduce the frequency of colds[77]. However, Rupintrivir did not significantly reduce viral loads and symptom severity in trials of natural infection and was thus

terminated from clinical development[78]. Interestingly, Rupintrivir is effective against RV-C15 and EV-71 *in vitro*, possibly indicating clinical utility of this approach for all three RV species[79,80].

Tremacamra, a soluble ICAM-1 receptor, did not reduce the incidence of RV infection in a placebo-controlled trial of experimental RV-A39 infection, but did reduce symptom severity[81]. Unfortunately, Tremacamra was not pursued due to the high cost of production and an impractical administration regimen, as well as a likely inability to inhibit RV-C infection. Finally, Enviroxime, a promising small molecule that may inhibit components of the RV replication complex, was proven clinically ineffective in multiple placebo-controlled clinical trials[82–88].

Interferons (IFN) have antiviral, antiproliferative, and immunological effects and have been pursued for RV prophylaxis and treatment in multiple studies[89–92]. While intranasal IFN-alpha 2b therapy was effective when administered prophylactically, there was no decrease in respiratory illness or severity when administered during or after RV infection. Furthermore, studies indicated that IFN alpha 2b therapy caused increased symptom burdens and intranasal bleeding, consequently this approach was abandoned. Promising initial studies using intranasal prophylactic administration of IFN-beta showed equivalent symptom burdens between experimental and placebo-controlled groups, and a significant reduction in the frequency of colds in the experimental group[93]. However, larger placebo-controlled clinical trials using IFN-beta for RV therapy were associated with nasal toxicity[94]. Interestingly, a recent trial of inhaled IFN-beta in asthmatics with natural respiratory virus infections indicated a significant reduction in the frequency of exacerbations for patients with severe asthma, suggesting that inhaled IFN-beta may prove to be a useful treatment for virus-induced exacerbations of asthma in this patient population[95].

Many clinical trials have been conducted to test nutritional supplementation to treat or prevent cold, with results that range from limited to no efficacy. Zinc has been evaluated for activity against RV for decades, and can inhibit viral replication *in vitro*, block RV binding to ICAM-1, alter configuration of capsid proteins thus preventing their subsequent proteolysis, directly inhibit RV proteases, and decrease

histamine release[96–100]. Multiple clinical trials and systematic reviews indicated that zinc supplementation within 24 hours of cold onset was associated with decreased duration of illness, but presented contrasting effects on reduction of symptoms[101,102]. One promising study indicated that long-term zinc supplementation reduced the incidence of colds, sick days, and antibiotic prescriptions in school-age children[103]. In contrast to oral zinc, topical zinc has significant toxicity in olfactory epithelium, and the resulting anosmia outweighs the benefit of small reductions in cold severity and length for many affected people[104].

Echinacea has been a popular herbal remedy for the treatment of the common cold for many years, and was initially touted for its ability to reduce cold length and symptom severity[105,106]. However, large clinical or experimental studies of Echinacea have failed to document efficacy[107–111]. Vitamin C, which protects against oxidative stress, has been tested repeatedly for prevention and treatment of the common cold since 1942[19]. A meta-analysis of 29 placebo-controlled trials investigating the efficacy of 0.2 g per day of vitamin C in the augmentation and prevention of the common cold indicated no significant effects in the general population[112]. However, the authors noted a slight benefit of vitamin C supplementation in the reduction of cold illness length and severity in people exposed to brief periods of "severe physical exercise." Similarly, culturing human bronchial epithelial cells (HBECs) with vitamin D indicated an influence on chemokine synthesis and alteration of cell growth and differentiation, but no effect on RV replication *in vitro*[113]. First-generation antihistamines, but not non-sedative antihistamines, have been shown to significantly reduce sneezing and rhinorrhea in placebo-controlled trials of experimental RV infection, but did not significantly reduce illness severity or duration[114–116]. Furthermore, the added side effects of dry eyes, nose, and mouth, and drowsiness limit their clinical practicality, and they are not recommended for treatment of colds in children[19].

THE RV-C: THEIR DISCOVERY, METHODS OF CULTURE, AND CELL ENTRY RECEPTOR.

RV-C Discovery

Historically, inoculation of tissue cultures was the gold standard for the identification of respiratory viruses, with fibroblast and HeLa cell lines primarily used for RV identification[117,118]. The major limitation with the tissue culture approach in virus identification is sensitivity, in that some viruses are very difficult to culture. The first evidence of RV-C, which was unable to grow under standard diagnostic culture conditions, was in Queensland, Australia, where molecular detection of virus in sputum samples from children presenting with acute respiratory exacerbations in the Brisbane respiratory virus research study revealed an unknown RV[119]. Furthermore, in 2004, a high incidence of influenza-negative (by molecular methods), and other respiratory virus-negative (by culture methods), influenza-like illnesses struck New York State that led investigators to suspect a non-cultivable pathogen[120,121]. Reanalysis of mucus samples from this New York outbreak by PCR resulted in the identification of multiple isolates of RV-C, making it clear that this virus was wide-spread[119–123].

Culture Methods

The inability to grow RV-C in standard tissue culture systems prevented its in-depth investigation for a number of years. In 2011, Bochkov *et al* reverse engineered RV-C sequences from clinical isolates that produced functional virions following transfection of Wis.L and HeLa cell monolayers with *in vitro*-transcribed vRNA[72]. These RV-C virions were also capable of infecting and replicating in sinus organ cultures, and were later shown to infect and replicate in bronchial and sinus cultures differentiated *in vitro* by the air-liquid-interface culture method[74,73,124]. The use of organ and ALI cultures enabled initial studies and characterization of the virus. These initial culture systems were limited by multiple logistical issues involving the following: sample acquisition from sinus or lung transplant surgery, a minimum of four weeks of culture preparation prior to the development of susceptible epithelial cultures, and the low

frequency of susceptible cells (~1.5%) within heterogeneous tissue samples and ALI cultures. It became clear that a susceptible immortalized cell line was needed to expedite molecular RV-C research, and in order to determine, or engineer a suitable line, a cell-entry receptor had to be found.

RV-C Cell Entry Receptor (Cadherin-related family member 3)

Since the discovery of the RV-C, basic molecular studies have focused on receptor and antiviral identification. Genome analysis made it clear that large spans of nucleotide insertions and deletions likely altered the RV-C capsid structure significantly from the RV-A and B[61,62]. Molecular models of the RV-C15 capsid based on genetic analyses demonstrated that there was a loss of mass in VP1 which results in a "shaved" topology at the 5-fold axis of symmetry and a less-pronounced receptor-binding canyon compared to known RV-A and B structures[125]. The evidence for a significantly different capsid structure combined with an inability to grow in standard tissue cultures unless viral genomic RNA (vRNA) was transfected into the cell supported the hypothesis that the RV-C bind and/or enter the cell via a different mechanism than the RV-A and B. Whole transcriptome analysis used to compare susceptible airway epithelial and organ cultures to nonsusceptible cultures revealed a list of receptor candidates that were highly expressed in permissive tissues[54]. Experimental transfection of HeLa cells with receptor candidates followed by inoculation with RV-C15 genetically engineered to express GFP during replication (C15-GFP) led to the identification of cadherin related family member 3 (CDHR3) as a factor permitting low-level RV-C entry and replication.

Interestingly, a variant allele of CDHR3, notable for a C529Y mutation in the protein's fifth extracellular domain (out of six), was recently identified as a strong asthma susceptibility determinant[126]. In early 2014, a Danish group performed a genome-wide association study (GWAS) to identify any genes that played a role in recurrent, severe asthma exacerbations in children 2-6 years of age[126]. The authors identified a single-nucleotide polymorphism of CDHR3 that was associated with severe and recurrent asthma exacerbations in young children. In fact, the asthma-associated polymorphism caused a

phenotype of increased surface presentation of CDHR3 compared to the wild type allele. Accordingly, transfection of the $CDHR3_{C529Y}$ allele into HeLa cells followed by C15-GFP inoculation resulted in robust, multi-cycle C15-GFP replication[54].

The identification of $CDHR3_{C529Y}$ as a RV-C entry factor for normally non-permissive cells led to the generation of a HeLa cell line that overexpresses this allele of CDHR3, which represents an important advance for conducting molecular studies of the RV-C. While it is clear that CDHR3 is necessary for RV-C entry, low levels of binding to normal HeLa cells indicate that other factors may also contribute to RV-C binding and entry into the host cell[54]. Regardless, the combined discoveries that a variant allele of CDHR3 is an asthma susceptibility determinant and that CDHR3 contributes to RV-C binding and entry into the host epithelium establishes a mechanistic, and possibly causal, link between RV-C infections and the subsequent development of asthma in children.

RV MOLECULAR BIOLOGY

Taxonomy

Rhinoviruses are members of the enterovirus genus and picornavirus family, and consist of three species (A-C)[16]. Rhinoviruses, like other picornaviruses, are small (capsid diameter 27-30nm), non-enveloped, positive-sense, single-stranded RNA viruses with ~7.2kb genomes[127]. Polioviruses, which are closely-related members of the enterovirus genus, have been studied extensively at the molecular level and much RV molecular biology is based upon initial work with polioviruses.

Capsid Structure

The RV capsid is icosahedral with pseudo-T3 symmetry consisting of 60 subunits each of the viral capsid proteins VP1-4, and serves the important functions of vRNA storage and transport between hosts and through the environment, cell entry, and immune evasion[128]. While VP1-3 have a molecular weight of ~ 32kDa and makeup the external face of the viral capsid, VP4 is only 5kDa and is

located beneath the other subunits, unexposed to the external environment prior to cell entry, and plays a crucial role in RNA transport during cell entry[127]. In each subunit, VP1-3 interact to form a wedge-shaped, beta-barrel motif, known as the jelly-roll fold, created by 8 antiparallel beta-strands, and is commonly seen in viral capsid subunits[127]. Cell entry occurs via interactions between the host receptor and canyons (depressions) within the viral capsid[129]. Antibodies that neutralize viral entry tend to bind within or near the canyon, thus preventing interactions with cellular receptors[130]. In order to prevent neutralization, RV has evolved a highly structured, "mountainous" capsid that makes it difficult for the immune system to raise antibodies to receptor binding sites tucked within narrow canyons[131,132]. Additionally, like many RNA viruses, RV encodes a low-fidelity RNA-dependent RNA polymerase (RDRP) that promotes the generation of a quasispecies of viruses with slightly dissimilar features, including capsid sequences that assist in evasion of host adaptive immune responses[131].

In comparing all known RV capsid sequences, three large deletions were identified in the VP1 capsid subunit of the RV-C that likely affect immunogenicity and receptor binding sites[61,62]. Modeling of the RV-C capsid further indicated a significantly different drug-binding pocket structure, and the pore that which exists in the RV-A and RV-B that is utilized by capsid binding agents is predicted to be closed in RV-C. This modeling predicts that the RV-C cannot be similarly inactivated by capsid-binding drugs developed for the RV-A and B, such as pleconaril, and in fact this has been demonstrated in tissue culture[71]. Thus, capsids within and between RV species are highly variable, and serve the functions of immune and antiviral evasion, as well as genomic vRNA storage and delivery.

Cell Entry

Cell entry for RV-A or RV-B is initiated by binding of a cellular receptor within the capsid canyon, and is mediated by either clathrin-dependent or independent endocytosis[133]. Known RV cell entry receptors include intercellular adhesion molecule-1 (ICAM-1), low-density lipoprotein receptor (LDLR), and cadherin-related family member 3 (CDHR3) for the major and minor groups, and RV-C species, respectively[54,134,135]. For RV-A and RV-B, capsid interaction with the host receptor induces a conformational change in the VP1 and VP2 subunits that allows for the amphipathic helices of VP1 to

interact with the endosomal membrane, and the VP2 subunits to reveal a pore large enough for the passage of ssRNA at the 2-fold axis of symmetry[136–141]. These conformational changes convert the virion into what is known as an A-particle, and is associated with the release of the hydrophobic, N-myristoylated VP4 subunit from deep within the capsid[141–143,139,144]. VP4 then likely destabilizes the endocytic membrane, promoting the formation of pores that allow viral genomic RNA entry into the host cell cytoplasm[138,141,145–149]. Some RV genotypes also require or may only require a shift towards low pH to initiate uncoating[133,147,150–157]. It was generally believed that the 5'-tail was extracted from the viral capsid by ribosomal scanning in the 5' to 3' direction, in an energetically favorable reaction, but recent structural and mechanistic studies have revealed that it is actually the 3' genomic end that first exits the capsid[133,149,158].

Genome Structure

The RV genome is a ~7.2kb RNA molecule, including a VPg protein covalently linked at the 5'-end and terminating at the 3'-end with a poly(A) tail[159–162]. Unlike mRNA, the viral genome lacks a 5' cap, and does not use cap-dependent translation—which is inhibited by cleavage from viral proteases—but rather initiates translation of the polyprotein via an RNA structural element, the internal ribosomal entry site (IRES), located upstream of the main open reading frame (ORF)[163–166]. Following ribosomal and translation initiation factor recruitment to the IRES, translation of the viral polyprotein begins.

Polyprotein Translation and Cleavage

The entire RV ORF is translated *en bloc* in the form of an ~2.2K amino acid polyprotein that self-cleaves (in *cis*) throughout translation (Figure 1-1)[167]. The polyprotein is divided into three main sections—P1, P2, and P3—which are formed by cleavage *in cis* by proteases within the nascent polyprotein. The first subunit, P1, is cleaved following the translation of 2A protease ($2A^{pro}$, just 3' to the VP1 sequence), and is the structural region, consisting of the RV capsid proteins in the following order: VP4, VP2, VP3, and VP1. Following translation of complete $2A^{pro}$ through $3C^{pro}$, $3CD^{pro}$ cleaves the junction between 2C and 3A, producing the P2 and eventually P3 nonstructural regions. $3CD^{pro}$ then cleaves multiple junctions, including VP0/VP3, VP3/VP2, $2A^{pro}$/2B, 2B/2C, 3A/3B, and 3B/3C.

Figure 1-1.

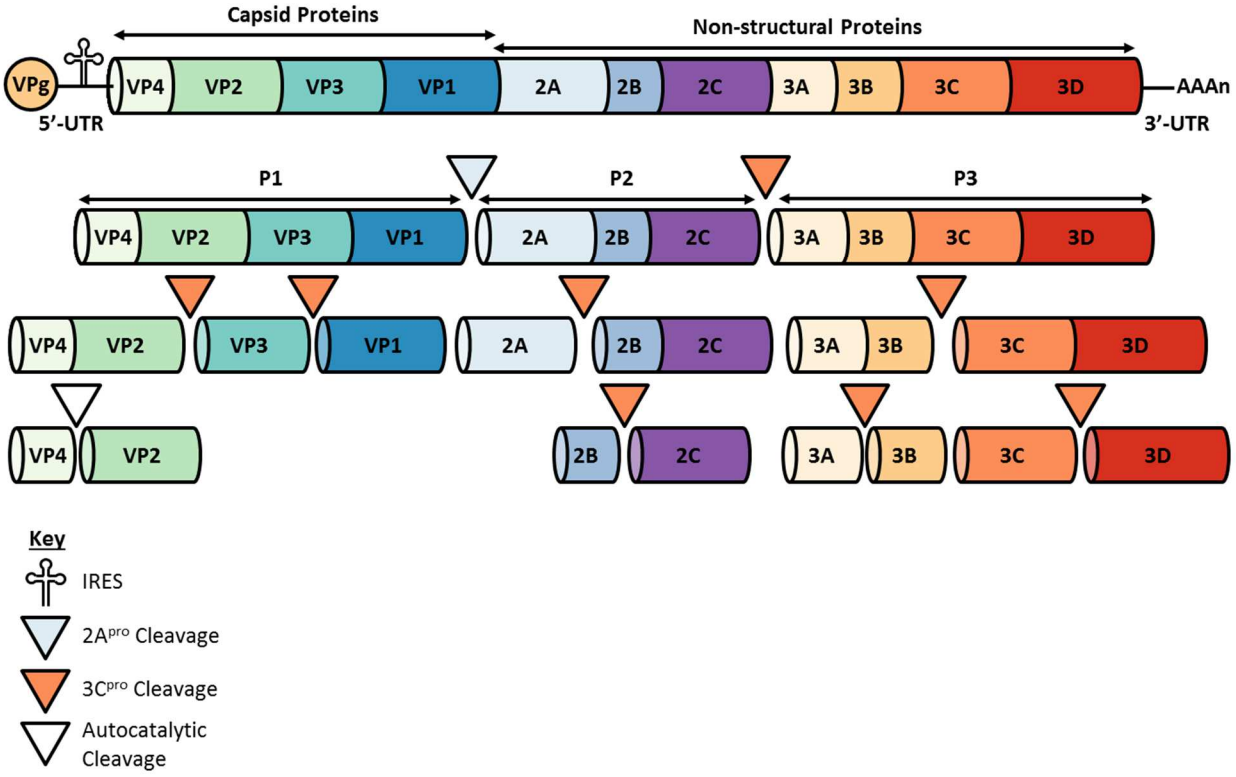
Capsid Proteins
Non-structural Proteins
VPg
VP4
VP2
VP3
VP1
2A
2B
2C
3A
3B
3C
3D
AAAn
5'-UTR
3'-UTR
P1
P2
P3
Key
IRES
2A^pro Cleavage
3C^pro Cleavage
Autocatalytic Cleavage

Figure 1-1. RV polyprotein cleavage map. Translation of the viral genome, which is initiated by a small VPg priming protein joined to the 5'-UTR containing the internal ribosomal entry site (IRES) and ends at the 3'-UTR with a polyadenylated tail, leads to the generation of a ~2.2kb polyprotein from a single open reading frame (ORF) that is processed by consecutive cleavage of viral proteases. P1 cleavage generates the viral capsid proteins, while cleavage of P2 and P3 generate VPg, viral proteases, and the RNA-dependent RNA polymerase (RDRP).

Interestingly, the mechanism involving the maturation cleavage of VP0 to form VP4 and VP2 is unknown, but is generally believed to be an autocatalytic process[168–172].

Replication, Assembly, and Egress

Picornavirus replication occurs on the membrane surfaces of vesicles[173–177]. Cleavage of the viral 3B protein produces VPg, which binds a hairpin in the 3'-untranslated region (UTR) of the viral genome and is uridylated by the viral $3D^{pol}$ subunit of 3CD[178,179]. Uridylation favors replication initiation of the viral negative-sense RNA genome through interactions with the poly-A tail, and cleavage of 3CD produces $3D^{pol}$ which serves as the processive viral RNA-dependent RNA Polymerase (RDRP) at the 3'-UTR[179–181]. This initial process leads to the synthesis of the negative genomic strand, which in turn serves as a template for the synthesis of multiple positive-sense vRNA genomes that can subsequently serve as templates for translation or replication, or be encapsidated once enough capsid proteins have been synthesized and assembled[177]. Cellular egress is generally believed to occur by cell lysis or an as-of-yet unidentified mechanism that may involve pathways more commonly associated with autophagy[182,183].

RV Evasion of Host Immunity

RV has evolved multiple methods of evading host antiviral responses including, but likely not limited to, genetically diverse capsid structural elements that prevent antibodies from blocking receptor binding sites, a low fidelity RDRP that promotes genetic diversity, proteolytic cleavage of multiple host cell proteins, disruption of cell death and signaling pathways, and the use of RNA sequence motifs that allow the virus to usurp host translational machinery and inhibit recognition by the host. As described previously, the low-fidelity RDRP allows for the production of a quasispecies of RV throughout the course of infection, promoting escape from host adaptive immune responses by allowing genetic drift to alter antigenic capsid motifs[131,180]. The proteolytic cleavage activities of the viral $2A^{pro}$ and $3C^{pro}$ have been well studied and play a central role in the dampening of the host response to RV infection. $2A^{pro}$ has been shown to cleave eIF4G shortly after its own translation, as well as nuclear pore proteins (Nups), thus halting translation and the nuclear import and export of many cellular proteins and mRNA[50,184–186]. Furthermore, the activity of $2A^{pro}$ has been correlated with RV disease severity, with the most pathogenic

genotypes (RV-A and C) possessing proteases with high cleavage kinetics on multiple Nups[52]. The $3C^{pro}$ has been shown to localize to the nucleus and inhibit eukaryotic RNA polymerases I, II, and III, thus preventing the synthesis of cellular mRNA in this location[187–190]. The 2B and 3A viral proteins also inhibit antiviral function of the host cell by inhibiting apoptosis and disrupting ER and Golgi trafficking, respectively[191–194].

RESEARCH METHODS & ADVANCES

Model Organisms

As humans are the only known reservoir for RV, there are no other natural animal models to study infection. Rodent models for specific genotypes of RV have been developed with some limitations. Blanco *et al*, noted that intranasal infection of the Cotton Rat (*Sigmodon hispidus*) with the major-type RV-16 but not the minor type RV-1B resulted in epithelial degeneration in the trachea and large airways, mild neutrophilic and histiocytic alveolitis, peribronchial infiltrates of neutrophils, macrophages, and lymphocytes, and mucous cell hypertrophy and hyperplasia[195]. Infectious RV-A16 was recovered up to 1 day post inoculation (p.i.) from the nose and trachea, and up to 2 days p.i. from the lung in the cotton rat model.

Bartlett *et al* in 2008 developed a transgenic mouse model that expresses human ICAM-1 and characterized the infection with RV-1B and RV-A16[196]. While an increase in BAL neutrophilia and lymphocytosis, Muc5B secretion, and viral RNA levels were promising indicators of viral-induced lung pathology, viral infections steeply declined from 12-24h, thus the model is of limited usefulness for studying effects on viral replication[196]. Another group used an OVA-sensitized mouse model of allergic airways disease and RV-1B (minor group, capable of growing in mouse cells *in vitro*) infection, and observed increased airway hyperresponsiveness, neutrophilia, and Th2 cytokine release in sensitized mice[197]. More recently, a mouse model of RV-induced exacerbation of COPD was developed that

involves the pretreatment of mice with elastase followed by inoculation with RV-1B, and led to airway neutrophilia and lymphocytic inflammation, the increased expression of TNF-alpha, CXCL-10, and other inflammatory cytokines, mucus hypersecretion, and increased airway hyperresponsiveness[198].

There are no animal models for RV-C infection at present. However, the identification of CDHR3 as a cell entry factor for the RV-C will likely allow for the identification or engineering of animal models for this RV species.

Tissue Culture Systems

RV-A and B were discovered in the 1950s using culture-based techniques, while the first RV-C types were discovered in 2006 with molecular techniques because they do not grow in standard culture systems[119,121,199]. The standard cell lines used to culture RV include HeLa cells and fetal lung fibroblasts (WI38, MRC5 and Wis.L). Growth of RV-A (both major and minor types) and RV-B on these cells were permitted due to the high expression of the two receptors (ICAM-1 and LDL-R) that bind the major and minor type viruses respectively[152]. A recent study has shown that these lines express little or no CDHR3, which is the only known RV-C cell entry factor[54].

Due to the lack of a standardized cell line permissive to infection with the RV-C, the gold standard for RV study has been the *in vitro* air-liquid interface (ALI) culture method using either sinus or bronchial tissue from human donors[73,74]. The ALI culture technique involves the acquisition of respiratory tissues (usually tracheal, bronchial, or sinus tissues), enzymatically stripping them of their epithelial cells, and dedifferentiating the stripped cells to grow in a monolayer *in vitro*. In order to differentiate respiratory stem cell cultures into pseudostratified respiratory epithelium, cells are grown on a semi-permeable membrane exposed to differentiation media on the basal surface and air on the apical surface. Over the course of ~30 days, the monolayer differentiates into respiratory epithelium and is susceptible to RV-C infection similarly to RV-A16[73,74]. These cultures closely resemble respiratory epithelium, and are composed mainly of ciliated, secretory, and basal cells[73,74].

Protocols Used to Purify Rhinovirus

As with all proteins and compounds, the first step to determining structure and function is to obtain a pure form of the substance of interest. Viral capsid purification has been practiced since the 1920s, and the first protocols to purify picornaviruses were published in the 1950s[200,201]. Picornavirus purification is necessary for multiple research purposes including structural determination by x-ray crystallography and cryo-electron microscopy, development of antibody reagents and vaccines (both attenuated and inactivated), modeling of capsid-binding antivirals, and elucidation of immune responses to viral components[46,202–206]. Standard RV purification protocols were based on those developed for the cardioviruses in the early 80s, and involves high speed centrifugation of infectious HeLa or Wis.L cell lysates through a 30% sucrose cushion[207,170,208–210]. Through the course of centrifugation, only small particles with a density greater than ~1.127 g/cm^3 (the density of 30% sucrose) will pass to the bottom of the ultracentrifuge tube, leaving the majority of cell lysate contents behind[207]. Furthermore, sucrose gradients have been employed for high-resolution focusing of particles with similar densities[211].

While the purification protocols optimized for the RV-A and B worked well to purify the RV-C15 clinical isolate, marked loss in viral yield and infectivity was consistently observed when the protocol was applied to other genotypes of RV-C (e.g. C41 and C2)[46,170,208–210,212]. An inability to robustly purify multiple genotypes of the RV-C coupled with the limitations of the primary airway epithelial cell tissue culture system inhibited RV-C molecular research. These limitations provided the rationale for conducting experiments to determine a robust and efficient mechanism for growth and purification of all isolates of the RV-C species, and the results of these studies are described in Chapter 2[212].

AIRWAY EPITHELIAL CELL BIOLOGY

Structure and Function of the Human Airways

The airways are divided anatomically into upper (nasal cavity, pharynx, and larynx) and lower (trachea, bronchi, bronchioles, terminal bronchioles, and alveoli) at the sternal angle, and are further organized into functionally distinct units, each with distinct epithelia[213]. The nasal cavity and proximal trachea are exposed to the greatest concentrations of inhaled particles, pathogens, pollutants, and aeroallergens. Thus, barrier function is well developed in the upper airways which are lined with thick, highly-ciliated, pseudostratified columnar epithelium with goblet cells (respiratory epithelium). The combination of ciliated epithelium and airway fluids and mucins provide a functional barrier by sweeping inhaled particles out of the airways via mucociliary transport[213]. The epithelium is firmly anchored by the basement membrane (BM), which is required for epithelial adhesion, maintenance of correct cell polarity, preservation of a selective barrier between the surface and underlying mesenchymal compartments, and the relay of essential survival signals to the epithelium[214–216].

Basal cells form tight integrin-mediated attachments to the BM in the form of hemidesmosomes[217]. They are highly abundant in the large airways and decrease in frequency more distally, and are the only respiratory epithelial cell type that does not reach the apical surface[217–219]. Basal cells can self-renew and differentiate into ciliated and secretory epithelial cells in response to injury, and also secrete multiple bioactive compounds including neutral endopeptidase, 15-lipoxygenase products, and cytokines[220,221].

In between the surface epithelium and cartilage of the trachea through the bronchi are submucosal glands (SMGs) that secrete mucus (mainly Muc5B) and serous fluids containing antimicrobials (such as lysozyme, lactoferrin, and lactoperoxidase) that moisten and disinfect the inner lining of the airways[213]. Similar to the SMGs, goblet cells, located from the proximal trachea (and sinuses) through the terminal bronchioles, primarily function to secrete a mixture of highly glycosylated mucin proteins (mainly

Muc5AC) into the airways for the entrapment of foreign objects, such as pathogens, pollutants, and allergens. They also can self-renew and transdifferentiate during inflammation and wound healing[218,222,223].

Ciliated cells represent over 50% of the epithelial population in human airways, and are mainly responsible for the coordinated movement of the mucus layer from the airways to the pharynx. These cells have limited ability to transdifferentiate and mediated wound healing capacity[224–226]. Ciliary clearance and mucus secretion are well-balanced in normal airways, but this equilibrium can be perturbed by chronic airway inflammation (as in asthma, or COPD) and viral infections that may lead to mucus cell metaplasia (MCM), epithelial hyperplasia, an increase in airway smooth muscle (ASM) mass, reticular basement membrane (RBM) thickening, and neovascularization[227–229]. MCM, mediated *in vitro* by IL-9 and IL-13 inflammatory cytokines, is defined as the replication of mucus-secreting cells and SMGs along the airways where they are not normally present, often accompanied by a loss of ciliated cells, the overproduction of mucus, and epithelial hyperplasia. This combination is known as airway remodeling, and is associated with airway obstruction and hyperresponsiveness to noxious stimuli[230,231]. Virus-induced overproduction of mucus, impaired ciliary transport, and airway hyperresponsiveness are important contributors to respiratory compromise during acute exacerbations of chronic airways diseases.

The epithelial lining thins in the distal airways, and cell height decreases with smaller airway diameter. Many cells found in the proximal conducting airways (e.g. secretory cells, SMGs) are replaced by smaller, cuboidal cells (e.g. clara, brush cells)[232]. Clara cells secrete surfactants, antiproteases, and p450 oxidases that promote proper lung inflation, neutralize allergens and excreted proteases during inflammation, and metabolize xenobiotic compounds such as aromatic hydrocarbons found in cigarette smoke[221,233,234]. Interestingly, clara cells can self-renew and differentiate into both secretory and ciliated respiratory epithelial cell types[235].

Finally, at the furthest distal pouches of the airways are the alveoli, which are lined with type I (TI) and type II (TII) pneumocytes that are specialized for gas exchange[236,237]. TI cells cover ~98% of the internal alveolar surface with thin cytoplasmic extensions and act as the main selective barrier for diffusion and gas exchange between inhaled air and blood in the lung parenchyma[238]. TII cells are much smaller, cuboidal cells that secrete and reabsorb pulmonary surfactants, and regenerate the alveolar epithelium following injury[236,237]. While it is generally believed that cells of the alveoli are not targeted by any species of RV, there are many other respiratory viruses and bacteria that can infect this compartment[10,239–241].

Role of the Epithelial Cell during Infection

Along with its barrier and mucociliary transport functions, the respiratory epithelium has a dynamic role in the control of immunity and regulation of inflammation in response to infection. The epithelium is the first line of defense exposed to the inhalation of foreign particles or pathogens and thus expresses a number of pathogen recognition receptors (PRRs), including Toll-like receptors (TLRs) and retinoic acid inducible gene-I (RIG-I)-like receptors (RLRs)[242]. These proteins serve to detect and respond to unique pathogen-associated molecular patterns (PAMPs) on infectious agents such as bacteria or viruses[242]. PAMPs include molecules that are not produced by the host organism, such as lipopolysaccharide (LPS) or chitin, or that may appear in the wrong host cell compartment, such as cytoplasmic double-stranded RNA (dsRNA). Using the RV life cycle as an example, RV capsid binding to the epithelial surface is detected by and activates TLR2[243]. Furthermore, the subsequent entry and initiation of replication in the host cytoplasm leads to the formation of dsRNA replication intermediates that activate TLR3, leading to downstream activation of inflammatory and antiviral effector genes. Cytoplasmic proteins such as RIG-I and melanoma differentiation associate gene 5 (MDA5) can also recognize viral RNA and further amplify the inflammatory response[244–246]. Some controversy exists whether or not the endosomal PRRs TLR7 and TLR8 play important roles in the detection of RV in HBECs, but the current consensus suggests they are less important than TLR3 and RLRs[245,247–251].

The activation of PRRs then leads to the downstream expression of proinflammatory cytokines and type I IFN production. For example, TLR2 activation causes the upregulation of IL-1 beta, IL-6, IL-8, and TNF-alpha, while the activation of TLR3 leads to the upregulation of IFN-beta in epithelial cells[252]. Proinflammatory cytokines produced this way recruit immune cells to the site of infection, while IFNs have para-and autocrine functions to signal for the activation of antiviral responses in surrounding cells and further amplify their own antiviral responses. IFN signaling thus promotes the production of IFN-stimulated genes (ISGs) which tend to inhibit cellular growth and survival, and require multiple ligands for activation (such as IFN and cytoplasmic dsRNA)[253].

The need for multiple ligands prior to the activation of ISGs allows uninfected cells to be primed for oncoming infection by upregulating a subset of these genes, without causing growth arrest or cellular destruction by activating the full range of antiviral defenses [253]. Furthermore, dendritic cells located in the basolateral compartment of the epithelium serve as cellular sensors for invading pathogens and will migrate to regional lymph nodes to promote the activation and differentiation of T and B immune cells in response to inciting stimuli, thus promoting the activation of cell-mediated and humoral immunity[254,255].

Role of Cadherins in Airway Epithelium

An important function of respiratory epithelium is to maintain an intact barrier between the submucosa and the airway lumen, and yet allow the selective transport of small molecules and immune cells between the two compartments. Cadherins and integrins play essential roles in maintaining the epithelium's selective barrier and cell polarity as well as coordination of inflammation and immune cell function. From apical to basal, three main intracellular junction complexes maintain the epithelial barrier. Tight junctions (TJs) are composed of occludens, claudins, and junctional adhesion molecules (JAMs) and regulate the paracellular permeability and maintain cell polarity by circumferential membrane expression of Zona occludens protein 1 (ZO-1)[256–258]. Adherens junctions (AJs) mechanically connect adjacent cells and initiate the formation and maturation of cell-cell contacts through the expression of

cadherins[256]. Finally, desmosomes and hemidesmosomes connect cells to each other and to the basement membrane, respectively using strong non-classical cadherins and integrins that connect the intermediate filaments of cells providing mechanical support to the entire tissue[217–219,256].

The AJs, and epithelial cadherin (E-cadherin) in particular, have been closely studied for their roles in the mediation of inflammation and allergy[256]. E-cadherin is a type I cadherin transmembrane protein, and has five extracellular cadherin repeats (ECRs) in its extracellular domain, and a conserved HAV tripeptide motif in the most distal ECR[259]. The extracellular domain of E-cadherin forms a homotypic, calcium-dependent trimer for adhesion between epithelial cells, while the cytoplasmic tail interacts with anchor proteins p120 catenin, beta-catenin, and alpha-catenin which all serve as an interface with the microtubular network and actin cytoskeleton[260,261]. Thus, E-cadherin, along with its role in cell-cell adhesion, participates in a number of cellular functions related to the maintenance of cell-shape, ciliary motion, intracellular vesicle transport, and cell division/proliferation.

Along with their structural roles, cadherins regulate inflammatory responses and mucosal immunity both directly and indirectly. For example, E-cadherin expression causes the repression of NF-kB, a protein complex that is a principal regulator of proinflammatory responses in the airways[262–265]. On the other hand, the downregulation of E-cadherin inversely leads to the upregulation of NF-kB and other proinflammatory mediators such as the Th2 signaling molecules chemokine ligand (CCL)-17 and thymic stromal lymphopoietin protein (TSLP), molecules that are well known to instigate exacerbations of chronic airway diseases[258,266,267]. E-cadherin binds to multiple cells of the innate and adaptive immune system. For example, E-cadherin is a ligand for the $\alpha_E\beta_7$ integrin, CD103 found on dendritic cells (DCs), the majority of CD4+ and CD8+ Tcells, and Tregs, and provides a tolerogenic signal to these cells as well as assisting in their transmigration through the epithelium to the airway lumen and to sites of infection[256,268,269]. E-cadherin also binds the killer cell lectin-like receptor 1 (KLRG1), which is expressed on activated natural killer cells, effector/memory T cells, and Tregs, and provides an immunosuppressive stimulus to these cells, leading to the inhibition of cytokine release[270].

While cadherins have been shown to directly damper immune responses through receptor binding, the proteolysis of cadherins, either by enzymes excreted by transmigrating leukocytes or allergens possessing proteolytic activity (e.g. dust mite, cockroach, fungi, cat, and pollen), can lead to the loss of epithelial integrity and an increased permeability of the epithelium to airway allergens and immune cells. The net result of reduced barrier function is a stressed and activated mucosal phenotype with increased NF-kB activity[271–277]. As a side note, the activation of a proinflammatory state following proteolytic cleavage could be an evolutionary tactic to combat parasitic helminth infections, which secrete proteases in order to invade host tissues[278]. As parasitic worm infections are controlled by Th2-type responses, proteolytic destruction of cadherins likely plays an integral role in the exacerbation of Th2-type cytokine and cellular responses in allergic disease. Taken together, it is clear that cadherins play an important role in the regulation of mucosal immunity and inflammation through maintenance of an intact epithelial barrier, intracellular signaling, and cross-talk with cells of both the innate and adaptive immune system.

SUMMARY

In summary, RVs are the major pathogen responsible for the most common disease in humans, the common cold. While most RV infections result in mild illness, young and old patients and those with chronic airway inflammatory diseases, CF, and immunodeficiencies are predisposed to higher symptom burdens and respiratory distress. Many studies have demonstrated an increased disease severity with the RV-C in all of these populations, however there is still very little known about the mechanism by which the RV-C are able to cause more severe respiratory disease. Many structural and physical characteristics of the RV-C remain largely unknown, primarily due to their recent discovery and the lack of a robust method for culture and purification. The development of a robust RV-C growth and purification protocol would enable detailed studies of structural and molecular characteristics of the viral capsid. Further, even with the recent discovery of CDHR3, the identity of the cellular target for the RV-C within the epithelium

is unknown. Understanding the primary cellular tropism of the RV-C is needed to understand additional mechanisms of RV-C entry, and host-virus interactions that influence the course of infection to produce mild or severe respiratory illness in different patient populations. These questions provide the rationale for the two primary goals of this dissertation: 1) develop a more robust growth and purification protocol for all RV-C genotypes, and 2) to identify the cellular target of the RV-C in respiratory epithelium, and determine the relationship of CDHR3 expression with RV-C tropism.

Briefly, this dissertation will demonstrate:

i) The standard purification procedures developed for the RV-A and B result in the loss of infectivity for multiple RV-C genotypes. The disparity is not due to an intrinsic instability of the RV-C capsid, but is more likely due to more profound aggregative and adhesive forces between the RV-C capsid and other capsids or materials. A reduction in centrifugal force with commensurate increase in centrifugation time increases the yield of infectious particles, presumably by reducing interactions between virus particles and with purification materials. In conducting these studies, we identified an increased sensitivity to low pH in all RV-C genotypes examined, and demonstrated an increased capacity for virion production in Wis.L cells (embryonic fibroblasts).

ii) The exclusive cellular target for the RV-C is the ciliated, respiratory epithelial cell. Ciliated cells express the majority and highest concentrations of CDHR3, the only known cell entry factor for the RV-C, and infection with RV-C results in diminished CDHR3+ populations as well as decreased CDHR3 expression in RV-C+ cells. Furthermore, we present preliminary evidence that RV-C results in cellular shedding, and infects pharyngeal but not palatine tonsillar epithelium.

CHAPTER TWO

Production, Purification, and Capsid Stability of Rhinovirus C Types

Adapted from

Theodor F. Griggs, Yury A. Bochkov, Kazuyuki Nakagome, Ann C. Palmenberg, and James E. Gern.

Journal of Virological Methods; June 1, 2015; 217:18-23

ABSTRACT

The Rhinovirus C (RV-C) were discovered in 2006 and these agents are an important cause of respiratory morbidity. Little is known about their biology. RV-C15 (C15) can be produced by transfection of recombinant viral RNA into cells and subsequent purification over a 30% sucrose cushion, even though yields and infectivity of other RV-C genotypes with this protocol are low. The goal of this study was to determine whether poor RV-C yields were due to capsid instability, and moreover, to develop a robust protocol suitable for the purification of many RV-C types. Capsid stability assays indicated that virions of RV-C41 (refractory to purification) have similar tolerance for osmotic and temperature stress as RV-A16 (purified readily), although C41 is more sensitive to low pH. Modification to the purification protocol by removing detergent increased the yield of RV-C. Addition of nonfat dry milk to the sucrose cushion increased the virus yield but sacrificed purity of the viral suspension. Analysis of virus distribution following centrifugation indicated that the majority of detectable viral RNA (vRNA) was found in pellets refractory to resuspension. Reduction of the centrifugal force with commiserate increase in spin-time improved the recovery of RV-C for both C41 and C2. Transfection of primary lung fibroblasts (Wis.L cells) followed by a modified purification protocol further improved yields of infectious C41 and C2. Described herein is a higher-yield purification protocol suitable for RV-C types refractory to the standard purification procedure. The findings suggest that aggregation-adhesion problems rather than capsid instability influence RV-C yield during purification.

INTRODUCTION

Rhinoviruses (RVs), the agents of most common colds, can contribute to more severe illnesses in susceptible individuals. For example, children, the elderly, the immunosuppressed and those with chronic respiratory conditions, such as asthma or COPD, are more predisposed to lower respiratory illnesses resulting in hospitalization [4–8]. Recent studies have demonstrated that respiratory illness severity is correlated with the type of RV, and the most severe colds and asthma exacerbations are likely caused by isolates in the RV-A and C species [8,41].

Of the three RV species, the RV-A and B were identified decades ago, while RV-C were only recently discovered (2006) via molecular techniques [119,121,199]. RV-C isolates are unable to grow in standard immortalized cell lines used to culture other species of RV, because these cells lack the required cellular receptor. Sequence analysis and molecular modeling has made it clear the RV-C have large capsid protein alterations that are associated with receptor specificity [125]. The inability to grow RV-C in standard tissue culture initially prevented a detailed investigation of these isolates, until Bochkov *et al* developed a reverse genetics system for RV-C15 (C15) that produced functional virions after transfection of RNA synthesized *in vitro* into cell monolayers [72]. The resultant C15 material was successfully purified using centrifugation through sucrose cushions and related protocols developed for the A and B viruses [170,208–210].

While this protocol worked well for C15, a marked loss in viral yield and infectivity was consistently observed when the protocol was applied to other C genotypes (e.g. C41 and C2) [46]. To date, obtaining high yields of RV-C other than C15 has been problematic because of technical difficulties in virus recovery procedures. Large stocks of purified RV-C are needed for structure determinations, monoclonal antibody production, immunological studies, and other RV-C investigations [46,127,279].

The hypothesis that some C types may have unstable capsid structures that cause apparent low viral yields following standard purification procedures is tested here. The data do not support this idea, and

instead led to a revised purification protocol, reducing virion aggregation, that results in higher viral yields. Virions isolated in this fashion retain infectivity for primary cultures of differentiated airway epithelial cells.

MATERIALS & METHODS

Viruses: RV-A16, C2, C15, and C41 samples from clinical isolates were cloned into cDNA, followed by linearization, *in vitro* transcription into infectious RNA (RiboMAX™ Large Scale RNA Production System-T7, Promega, Madison, WI), and transfection into HeLa or Wis.L (fetal lung fibroblast) cells (Lipofectamine® 2000 transfection reagent, Life Technologies, Grand Island, NY) as previously described [46,72,208,210].

Cell Culture: HeLa (ATCC CRL-1958) and Wis.L cells were grown in monolayers as previously described [52,72]. All experiments utilized HeLa cells for virus production, unless otherwise specified. Primary human bronchial epithelial cells (HBECs) were extracted from surgical specimens provided by the University of Wisconsin Department of Surgery, Division of Transplantation and grown by the air-liquid interface (ALI) culture method as described previously [73,74]. HBEC ALI cultures were inoculated with ~10^6 units of purified virions (PCR genome equivalents) per well or with BEGM (Lonza) alone for infectivity assay.

Solutions: Stock solutions of 50X 4-(2-hydroxyethyl)-1-piperazineethanesulfonic acid (HEPES) buffer were prepared by adding dry HEPES (Sigma) to a final concentration of 1.25M in DPBS, and adjusting the pH to 7.3-7.4. Sucrose (30% w/v, pH 7.1-7.2) was prepared in DPBS and 2% (v/v) 50X HEPES. Stocks of 0.1M citric acid and 0.2M Na_2HPO_4 were prepared and then mixed in required combinations (Table 2-1) to attain pH 5.5 – 7.0.

Rhinovirus C Concentration, Revised Protocol: All steps of this procedure were performed in a laminar flow hood using sterile cell culture material and solutions. 24 hours post transfection of Wis.L cells, T-75 flasks were removed from incubator and 200ul of 50X HEPES was added per 10mL of media in each flask. Flasks were incubated at -80ºC for 20min, and then at room temperature for 30min or at 37ºC for 15min (until cultures were thawed fully). This cycle was repeated twice more. After the third thaw, adherent cellular debris was scraped from the flasks, and cell lysates were transferred to 30mL

Table 2-1.

pH	X mL 0.1M Citric Acid	Y mL 0.2M Na_2HPO_4
5.5	43.1	56.9
6.0	36.9	63.2
6.5	29.0	70.9
7.0	17.7	82.4

round-bottom centrifuge tubes (Thermo Scientific Nalgene Oak Ridge, Cole-Parmer, Vernon Hills, IL). Lysates were vortexed and pelleted (10,000 x g, 10min, 4ºC). Supernatants were decanted into sterile 50mL conical tubes, and treated with RNAse A (100 µg/mL, 37ºC, 10min; Qiagen) to remove transfection input RNA. B-mercaptoethanol was then added to a final concentration of 0.2% (v/v). Lysates were mixed briefly, and 10µl aliquots were saved in 90µl DPBS for qPCR assay of treated lysate. Sucrose cushions (1mL/tube) were prepared in 14 x 89mm centrifuge tubes (Ultra-Clear™, Beckman Coulter, Brea, CA), and 10-11mL of lysate was overlaid onto each cushion. Following ultracentrifugation (100,000 x g, 4h, 10ºC), supernatants and cushions were aspirated from ultracentrifuge tubes and 200-250µl calcium and magnesium-free DPBS (CMF-PBS) was added. Samples were left overnight at 4ºC, and pellets were resuspended the next day by pipetting vigorously until observable clumps disappeared. Aliquots of 10µl per sample were diluted in 90µl DPBS for quantitation of virus, and aliquots of concentrated viral suspensions were stored at -80°C.

RNA extraction and quantitative (q) RT-PCR: Viral (v) RNA was extracted from cell lysates or concentrated virus aliquots using RNeasy Mini kits (Qiagen), using the QiaShredder (Qiagen) preliminarily if extracting from ALI culture [73]. vRNA concentrations were determined by qRT-PCR as described previously [72].

Osmotic Stability Assay: Clarified lysates from C41 or A16-infected cells were diluted 1:10 in DPBS with added sucrose to produce final concentrations of 0-30% w/v sucrose. Samples (100µL) were incubated for 1 hour at RT with shaking (500 rpm). Aliquots were then diluted 1:10 with DPBS (to decrease the sucrose concentration) and incubated (10min, 37°C) with RNAse A (100µg/mL, Qiagen) to remove unprotected vRNA. vRNA content was analyzed by qRT-PCR.

Thermostability Assay: Clarified lysates from C41 or A16-infected cells were diluted 1:10 in DPBS and then incubated at 4, 37, 46, 55, or 65ºC for 1h, followed by 10 min incubation at 37°C in the presence of 100µg/mL RNAse A (Qiagen) to remove unprotected vRNA. vRNA content was analyzed by qRT-PCR.

pH Stability Assay: Clarified cell lysates containing C41, A16, C2, or C15 were diluted 1:10 into various citrate-phosphate buffer combinations (Table 1) thereby exposing virions to a range of pH (7.0, 6.5, 6.0, or 5.5). The samples were incubated at RT with shaking (500 rpm) for 1h, followed by 10min incubation at 37°C with 100µg/mL RNAse A (Qiagen), and analysis for vRNA by qRT-PCR.

Statistics: Statistical significance of collected data was assessed with SigmaPlot programs (version 11.0 Systat Software, Inc., San Jose, CA). Log-transformed values were used for most comparisons. Paired t-tests, one-way ANOVAs, and repeated measures ANOVAs, were used when comparing two groups, three or more groups with one variable, and three or more groups with two variables, respectively. Yield (%) values were determined by dividing the total number of vRNA copies detected per purified sample, by the total number of vRNA copies detected in the starting input lysate.

RESULTS

C41 and C2 yields are lower than C15, following standard concentration protocols.

In standard RV concentration protocols [170,208–210], lysates from cells transfected with A16, C2, C15, or C41 are incubated with N-lauroylsarcosine to release virus from cell membranes, RNAse A to eliminate transfection input RNA, and β-mercaptoethanol to inhibit RNAses. Viral particles are then pelleted by centrifugation (200,000 x g, 2h) through a 30% sucrose cushion. Approximately 65% and 60% of A16 and C15 PCR signals were recovered with this procedure, respectively (Figure 2-1), compared to the RNAse-protected signals in starting lysates. However, for C2 and C41, the comparative yields were significantly lower (<15% and <5%, respectively, $p < 0.001$). Since detergents can adversely affect RV infectivity [280], the first tested protocol variation was to omit N-lauroylsarcosine (Figure 2-2). The result was a decrease in A16 recovery by approximately 20% ($p < 0.05$), with only a slight increase in C41 yield, from 2 to 5% ($p < 0.01$).

Effects of stabilizer additions.

During purification, other picornaviruses have been stabilized using $MgCl_2$, gelatin, or casein [281–283]. Nonfat dry milk (NFDM) or other lipid sources (myristate) have been shown to protect poliovirus and foot and mouth disease virus (FMDV) from thermal inactivation [284,285]. The effects of these compounds on RV-C yield were tested. There was no increase in viral yield following addition of $MgCl_2$, gelatin, casein, or whey to transfected cell lysates, the sucrose cushions, or both (data not shown). In contrast, when 1% NFDM was included in the cushions, the yields of C41 and C2 (the RNAse-resistant PCR signals in the resultant pellets) increased to ~60% and ~35% of the input signals, respectively ($p < 0.01$ and < 0.05, Figure 2-3). Unfortunately, the final product in both cases consisted of large aggregates of non-viral proteins, lipids, and carbohydrates, and therefore was not suitable for most downstream applications.

Figure 2-1

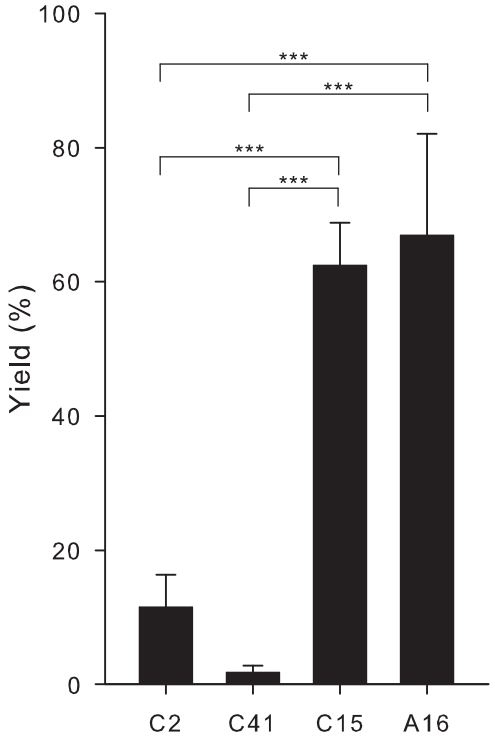

Figure 2-1. Variable RV-C yield with standard purification protocol. HeLa cell lysates transfected with either C2, C41, C15, or A16 were purified using the standard protocol (n=3)[72,170,208,210]. *** p-value <0.001.

Figure 2-2.

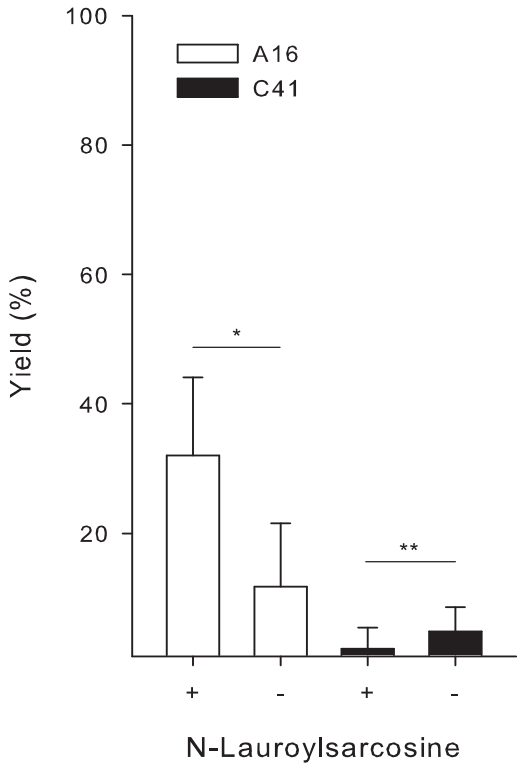

Figure 2-2. Effects of detergent on virus yield. Cell lysates were treated (+) or not (-) with N-lauroylsarcosine. RNAse protected virus signals recovered by each protocol was recorded (n=3). *, ** p-value <0.05 and <0.01, respectively.

Figure 2-3.

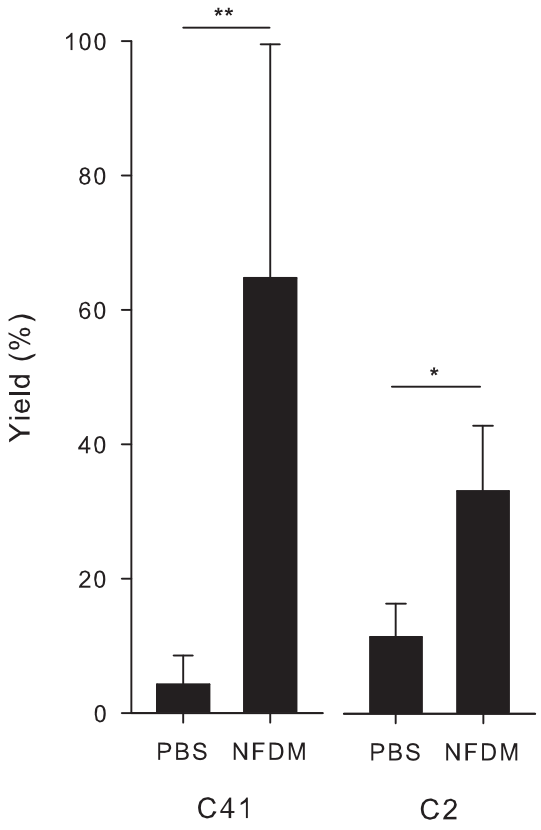

Figure 2-3. Effect of NFDM on virus yield. Following transfection of HeLa cells with recombinant transcripts, C41- or C2-containing clarified cell lysates were fractionated by pelleting through a 30% sucrose cushion containing PBS with 1% nonfat dry milk (NFDM), or PBS alone (n=4 and n=3 for C41 and C2 experiments, respectively). *, ** p-value < 0.05 and <0.01, respectively.

RV-C capsid stability to physical stress.

The previous experiments suggested that C2 and C41 capsids were less stable than those of C15 and A16. To test this hypothesis, HeLa cell lysates clarified without detergent containing A16 and C41 capsids were subjected to osmotic, temperature, and pH stresses, and then measured for changes in RNAse-protected PCR signals, indicative of particle disruption (Figure 2-4). Both C41 and A16 responded similarly to osmotic and thermal stress (Figure 2-4A and B). Both treatments reduced the recovery of protected PCR signals, incrementally, with higher osmotic and temperature shocks. To a degree, the same was true for the pH experiment, except C41 became sensitive to disruption at pH 6.0, losing 1-log in titer relative to A16 ($p<0.01$). At a lower pH (5.5), both samples lost PCR signal, indicating common capsid disruption. To determine whether this disparity was common also to C2 and C15 particles, the experiment was repeated with lysates containing these viruses (Figure 2-5). As with C41, these too had reduced capsid stabilities at pH 6.0. Since C15 yield is not severely reduced following standard purification, and solutions used are buffered at a pH of ~7.2, RV-C acid lability is an unlikely explanation for the comparatively reduced C2 and C41 yields in standard purification procedures.

Role of centrifugation in RV-C purification.

The above experiments showed there were no overt physical distinctions among C15, C2 and C41 particles that might account for their discrepant recoveries during the standard purification procedure. The NFDM experiment hinted, however, that pelleted aggregates during the centrifugation step might be a source of considerable lost materials. To test this idea, standard purification of C2 was carried out, with or without added NFDM. After centrifugation, the supernatant was decanted and total RNA was extracted from the bottom of the ultracentrifuge tube (Figure 2-6A). All C2 vRNA signal was detected in this location, even in the absence of NFDM. These pellets resisted resuspension even when they were incubated overnight in CMF-PBS (data not shown). Reasoning these pellets were irretrievably aggregated, the experiment was repeated with lower centrifugal force (100K x g) and commensurately

Figure 2-4.

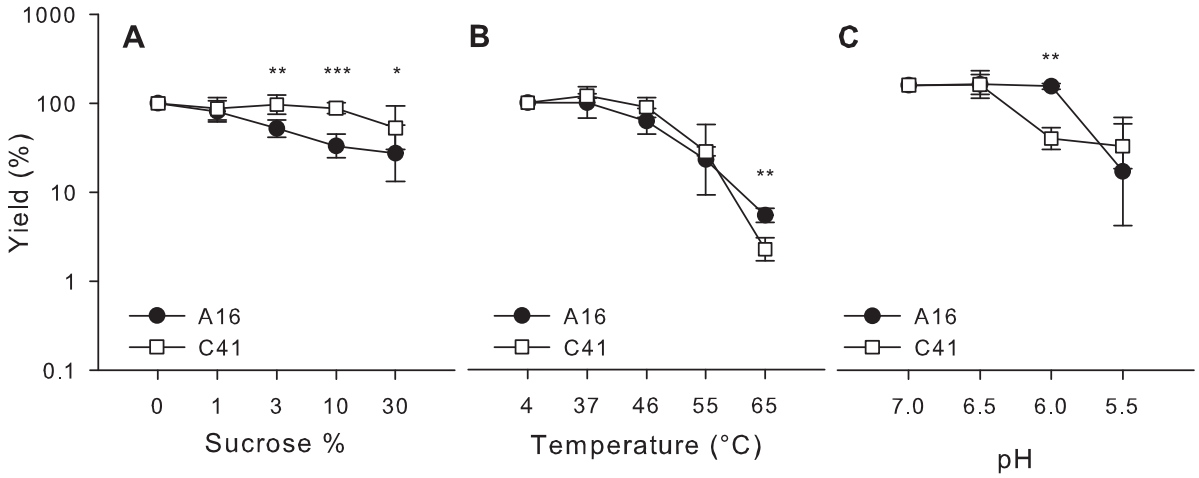
1000
100
10
1
0.1
Yield (%)
A
B
C
**
***
*
**
**
A16
C41
A16
C41
A16
C41
0
1
3
10
30
Sucrose %
4
37
46
55
65
Temperature (°C)
7.0
6.5
6.0
5.5
pH

Figure 2-4. Response of RV-C41 to physical stress. HeLa cell lysates containing newly synthesized A16 or C41 were subjected to conditions intended to induce potential capsid disassembly. The assays measured gain/loss of vRNA PCR signal, following treatment with RNAse A. To assay osmotic stress factors, (A), lysates were incubated for 1h, with shaking at RT in PBS containing 0, 1, 3, 10, or 30% sucrose (w/v, n=3). To assay thermal stress (B), lysates were incubated for 1h at 4, 37, 46, 55, or 65°C (n=5). To assay pH stress (C), lysates were diluted into citrate-phosphate buffers with the indicated pH, and then incubated for 1h with shaking (n=3). *, **, *** p-value <0.05, <0.01, and <0.001, respectively.

Figure 2-5.

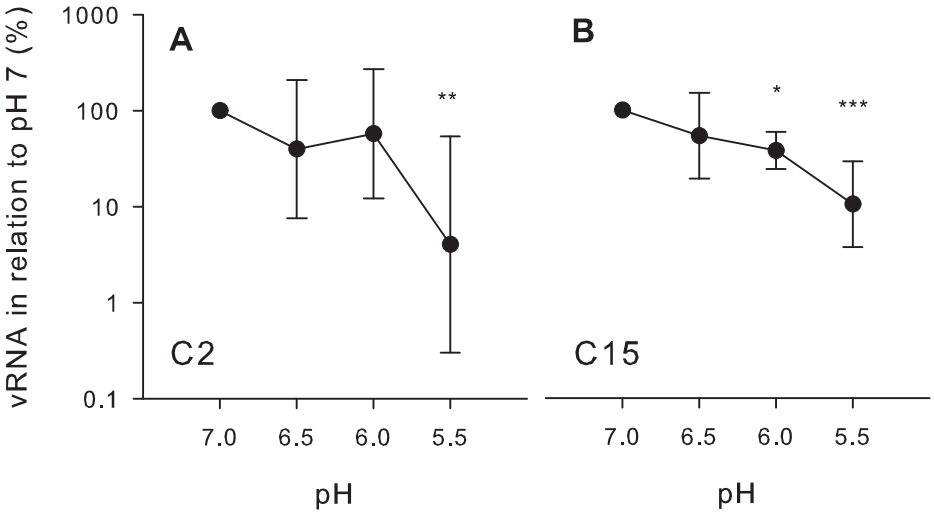

Figure 2-5. Response of C2 and C15 to pH stress. HeLa cell lysates containing newly synthesized C2 and C15 were diluted in citrate-phosphate buffers to yield a pH range from 7.0 to 5.5 and incubated for 1h with shaking followed by RNase A (Qiagen) treatment and analysis via qPCR (n=3). vRNA measurements at low pH were then compared to vRNA at pH 7. *, **, *** p-value <0.05, 0.01, 0.001, respectively.

Figure 2-6.

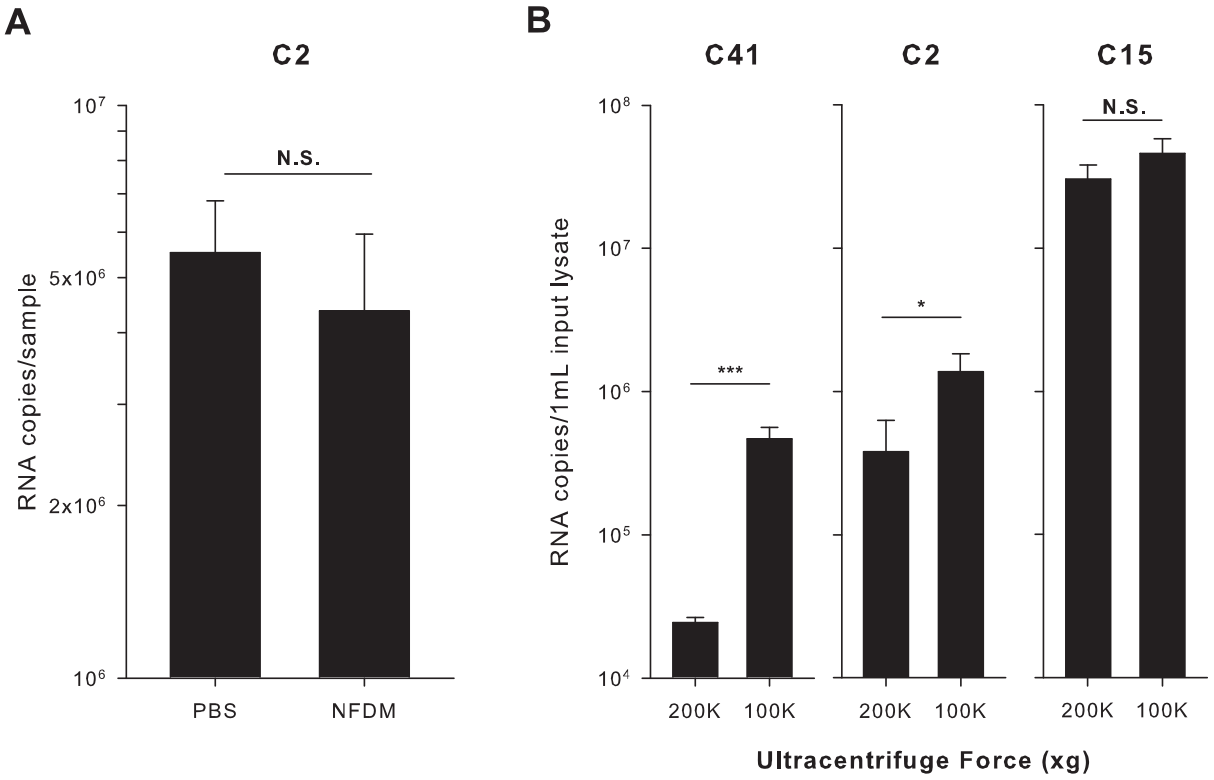
A
C2
RNA copies/sample
10^7
5x10^6
2x10^6
10^6
N.S.
PBS
NFDM
B
C41
C2
C15
RNA copies/1mL input lysate
10^8
10^7
10^6
10^5
10^4
***
*
N.S.
200K
100K
200K
100K
200K
100K
Ultracentrifuge Force (xg)

Figure 2-6. RV yield with modified centrifugation protocol. (A) Following purification of C2 through 30% sucrose with (NFDM) or without (PBS) NFDM, total RNA was extracted and quantified via qPCR to determine the total RNAse-protected material in the pellet prior to resuspension (n=3). (B) HeLa cell lysates containing C41, C2, or C15 were loaded over 30% sucrose cushions and subjected to centrifugation at either 200K x g for 2h, or 100K x g for 4h (n=3). The resultant pellets were quantified for RNAse-resistant PCR signals. N.S., *, *** p-value >0.05, <0.05, and <0.001, respectively.

greater time (4h) for sedimentation. Pellet resuspension was again overnight in CMF-PBS (Figure 2-6B). This simple protocol alteration increased the yield of resuspended C2 and C41 signals by 4-fold and 20-fold respectively compared to the standard protocol ($p < 0.05$ and < 0.01 respectively), while maintaining a similarly high recovery of C15.

Improved RV-C yields from transfected Wis.L cells.

Preliminary experiments demonstrated greater RV-C replication in transfected Wis.L cells compared to HeLa cells (data not shown). To capitalize on this observation, the revised centrifugation protocol was applied to virus-containing lysates from these cells, (Figure 2-7). The combined higher initial titers, and improved collection procedures gave excellent C2 and C41 preparations with vRNA concentrations near those observed for parallel C15 preparations ($1.7x10^9$, $7.4x10^8$, and $5.2x10^9$ vRNA copies/µl, respectively).

Infectivity of purified C41 and C2 to differentiated HBECs.

C41 and C2 suspensions prepared with the improved protocol were tested for binding and infectivity to ALI cultures of HBECs (Figure 2-8). HBEC ALI cultures were inoculated with $1x10^6$ units of purified virions per well or with medium alone. The amplification of C2 was greater than that of C41, but both viruses increased their vRNA signals by nearly 2 logs, over 24h, compared to the amount of cell associated signal at 3 hours post-inoculation (hpi).

Figure 2-7.

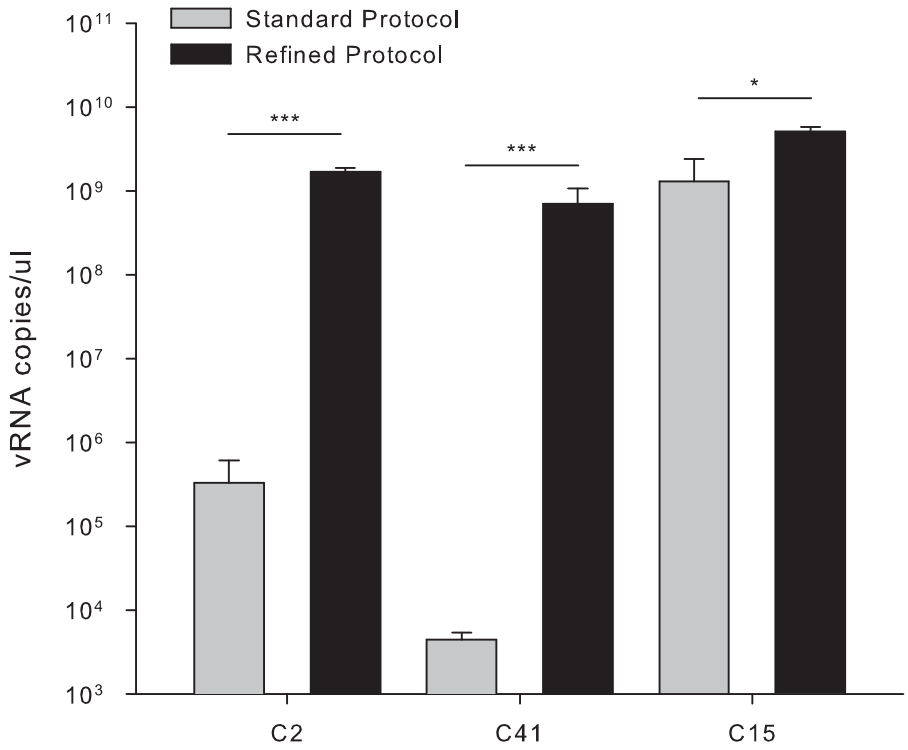
Standard Protocol
Refined Protocol
vRNA copies/ul
10^{11}
10^{10}
10^{9}
10^{8}
10^{7}
10^{6}
10^{5}
10^{4}
10^{3}
***
***
*
C2
C41
C15

Figure 2-7. Purification of C2, C41, and C15 from Wis.L cells, using the revised protocol. Following transfection of Wis.L cells with C2, C41, or C15 RNA, lysates were harvested (~10mL each) and pelleted (100K x g for 4h) through 30% sucrose cushions and then resuspended overnight in CMF-PBS (250µl) (black bars, n=3). Gray bars indicate yields obtained with standard, previous purification procedures, from HeLa cells, resuspended in the same volume (n=3). *, *** p-value <0.05 and <0.001, respectively.

Figure 2-8.

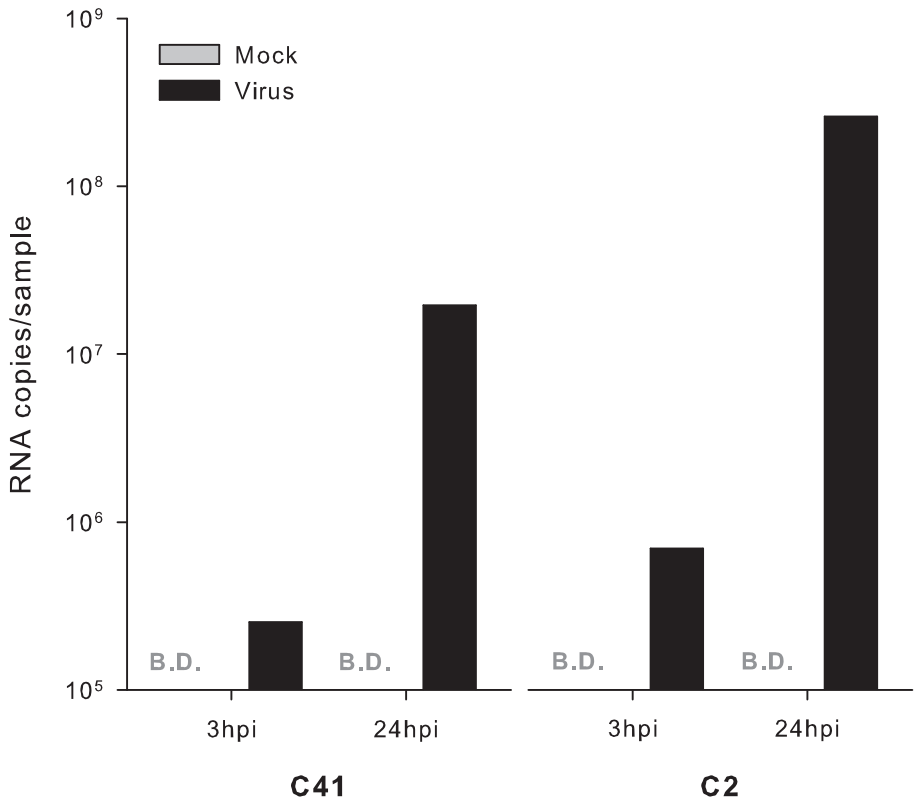
RNA copies/sample
10^9
10^8
10^7
10^6
10^5
Mock
Virus
B.D.
B.D.
B.D.
B.D.
3hpi
24hpi
3hpi
24hpi
C41
C2

Figure 2-8. Infectivity of purified RV-C preps. Cultures of differentiated epithelial cells (ALI) were inoculated with 106 vRNA copies/well of C41 or C2 produced using the revised protocol. BEGM media alone served as a control (mock). vRNA was assayed by qPCR at 3 hours post-inoculation (3hpi) and again at 24hpi to determine cell-associated virus prior to and post viral replication, respectively (n=1). vRNA was not detected in mock-infected samples. Abbreviations: B.D., below detection.

DISCUSSION

The RV-C are clinically important viruses that were first discovered in 2006. Research on these viruses has been hampered by difficulties in producing adequate preparations of purified viral particles. The standard RV purification protocol was adapted from methods used for cardioviruses [207]. While successful for multiple RV-A and B types, and for recombinant virus derived from the C15 cDNA, this protocol was unable to recover high yields for other RV-C types [72,170,208,286]. Accordingly, the protocol was adapted so it would be more ubiquitous. Only minor differences in capsid stability between those RV refractory to purification (e.g., C2 and C41), and the RV that were not (e.g., C15 and A16) were found. However, it was observed that the former formed tight aggregates following high-speed centrifugation, and these pellets were resistant to resuspension. By reducing the centrifugal force and increasing the spin-time, the resulting pellets could be resuspended, which led to significantly improved virus recovery. Using the revised protocol, C41 and C2 yields were comparable to those attained with C15 or the standard RV-A and RV-B types.

Additional variables were tested as part of this protocol. The removal of detergent negatively affected the recovery of A16, but did not substantially impact C41. This may reflect differential association of newly formed particles with cell membranes which may or may not contain viral receptors. Such membranes, possibly trapping some virus, particularly A16, would not have been disrupted in the absence of detergents, and could account for the loss. None of the putative stabilizing agents tested here had a positive impact on virus recovery. NFDM, while improving purification yield, produced large aggregates inadequate for downstream applications. Although some of these agents are useful for other picornavirus purifications, they do not add much to efficiency of RV yields [207,281,282,285].

Instead, the most important observation described here was that ultracentrifugation of C2 and C41 could lead to tight pellets that were resistant to resuspension. This suggests that the physical properties of some RV-C may promote aggregation. Gassilloud and Gantzer made similar observations with poliovirus,

and further noted that incubating poliovirus in a buffer with pH near its isoelectric point (pI) promoted the highest degree of aggregative and adherent properties [287].

Relative to the original protocol, a simple reduction in centrifugal force, and increase in spin time had a large effect on viral yield (~0.5-1.5 log). Furthermore, the use of Wis.L cells as targets for RNA transfection increased the apparent amount of virus produced per cell by ~1 log. These larger starting yields when coupled to the reduced-g procedures converted directly into highly concentrated and infectious samples for all tested RV-C.

In conclusion, the modified RV purification protocol enables production of multiple RV genotypes, while maintaining excellent infectivity. The three RV-C genotypes examined have slightly different physical properties, and additional experiments may reveal whether these differences influence virus binding, replication, or transmission. The protocol revisions and stability data presented in this work will assist and expedite RV-C research related to antiviral development, characterization of RV-C physical and immunological properties, and exploration of the RV-C lifecycle.

CHAPTER THREE

Rhinovirus C Targets Ciliated Respiratory Epithelial Cells

Adapted from

Theodor F. Griggs, Yury A. Bochkov, Thomas R. Pasic, Rebecca A. Brockman-Schneider,

Ann C. Palmenberg, and James E. Gern.

Manuscript in preparation. 2015

ABSTRACT

The Rhinovirus C (RV-C), identified in 2006, produce high symptom burdens in children and asthmatics, however, their primary target host cell in the airways remains unknown. Our primary hypotheses were that the RV-C target ciliated respiratory epithelial cells (RECs), and that cell specificity is determined by restricted and high expression of the only known RV-C cell-entry factor, cadherin related family member 3 (CDHR3). We also hypothesized that ciliated tissues are required for susceptibility to the RV-C in the upper respiratory tract. RV-C15 infection in HBEC cultures was assessed using immunofluorescent and time-lapse epifluorescent imaging. RV-C15 infected cell and tissue morphology were assessed by immunohistochemistry and flow cytometry of differentiated RECs, adenoids, and tonsils. RV-C15 produced a scattered pattern of infection, and infected cells were shed from the epithelium. The percentage of cells infected with C15 varied from 1.4-12% with cell culture conditions. Infected cells stained positively for acetylated-alpha-tubulin (aat, $p<0.001$) but not wheat germ agglutinin or Muc5AC (p=ns). 70% of aat+ cells were CDHR3+ ($p<0.001$) and decreased to 58% following RV-C15 inoculation ($p<0.001$). Uninfected ciliated cells expressed 2.2-fold higher CDHR3 than all other cell populations ($p<0.001$). Following inoculation *ex vivo*, C15 replication was identified in adenoids but not tonsils. In summary, the RV-C replicate only in ciliated RECs *in vitro* and cause infected cell shedding, CDHR3 expression is largely confined to ciliated RECs, and adenoids are susceptible to RV-C infection *ex vivo*. Our data indicate that factors regulating differentiation and CDHR3 production may be important determinants of RV-C illness severity.

INTRODUCTION

Non-influenza viral respiratory infections cost the US an estimated $39.5 billion annually from both direct healthcare costs and loss of productivity[288]. Rhinovirus (RV) is the most common cause of viral upper respiratory infection resulting in rhinitis, sinusitis, pharyngitis, or otitis media, and can lead to the development of bacterial superinfections[10,289–292,9]. While most individuals only experience mild symptoms during a RV infection, children, the elderly, the immunosuppressed, and those with asthma, COPD, or cystic fibrosis are predisposed to lower respiratory illnesses including wheezing, asthma exacerbations, and respiratory distress that can often result in hospitalization[2–8]. RV has also been implicated in the initiation of asthma, as the presence of wheeze during acute RV infection in the first few years of life is strongly correlated with the development of asthma later in life[293–297]. Three RV species have been identified, A-C, and recent studies have established a link between RV species and illness severity[8,41]. For example, the RV-C, discovered in 2006, appear to instigate the most severe upper and lower respiratory tract symptoms in infants and children under 5 years of age[8,41]. In an effort to explain this phenomenon, Nakagome *et al.* inoculated airway epithelial cells with multiple members of each RV species, and observed the highest levels of viral replication, cytotoxicity, and release of inflammatory cytokines following inoculation with either RV-A or C[46].

Clearly, the way a virus interacts with the host epithelium in an important determinant of illness severity, and at the center of this interplay is the target cell and cell entry receptor. Consider, for example, that cellular retargeting of avian influenza virus in human tissue from ciliated to secretory cells is necessary to produce severe and clinically apparent disease, and also that a broadening of the human coronavirus tropism to alveolar pneumocytes contributed to the Severe Acute Respiratory Syndrome and Middle East Respiratory Syndrome pandemics[240,241,298–304]. For RVs, the cellular targets of the RV-A and B have been studied with varying results[305–309]. For example, RV-B14 and the major group RV receptor, ICAM-1, have been identified in non-ciliated cells derived from the palatine tonsils (tonsils), and higher levels of RV-A16 replication were noted in cultures with mucus cell metaplasia (MCM), which can occur

in asthma or COPD[305,306,308]. High levels of ICAM-1 expression and RV-A16 binding were also observed on basal epithelial cells[307,310]. More recently, Jakiela *et al.* contradicted previous studies by identifying ciliated cells as the primary target for RV-A16, and further indicated MCM as a protective factor against RV-A16 infection[308,309]. Regarding the RV-C, while Bochkov *et al.* demonstrated the presence of viral RNA in sinus tissue organ cultures, and subsequently identified cadherin-related family member 3 (CDHR3) as the first and only known RV-C entry factor, the specific host cell for the RV-C remains unknown[54,72].

We therefore performed a series of experiments to identify the cellular target and tissue tropism of the RV-C. Our primary hypotheses were that the RV-C target ciliated respiratory epithelial cells (RECs) *in vitro*, and that cell specificity was restricted to cells expressing CDHR3. We also hypothesized that ciliated tissues are required for susceptibility to the RV-C in the upper respiratory tract (e.g. pharyngeal [adenoid] but not palatine [tonsil] tonsils).

MATERIALS & METHODS

Viruses: RV-C15 and RV-C15-GFP suspensions were prepared from the pC15 plasmid by reverse genetics as previously described[72,46,212,54].

Cell Culture: Primary human bronchial epithelial cells (HBECs) were extracted from surgical specimens provided by the University of Wisconsin Department of Surgery, Division of Transplantation and grown by the air–liquid interface (ALI) culture method as described previously[73,74]. For some experiments, we used a second culture medium (PneumaCult™, Stem Cell Technologies, Vancouver, BC, Canada) after preliminary experiments demonstrated improved differentiation and susceptibility to RV-C infection.

ALI Infections: Basal media was aspirated from 30-50 day-old ALI cultures that were then washed apically 5x and incubated with 100 µl of apical BEGM containing 1 x 10^7 plaque forming unit equivalents (PFUe) of RV-C15 (3.5h, 34°C). The inoculum was then aspirated, basal ALI media replenished, and cultures were incubated for an additional 14.5h.

Immunofluorescence: Following overnight incubation with RV-C15, ALI cultures were washed 3x apically and basally with PBS and fixed with ice cold 4% PFA (15 min, RT). Membrane inserts were cut in half and removed from transwell plates and placed into a 24-well plate for staining. Cells were permeabilized in 0.3% (v/v) Triton-X100 (10 min, RT), blocked in 0.5% nonfat dry milk in PBST (1h, RT), incubated in primary antibody (1:200 in blocking buffer, 1h, RT), secondary antibody (1:250 in PBST, 1h, RT) and Syto-13 (0.5uM, 10 min, RT, Life Technologies, Grand Island, NY). Inserts were washed in between staining with PBST, and mounted with ProLong® Gold Antifade Reagent (Life Technologies, Grand Island, NY). Cells were imaged on an Olympus 1X71 fluorescent microscope with a Q imaging Retiga2000R camera, a Nikon Eclipse T*i* fluorescent microscope, or Nikon C1 laser scanning confocal microscope (Chiyoda, Tokyo, Japan) with a 60x oil immersion objective. Analysis of digitized images was performed with FIJI/Image J version 1.49h (NIH, Bethesda, MD).

Immunohistochemistry: Differentiated and *ex vivo* organ cultures were fixed with 10% normal-buffer formalin, and embedded in paraffin (University of Wisconsin Histology Lab, Madison, WI). Five or 10um sections were adhered to slides which were deparaffinized and then rehydrated. For antigen retrieval, slides were incubated with proteinase K (40ug/mL in PBS, 10 min, 37°C). Peroxidases were blocked (5 min, RT, Peroxidazed 1 (Biocare Medical, Concord, CA). Slides were blocked (3% FBS, 2% goat serum, 0.2% Tween-20, 1.25% Human BD Fc Block™, 1h, RT), incubated (1:200 in blocking buffer, 2h, RT) with anti-C15-VP2 mouse monoclonal antibody (kindly provided by MedImmune Inc., Gaithersberg MD), Mach 4 Universal Probe and then Polymer (15 min, RT each, Biocare Medical, Concord, CA), Betazoid DAB (5 min, RT, Biocare Medical, Concord, CA), and counterstained with CAT hematoxylin or eosin (30s, RT, Biocare Medical, Concord, CA). Images from labeled slides were acquired and analyzed using an Olympus BX60 light microscope with DP Controller and Manager software (Shinjuku-ku, Tokyo, Japan).

Flow Cytometry: Basal media was removed from each well, followed by three washes in calcium-and-magnesium-free-PBS (CMF-PBS) apically, and basally. Cells were trypsinized (200µl apical, 800µl basal, 8 min, 37°C) and suspended vigorously with FBS (200µl, apical), followed by centrifugation (700 x g, 5 min) and decanting. Samples were treated with 0.1% (v/v) Ghost Dye™ Red 780 (Tonbo Biosciences, San Diego, CA, 20 min, on ice), MeOH (15 min, -20°C), 0.3% Triton-X100 (10 min, RT) in CMF-PBS, prior to blocking (1h, RT) in 10% FBS, 0.05% Tween-20, and 1.25% Human BD Fc Block™ (BD Biosciences, San Jose, CA). The samples were then incubated with a first set of primary (1:200, 1h, RT, in blocking buffer), and secondary (1:1000, 1h, RT) antibodies, and the second set of primary (1:200, 30 min, RT) and secondary (1:1000, 30 min, RT) antibodies (all in blocking buffer, without Fc Block for secondary antibodies). Samples were washed in between all antibody steps (3x, 700 x g, 5 min). Primary antibodies were mouse anti-C15-VP2 (MedImmune, Gaithersburg, MD), mouse anti-FLJ23834 (anti-CDHR3), rabbit anti-acetylated-alpha-tubulin, rabbit anti-Muc5AC, mouse IgG1 isotype, and mouse IgG2b isotype (AbCam, Cambridge, MA). Secondary antibodies (Alexa Fluor 350, Alexa Fluor 568,

Alexa Fluor 647) and wheat germ agglutinin (Alexa Fluor 350-conjugated) were from Life Technologies (Grand Island, NY). Data from labelled cells were acquired on a Fortessa (BD Biosciences) that was calibrated using Rainbow Fluorescent Particles (RFP-30-5A, Spherotech, Lake Forest, IL) and analyzed with FlowJo software version 10 (Tree Star, San Carlos, CA).

Statistics: Data were analyzed using SigmaPlot version 11.0 (Systat Software, Inc., San Jose, CA). One-way Repeated Measures ANOVAs were used to compare three or more groups, and square-root-transformed data was used to analyze data from PneumaCult™-differentiated cultures.

RESULTS

RV-C15 infection of HBEC-ALI culture results in diffuse, apical shedding of intact cells.

To visualize RV-C-infected cells, human bronchial epithelial cells (HBECs) were differentiated *in vitro* at an air-liquid interface (ALI) for 30-50 days, and then inoculated with RV-C15. After 16-18h, RV-C15-positive (C15+) cells were distributed diffusely along the epithelium (Figure 3-1A). Immunofluorescent staining revealed cells with bright cytoplasmic staining for the viral capsid. These cells often appeared rounded, and the brightest C15+ cells were observed above the epithelial layer among the epithelial cilia.

Following inoculation, cell-sized holes in the epithelial layer were noted by confocal microscopy just basal to C15+ cells (Figure 3-1B and C). In order to determine whether these holes in the epithelium were created by shedding of infected cells, we inoculated HBEC-ALI cultures with a RV-C15 genetically engineered to express GFP during viral replication (C15-GFP) and performed time-lapse fluorescent imaging over the course of 30h of viral infection (Figure 3-2). Cells expressing GFP indeed rounded in place and were ejected from the epithelial layer, leaving gaps in the epithelium that subsequently contracted over the course of the experiment.

Ciliated cells are the host cell for RV-C15.

We next assessed by immunofluorescence the colocalization of C15 staining together with markers of secretory cells (wheat germ agglutinin [WGA]) and ciliated cells (acetylated-alpha-tubulin [aat]), respectively (Figure 3-3). Many C15+ cells had aat staining of cilia on the apical membrane. On the other hand, cells staining positive for both C15 and WGA were not observed.

To obtain more information about the morphology of infected cells, HBEC-ALI cultures infected for ~18h were analyzed by immunohistochemistry (IHC, Figure 3-4A). Again, C15 staining was noted primarily in the cytoplasm of ciliated cells. The majority of C15+ cells possessed notable cilia, while a

Figure 3-1

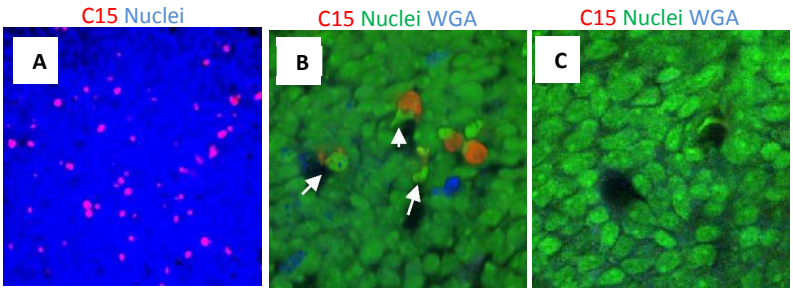

Figure 3-1. RV-C15 inoculation of airway epithelial cells causes a speckled pattern of infection and infected cell shedding. HBEC-ALI cultures were infected for 18h with RV-C15 and imaged by fluorescent microscopy (A). Nuclei stained with Hoechst (blue), RV-C15 capsid stained with monoclonal antibody against VP2 (red). Original magnification: 20x. Inoculated cultures were also imaged by confocal microscopy and analyzed by z-stacking (B) or apical surface views (C). Nuclei stained with Syto-13 (green), secretory cells stained with WGA (blue), and RV-C15 capsid stained with monoclonal antibody (orange). Original magnification: 60x.

Figure 3-2

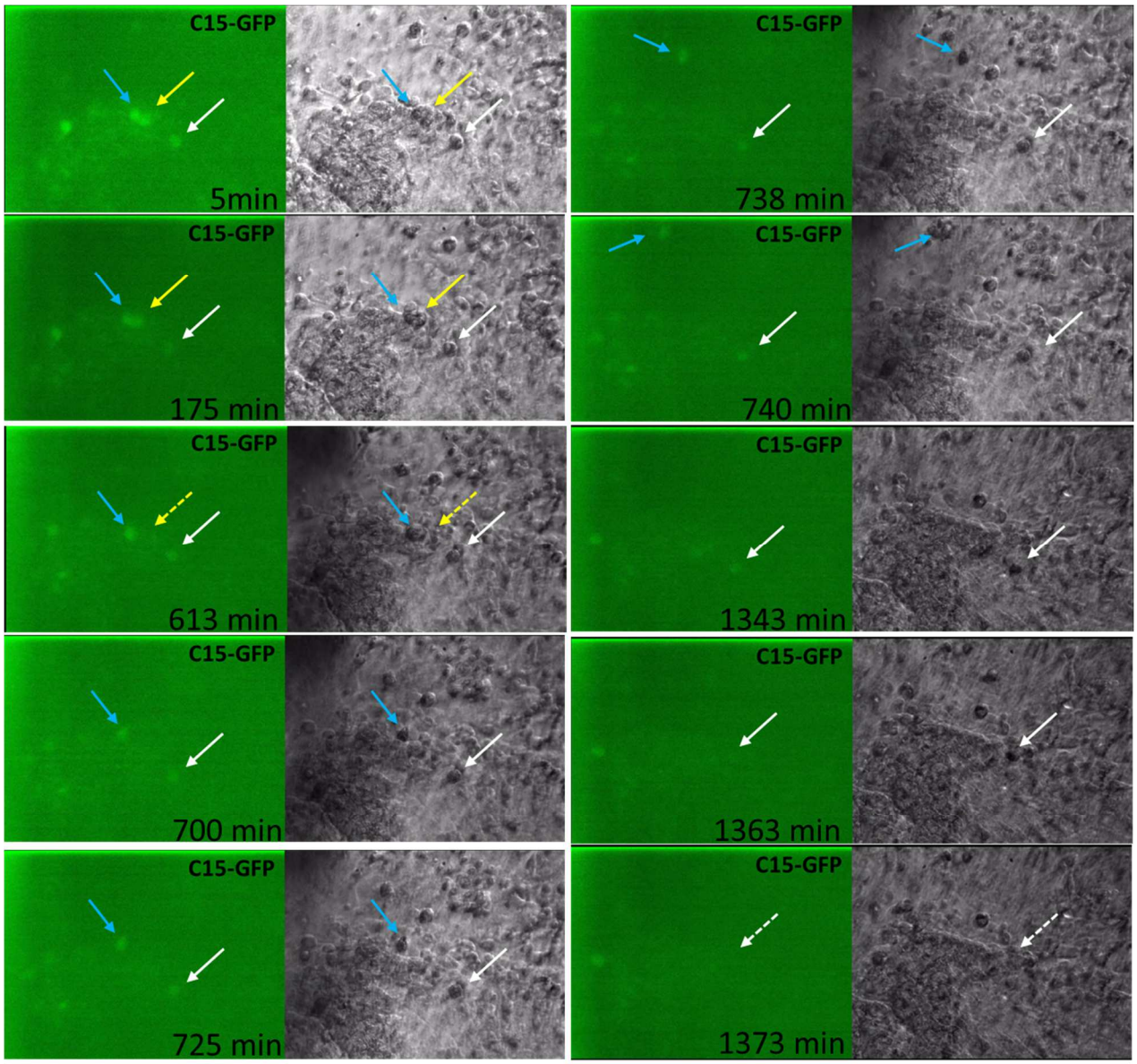
C15-GFP
5min
C15-GFP
738 min
C15-GFP
175 min
C15-GFP
740 min
C15-GFP
613 min
C15-GFP
1343 min
C15-GFP
700 min
C15-GFP
1363 min
C15-GFP
725 min
C15-GFP
1373 min

Figure 3-2. RV-C15-infected cells are shed from intact respiratory epithelium *in vitro*. HBEC-ALI cultures were infected for 18h with RV-C15 that expresses GFP during replication (C15-GFP, green) and fluorescently (Left, green images) or phase-contrast (Right, grayscale images) imaged ever 10-15 min for 30h. Individually shed cells are labeled with colored arrows for differentiation (blue, yellow, and white). Dotted arrows indicate position of shed cell in previous frame. Original magnification: 20x.

Figure 3-3

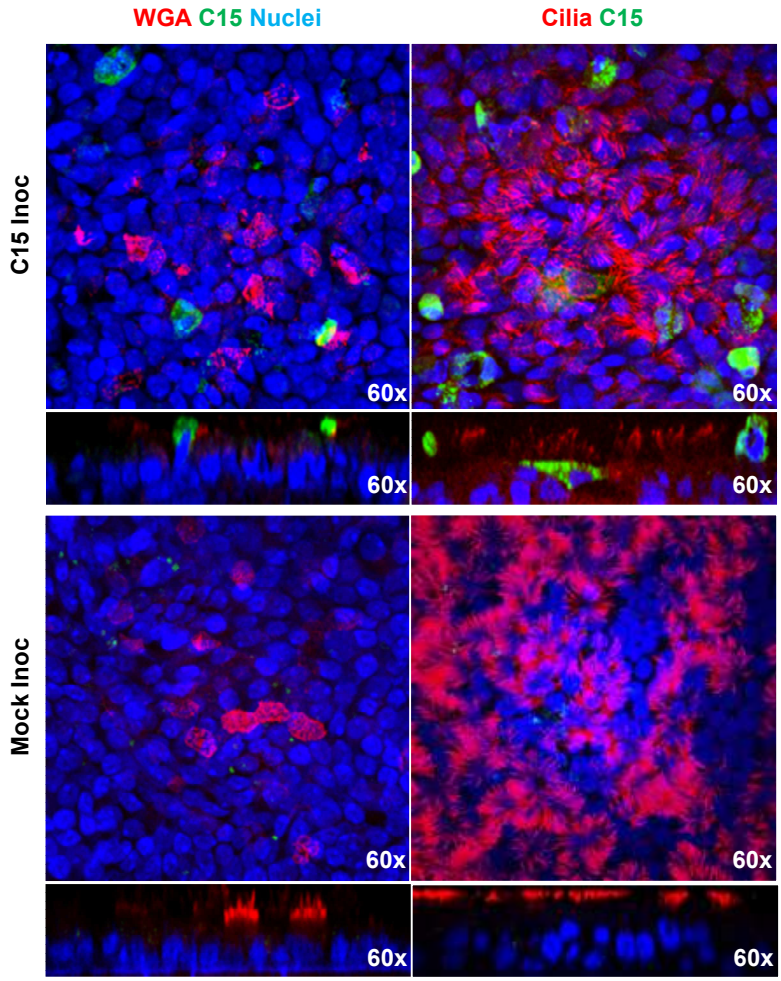
WGA C15 Nuclei
Cilia C15
C15 Inoc
Mock Inoc
60x
60x
60x
60x
60x
60x
60x
60x

Figure 3-3. Analysis of RV-C15 infectivity by immunofluorescent staining. HBEC-ALI cultures were infected for 18h with RV-C15 and imaged apically and z-stacked orthogonally by confocal microscopy. Secretory and ciliated cells were stained with WGA and rabbit polyclonal antibody against aat, respectively (false color red), RV-C15 capsid stained with monoclonal antibody (false color green), nuclei stained with Syto-13 (false color blue).

Figure 3-4

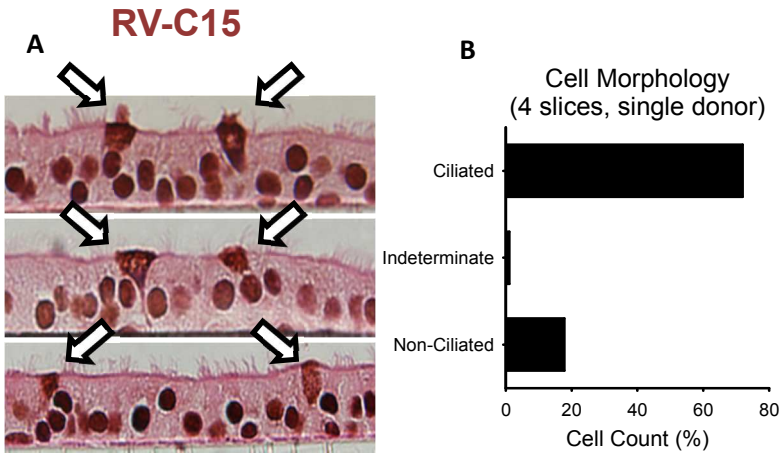
RV-C15
A
B
Cell Morphology
(4 slices, single donor)
Ciliated
Indeterminate
Non-Ciliated
0
20
40
60
80
Cell Count (%)

Figure 3-4. Immunohistochemical analysis of RV-C15 infectivity in HBEC-ALI cultures. HBEC-ALI cultures were infected for 18h with RV-C15, immunohistochemically stained for RV-C15 capsid, and imaged by light microscopy. RV-C15 capsid (brown, arrows [A]). Dark nuclei staining is nonspecific, secondary to incomplete nuclear peroxidase blockade. (B) Graph is representative of the quantification of infected cells from 4 membrane slices from a single donor.

minority were either non-ciliated or indeterminate (Figure 3-4B). Interestingly, the cilia of C15+ cells also stained positive for RV-C15 capsid protein, while the cilia of adjacent, uninfected cells did not.

Next, we performed a single cell analysis of C15 infection with markers of airway epithelial cell subsets. Differentiated epithelial cell cultures were inoculated (18 h) with RV-C15, and then single cell suspensions were analyzed for markers of ciliated or secretory phenotype (Figure 3-5). We consistently observed low frequencies of C15 infection (1.2-1.4% C15+ cells, Figure 3-5). C15+ cells were significantly more likely to be ciliated rather than nonciliated (92% ciliated, $p<0.001$, Figure 3-5A), and 3-4% of the ciliated cell population was C15+. There was no significant difference in C15 staining of nonciliated cells compared to mock-inoculated cells (p-value > 0.05). Analysis of cells stained with WGA further confirmed that secretory cells were not infected with RV-C15 (Figure 3-5B).

Highly differentiated cells are more susceptible to RV-C15 infection.

We consistently observed that highly differentiated cells were more susceptible to RV-C infection[73,311]. Preliminary experiments revealed cells cultured using a different HBEC culture medium (PneumaCult™, Stem Cell Technologies, Vancouver, Canada) had more plentiful ciliated cells[312]. We hypothesized that the greater differentiation of ciliated cells achieved using PneumaCult™ media (PCM) would lead to greater susceptibility to RV-C infection. Thus, we infected HBEC-ALI cells for 18h with either RV-C15 or BEGM alone, stained single cell suspensions with antibodies against viral capsid (C15), aat, or Muc5AC, and analyzed by flow cytometry (Figure 3-6). C15 staining was observed in 6-12% of HBECs differentiated in PCM, which represented a 5-10-fold increased frequency of infected cells compared to cells differentiated in BEGM (Figure 3-6, $p=0.004$). Again, RV-C15 replicated only in ciliated cells, as there was no significant C15 staining of non-ciliated cells or Muc5AC+ cells compared to mock-inoculated cells.

Figure 3-5

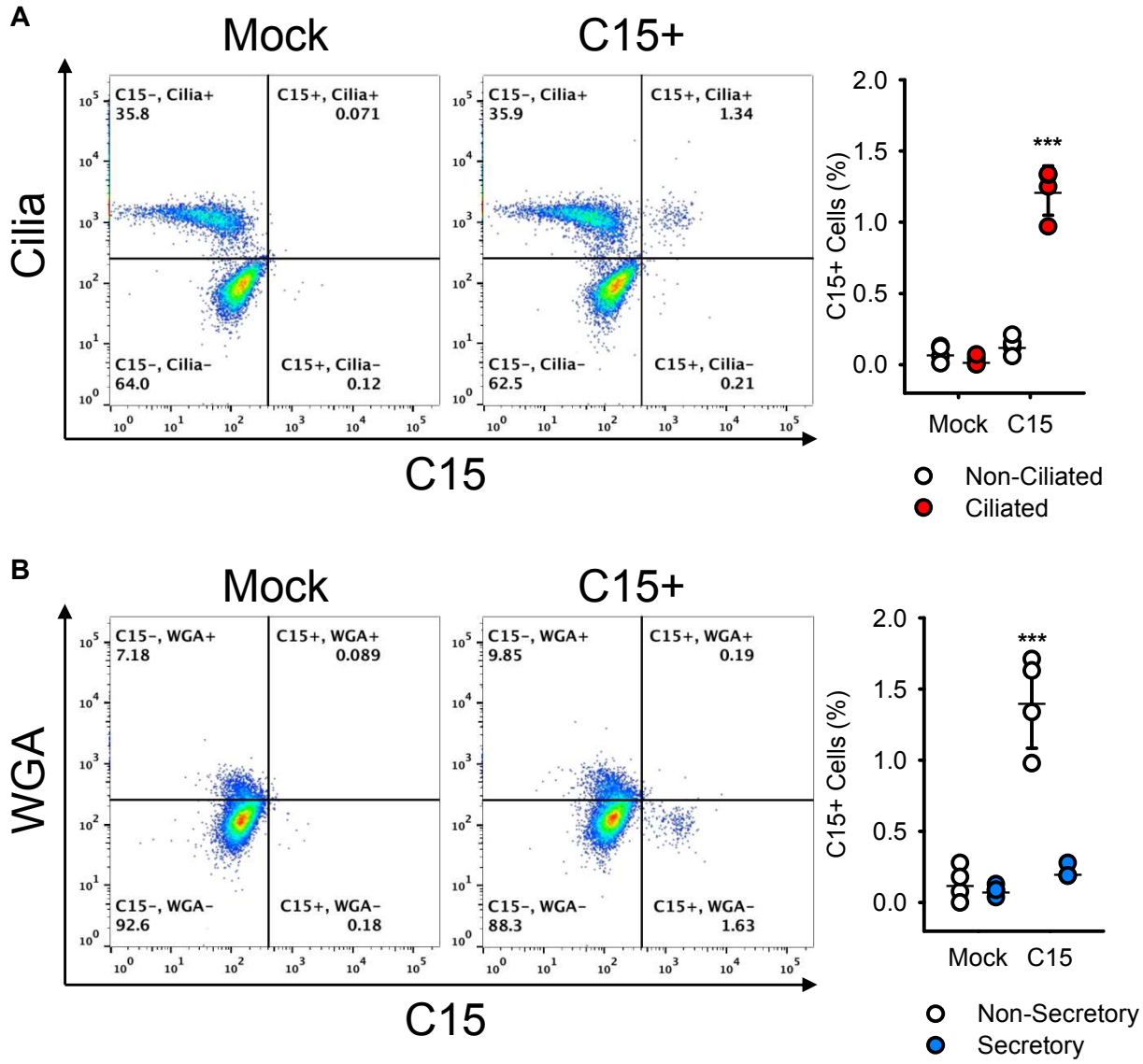
A
Mock
C15+
Cilia
C15
C15−, Cilia+
35.8
C15+, Cilia+
0.071
C15−, Cilia−
64.0
C15+, Cilia−
0.12
C15−, Cilia+
35.9
C15+, Cilia+
1.34
C15−, Cilia−
62.5
C15+, Cilia−
0.21
C15+ Cells (%)
2.0
1.5
1.0
0.5
0.0
***
Mock
C15
Non-Ciliated
Ciliated
B
Mock
C15+
WGA
C15
C15−, WGA+
7.18
C15+, WGA+
0.089
C15−, WGA−
92.6
C15+, WGA−
0.18
C15−, WGA+
9.85
C15+, WGA+
0.19
C15−, WGA−
88.3
C15+, WGA−
1.63
C15+ Cells (%)
2.0
1.5
1.0
0.5
0.0
***
Mock
C15
Non-Secretory
Secretory

Figure 3-5. Single cell analysis of RV-C infection and epithelial cell surface markers. HBEC-ALI cultures infected or mock-infected for 18h with RV-C15 or BEGM alone, respectively, were labeled with antibodies against RV-C15 capsid (C15), and (A) acetylated-alpha-tubulin (aat, Cilia) or (B) fluorescently labeled-WGA (WGA) and analyzed by flow cytometry. Graph is representative of the percentage of C15+ cells quantified by cell type (n=4 independent experiments, two donors). Mock, mock-inoculated cultures; C15, RV-C15-inoculated cultures; Non-Ciliated, aat- cells staining; Ciliated, aat+ cells; Non-Secretory, WGA- cells; Secretory, WGA+ cells. *** indicates p-value < 0.001.

Figure 3-6

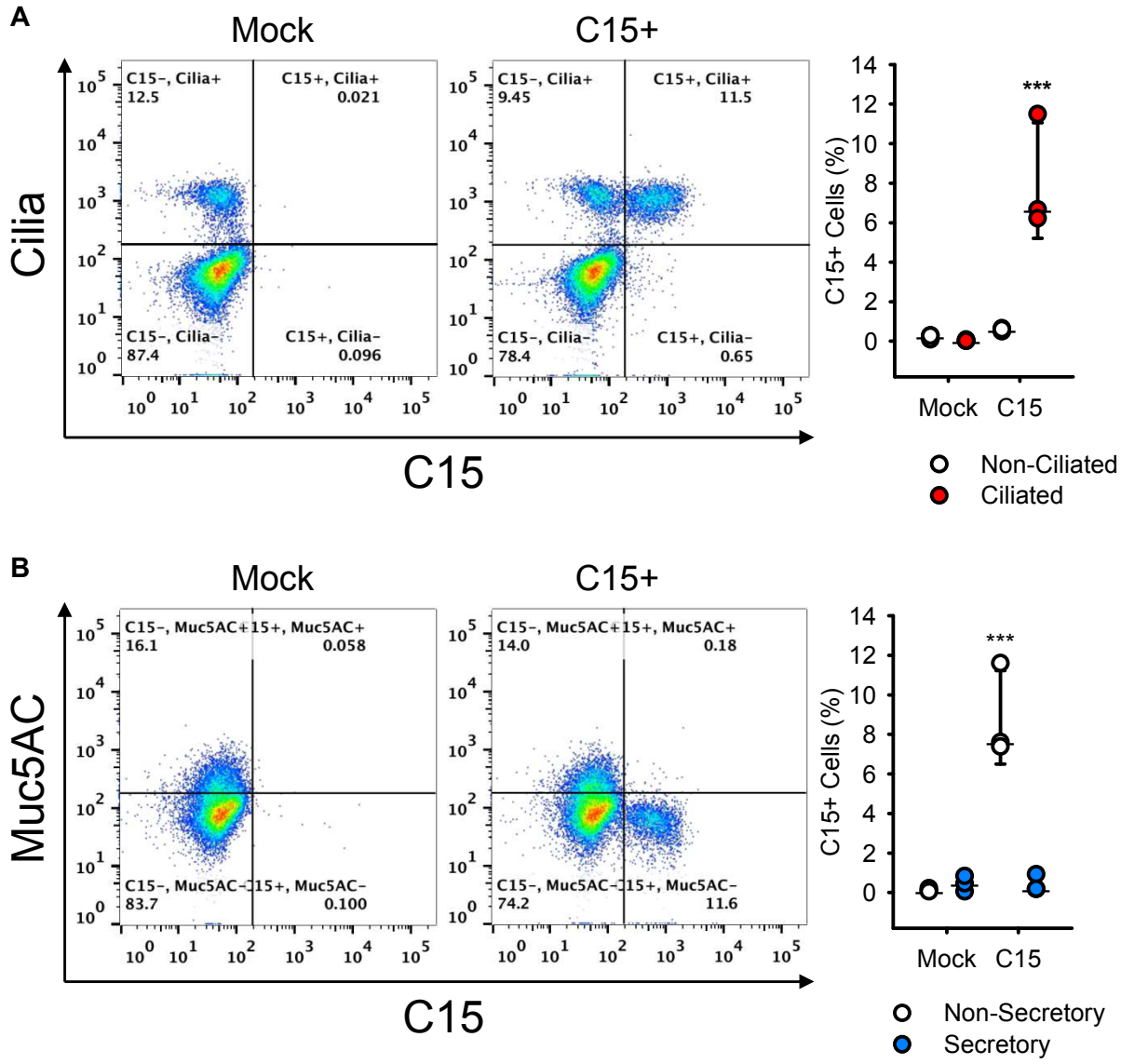
A
Mock
C15+
Cilia
C15
C15−, Cilia+
12.5
C15+, Cilia+
0.021
C15−, Cilia−
87.4
C15+, Cilia−
0.096
C15−, Cilia+
9.45
C15+, Cilia+
11.5
C15−, Cilia−
78.4
C15+, Cilia−
0.65
C15+ Cells (%)
***
Mock
C15
Non-Ciliated
Ciliated
B
Mock
C15+
Muc5AC
C15
C15−, Muc5AC+15+, Muc5AC+
16.1
0.058
C15−, Muc5AC−15+, Muc5AC−
83.7
0.100
C15−, Muc5AC+15+, Muc5AC+
14.0
0.18
C15−, Muc5AC−15+, Muc5AC−
74.2
11.6
C15+ Cells (%)
***
Mock
C15
Non-Secretory
Secretory

Figure 3-6. Highly differentiated cells are more susceptible to RV-C infection. PC-differentiated cultures infected or mock-infected for 18h with RV-C15 or BEGM alone, respectively, were labeled with antibodies against RV-C15 capsid (C15), and (A) aat (Cilia) or (B) muc5ac (Muc5AC) and analyzed by flow cytometry. Graph is representative of the percentage of RV-C15-positive cells quantified by cell type (n=3 independent experiments, two donors). Mock, mock-inoculated cultures; C15, RV-C15-inoculated cultures; Non-Ciliated, aat- cells; Ciliated, aat+ cells; Non-Secretory, muc5ac- cells; Secretory, muc5ac+ cells. *** indicates p-value < 0.001.

Ciliated bronchial epithelial cells express the highest levels of CDHR3.

We recently demonstrated that cadherin-related family member 3 (CDHR3) enabled RV-C entry into normally non-permissive HeLa cells [54]. Replication of C15 in ciliated cells suggested that CDHR3 expression might be restricted to these cells. To test this hypothesis, we analyzed total CDHR3 expression in single cells prepared from differentiated HBEC cultures (Figure 3-7). CDHR3 was expressed mainly by ciliated cells, with 70% of these cells expressing CDHR3 levels above the limit of detection, compared to 19% of the nonciliated population in uninfected cultures (Figure 3-7A and B, triangles).

We then tested whether C15 infection led to a reduction in the CDHR3+ population, perhaps by killing CDHR3-positive cells (Figure 3-7B). RV-C15 inoculation significantly reduced the percentage of CDHR3+ ciliated cells to 58%, but did not significantly reduce the CDHR3+, nonciliated cell population (18%, Figure 3-7B, circles). We followed up this result by examining CDHR3 staining in RV-C15-inoculated and mock-inoculated cultures (Figure 3-7C). C15+ cells contained low levels of total CDHR3, similar to the C15-/CDHR3- (double-negative, DN) population, while a population of uninfected cells stained much brighter for CDHR3. We quantified the relative median fluorescence intensity (rMFI, normalized to non-ciliated cell populations) of CDHR3 per cell population (ciliated vs non-ciliated and C15+ vs C15-) to determine if uninfected, ciliated cells express the highest levels of CDHR3 (Figure 3-6D). C15-, ciliated cells had a CDHR3 rMFI 2.0-2.2 times higher than all other cell populations, regardless of whether the culture was previously inoculated with RV-C15 or BEGM alone (Figure 3-6D, p-value < 0.001). There was no significant difference in CDHR3 rMFI between C15+/ciliated cells and the C15-/nonciliated populations (Figure 3-6D, $p > 0.05$).

Pharyngeal, but not palatine tonsils were susceptible to RV-C15 infection ex vivo.

Having determined that RV-C exclusively targets ciliated respiratory epithelial cells (REC) *in vitro*, we hypothesized that RV-C requires ciliated respiratory epithelial cells for infection *in vivo*. Therefore, we obtained ciliated pharyngeal and non-ciliated palatine tonsils (adenoids and tonsils,

Figure 3-7

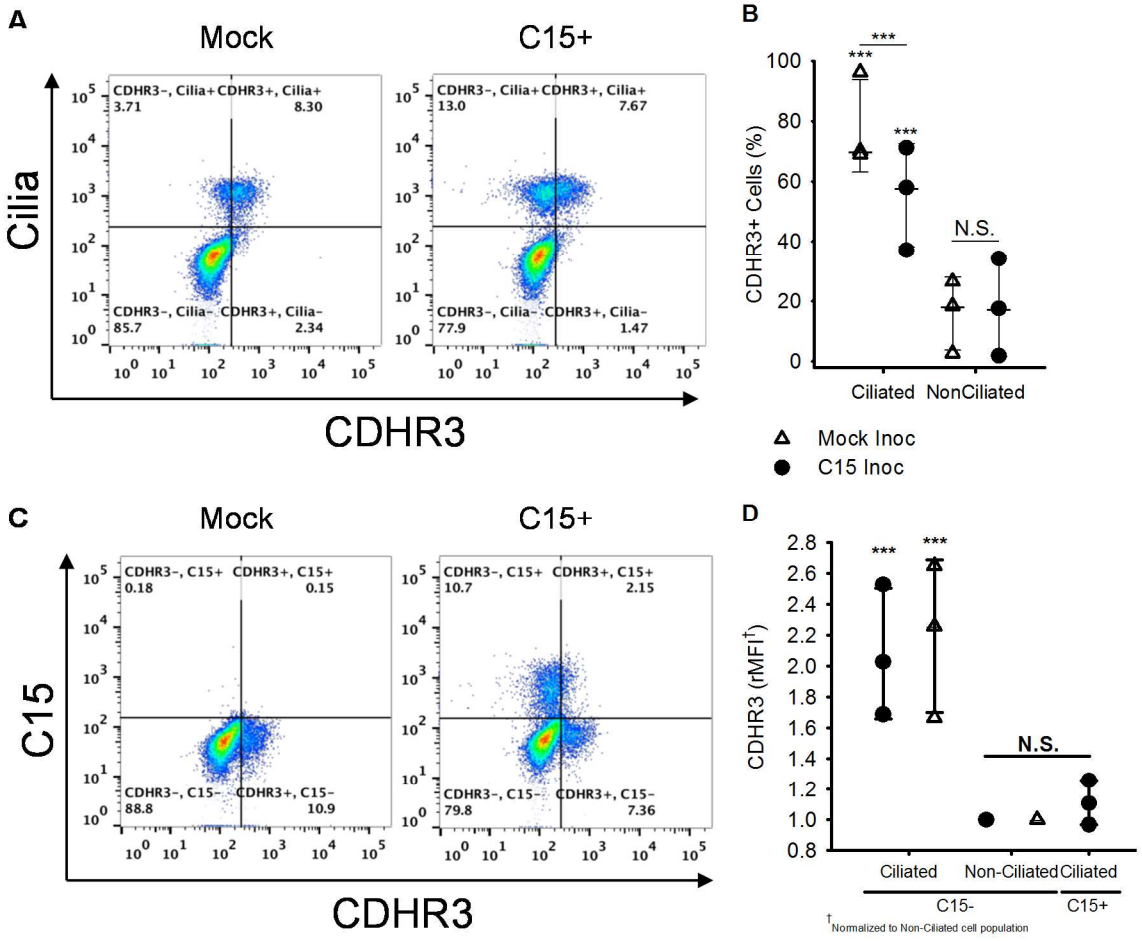
A
Mock
C15+
Cilia
CDHR3
CDHR3−, Cilia+ 3.71
CDHR3+, Cilia+ 8.30
CDHR3−, Cilia− 85.7
CDHR3+, Cilia− 2.34
CDHR3−, Cilia+ 13.0
CDHR3+, Cilia+ 7.67
CDHR3−, Cilia− 77.9
CDHR3+, Cilia− 1.47
B
CDHR3+ Cells (%)
***
N.S.
Ciliated
NonCiliated
Mock Inoc
C15 Inoc
C
Mock
C15+
C15
CDHR3
CDHR3−, C15+ 0.18
CDHR3+, C15+ 0.15
CDHR3−, C15− 88.8
CDHR3+, C15− 10.9
CDHR3−, C15+ 10.7
CDHR3+, C15+ 2.15
CDHR3−, C15− 79.8
CDHR3+, C15− 7.36
D
CDHR3 (rMFI†)
***
N.S.
Ciliated
Non-Ciliated
Ciliated
C15-
C15+
†Normalized to Non-Ciliated cell population

Figure 3-7. CDHR3 is predominantly expressed by ciliated epithelial cells and diminishes following RV-C15 inoculation. PC-differentiated cultures were infected or mock-infected for 18h with RV-C15 (C15+) or BEGM alone (Mock), respectively, were labeled with antibodies against RV-C15 capsid (C15), CDHR3, and aat (cilia) and analyzed by flow cytometry (n=3 independent experiments, two donors). (A) Representative plots of cilia and CDHR3 expression in mock-infected and C15-infected cells. (B) Summary (n=3) of frequency of CDHR3 expression in infected and mock-infected cells. (C) Representative plots of C15 and CDHR3 expression in mock-infected (C) and C15-infected cells. (D) Summary (n=3) of intensity of CDHR3 expression in ciliated and nonciliated cell populations. Values are normalized to the double-negative (DN) population in each experiment. *** and N.S. indicate p-values $\leq$ 0.001 and > 0.05, respectively.

respectively), from adenoidectomies and tonsillectomies (University of Wisconsin, School of Medicine & Public Health, Department of Surgery) and incubated them for 18h *ex vivo* with 1 x 10^8 PFUe of RV-C15 or BEGM alone (mock) (Figure 3-8). We observed intermittently C15-capsid stained cells within adenoidal tissue from a single donor (out of three). C15+ cells were confined to the surface-exposed, respiratory epithelium of the adenoidal culture. No C15+ staining was observed in any palatine tonsil tissue analyzed (three donors).

Figure 3-8

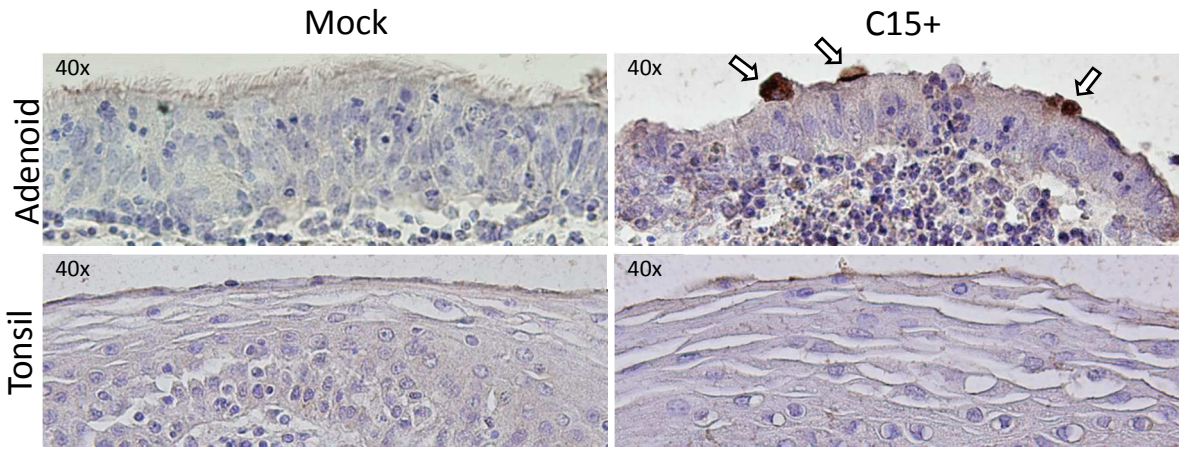

Figure 3-8. Pharyngeal but not palatine tonsils are susceptible to RV-C15 infection *ex vivo*. Pharyngeal (adenoid) and palatine (tonsil) tonsillar *ex vivo* organ cultures were infected for 18h with RV-C15 or BEGM alone, immunohistochemically stained, and imaged by light microscopy. Cells were labeled with monoclonal antibody against RV-C15 capsid (brown, arrows), and counterstained with haematoxylin (blue). Original magnification: 40x. RV-C15+ stain in adenoid is a single observation out of three donors, and RV-C15- tonsil and mock inoculated tissue stains are representative of three donors.

DISCUSSION

Since their discovery in 2006, the RV-C have been identified as important contributors to severe respiratory illness in infants and exacerbations of chronic airway disease, yet very little is known about how they interact with the human host. Here, we demonstrated that the RV-C replicate in ciliated RECs, but not secretory cells. Furthermore, the vast majority and highest levels of CDHR3 protein is expressed in ciliated cells, and its presence in airway epithelium is diminished by RV-C infection. We also present preliminary observations that pharyngeal but not palatine tonsillar epithelium is susceptible to RV-C infection *ex vivo*, indicating that the RV-C may have a different tissue tropism than the RV-A or B.

RV-C targeting of ciliated epithelial cells is consistent with observations for RV-A16, and indicates that RV-C-induced asthma exacerbations are not due to infection of secretory cells, which can be overrepresented in chronically inflamed airways[309,313]. Ciliated RECs have been identified as targets for multiple RNA viruses (e.g. avian influenza virus, coronavirus, RSV, parainfluenza virus, and RV-A), and infections thereof have been correlated to viral receptor expression[298,303,304,309,314–319]. Our data are consistent with this dogma as CDHR3 expression was high and fairly restricted to ciliated cells. The finding that CDHR3 staining is muted in C15-infected cells could represent viral shutoff of host protein synthesis, or may be a result of CDHR3 downregulation following internalization of the virus/receptor complex. On the other hand, our finding that some ciliated cells with high levels of total CDHR3 were not infected following high-MOI infections with RV-C15 may indicate the presence of unidentified cofactors or specific cellular properties required for RV-C binding or entry. Many viruses either utilize co-receptors or have cofactors that facilitate cellular binding. Poliovirus, for example, utilizes bacterial polysaccharides to increase the kinetics of binding to its host cells in the gut[320,321]. Alternatively, this cell population may be protected from RV-C infection due to diminished apical surface presentation of CDHR3 or reduced exposure of lateral membranes (a common location for intracellular cadherins) to viral particles[256]. Taken together, while CDHR3 is present in high concentrations on the majority of

ciliated RECs and diminishes following infection, other factors may play a role in augmenting RV-C binding and entry into these cells.

While our data indicate that CDHR3 expression is necessary for RV-C susceptibility in primary airway epithelial cells, other properties specific to the ciliated cell may promote RV binding or entry. For example, RV-A16 has been shown to primarily target ciliated cells, even though ICAM-1 is also expressed on some nonciliated cells[309]. Also, 40nm, virus-sized nanoparticles adhere to motile cilia *in vitro*, demonstrating a nonspecific mechanism for viral adhesion to ciliated cells[322]. These findings suggest that RV may adhere to cilia to facilitate cell entry. Whether it is receptor expression or localization, or properties intrinsic to the ciliated cell, further studies are needed to elucidate the mechanism of RV binding to and entry into its biologically relevant host cell.

The speckled pattern of RV-C15 infected RECs is consistent with what has been observed for RV-A16[309]. The shedding of infected cells, perhaps before the virus is able to spread to surrounding cells, could contribute to the patchy distribution of infection. The resulting gaps in the epithelium could impair barrier function and facilitate bacterial superinfection, which can lead to more severe RV illnesses [9,10,290,291]. These effects have been noted following Influenza A infections *in vitro*[323]. Taken together, the RV-C likely infect the host epithelium similarly to the RV-A, induce cell-shedding, and leave behind damaged epithelia that may support superinfections by other pathogens.

Finally, our *ex vivo* tissue inoculations indicate that RV-C infection is likely limited to highly-ciliated, respiratory epithelium *in vivo*. Analysis of gene expression on multiple normal human tissues using microarray data stored on the NCBI Gene Expression Omnibus indicates low-to-undetectable levels of CDHR3 on the palatine tonsils and greater expression in the trachea and the lungs[324]. These findings are in contrast to what has been observed for the RV-A and B, as the major group receptor, ICAM-1, has been localized to the palatine tonsils and evidence of RV-A and B infection in this tissue has been demonstrated previously[324–330]. These findings suggest that the tissue distribution of RV-C *in vivo* could differ from that of other RV species.

There are two limitations that should be considered in interpreting these findings. First, the only available anti-CDHR3 monoclonal antibody binds to an intracellular epitope, which prevented a discrete quantification of CDHR3 displayed on the cell surface, where it is putatively accessible to virus. Secondly, our experiments involved cultured cells and tissues, and additional studies are needed to map the distribution of RV-C infection *in vivo*.

In conclusion, our findings establish that RV-C primarily infects ciliated RECs throughout the airways, and that expression of CDHR3 is largely restricted to these cells. These findings provide a foundation for studying RV-C entry mechanisms into their primary host cell, establish a more robust *in vitro* model of RV-C infection, and suggest that factors that regulate CDHR3 expression or differentiation of ciliated cells may influence susceptibility to RV-C infection in vivo. These findings also suggest that tissue tropism may vary with RV species, and could be related to differences in patterns of clinical illness. Our work thus fills in multiple crucial knowledge gaps in the pathogenesis of the RV-C with the ultimate goal of fully understanding their biology and interactions with the human host.

CHAPTER FOUR

Summary, Conclusions, and Future Directions

SUMMARY AND CONCLUSIONS

In order to better understand RV-C biology and its interactions with the human host, the studies undertaken in this dissertation focused on methods for improving the purification of infectious viral materials, of which standard protocols fell short of isolating, required for basic virology. These techniques enabled us to define some basic characteristics of the viral capsid. Finally, we identified the RV-C cellular and tissue tropism and how these features relate to the expression of CDHR3 in various epithelial cell subsets. When considered together, these studies represent an important advance in our understanding of virus/host interactions, and provide the foundation for additional mechanistic studies of RV-C structure, binding, and cell entry.

The work in Chapter 2 focused on solving the problem of obtaining purified preparations of multiple infectious RV-C clones suitable for multiple experimental needs. Due to poor yields following high-speed centrifugation through a sucrose gradient, we hypothesized that some RV-C capsids were intrinsically less stable than those of RV-A16 and RV-C15, explaining why infectious material was lost following completion of the purification procedure. We thus conducted experiments to identify sources of instability in the RV-C41 and RV-C2 capsids, as compared to the easily purified RV-A16 capsid.

We demonstrated that the addition of nonfat dry milk (NFDM) to 30% sucrose cushions improves yield of all RV-C isolates studied (Figure 2-3). This interesting finding seemingly supported our instability hypothesis, as the data suggested that NFDM has a stabilizing effect on viral capsid, which was corroborated by previously published findings on the stabilizing effect of whole milk on the FMDV capsid subjected to thermal stress[285]. However, our data showed that the RV-C41 capsid is no less stable under hyperosmotic or thermal stress when compared to the RV-A16 capsid, thus refuting our hypothesis that the RV-C41 capsid is intrinsically less stable than capsids of other RV types. Interestingly, we did find that RV-C41, C2, and C15 capsids are all slightly more sensitive to low pH than the RV-A16 capsid (Figures 2-4, 5). This may have important implications for viral entry and uncoating, as the release of

vRNA into the cytoplasm is often mediated by drops in endosomal pH following entry[133]. We therefore suspect that the penetration of RV-C vRNA into the host cell cytoplasm may occur by a different mechanism or in a different cellular compartment than previously studied RVs.

Since the C41 capsid stability was similar to RV-A16, we then considered that some RV-C capsids may form tight aggregates and adhere to material surfaces, thus leading to difficulties with resuspension. We further suspected that centrifugal force increased the interaction of virus particles with each other and material surfaces, thus increasing the likelihood of aggregation and adhesion. To test this hypothesis, we analyzed the total protected virus material from the bottom of ultracentrifuge tubes following centrifugation of infected cell lysates, and determined that all input virus was indeed isolated from this location. Thus, we concluded that the loss of RV-C41 and C2 infectivity was not due to capsid instability, but an inability to overcome aggregative or adhesive forces that were preventing the efficient resuspension of purified virions. We concluded the study by demonstrating that the highest levels of purified RV-C can be obtained by growth (following transfection) in Wis.L cells, followed by purification under a reduced centrifugal force and increase spin-time procedure. Our revised protocol produces high levels of all three C types that were tested.

The studies presented in Chapter 3 focused on the identification of the cellular target of the RV-C, and how CDHR3 expression correlated with viral infectivity. We also conducted experiments to define the location of susceptible tissues in the upper airways. While no studies investigating RV-C cellular tropism have been published, results of studies regarding the cellular targets for the RV-A and B have been conflicting. However, a recent study conclusively determined that RV-A16 replicates in ciliated airway epithelial cells, therefore we tested the hypothesis that ciliated cells are also the primary target for the RV-C[309]. To test this hypothesis, we used a monoclonal antibody directed against the RV-C capsid protein VP2, received from MedImmune, and refined techniques for culturing RV-C in differentiated cultures of primary airway epithelial cells. We then tested the colocalization of infected cells with phenotypic markers of either ciliated or secretory respiratory epithelial cells and also with

CDHR3 in qualitative (immunofluorescence, immunohistochemistry) and quantitative (flow cytometry) assays. Our study is the first to identify that the ciliated cell is the exclusive cellular target for the RV-C in airway epithelial cell cultures, and further showed that the majority and highest expression of CDHR3 is expressed in ciliated cells. Our findings corroborate our recently published data that CDHR3 expression is required for cell susceptibility to the RV-C[54]. We also included preliminary data that pharyngeal, but not palatine tonsillar epithelium is susceptible to RV-C infection *ex vivo*, both tissues having previously been found susceptible to members of the RV-A and B, and that RV-C infection leads to the shedding of infected cells, a finding that has only been concretely reported for the RV-A16 isolate[58,306,309,331,332]. Our data indicate that RV-C likely targets ciliated respiratory epithelial cells due to high levels of CDHR3 expression, leading to cellular shedding that might be related to mechanisms of transmission and/or viral clearance.

REMAINING QUESTIONS AND FUTURE DIRECTIONS

The isoelectric point of the RV-C capsid

As the major conclusion from Chapter 2 is that the RV-C have a propensity for aggregation and adhesion that prevents their resuspension following high-speed spin, as well as an increased sensitivity to drops in pH that may alter the kinetics of genome delivery, it would be interesting and important to determine the isoelectric point (pI) of multiple RV-C capsids. A protein's pI is the point at which positive and negative surface charges are balanced, creating an overall neutral particle that has increased self-aggregative properties and a propensity to adhere to hydrophobic surfaces. Our findings suggest that the RV-C have an increased propensity to aggregate along with an increased sensitivity to low pH, and this could be secondary to a distinct capsid pI compared to other species of RV. In support of this hypothesis, poliovirus aggregation and adhesion is enhanced by low-pH buffers and groundwater that support the generation of electrically neutral virus particles[287,333]. Furthermore, multiple isolates of RV utilize

endosomal acidification to initiate capsid structural changes and melting with the endosomal membrane following the formation of an electrically neutral particle. The pI likely relates directly to these processes for genome delivery. While the pI has been determined for multiple vaccine strains of poliovirus, it is only known for a single isolate of minor group RV[334,335]. An understanding of the pI of the RV-C could provide insight into genome delivery, optimized purification and storage buffers, and even transmission characteristics.

To test this hypothesis, we need to analyze the pI of purified RV-C particles. Isoelectric focusing is the process by which proteins are run through a substrate holding a pH gradient, and separated based on charge, similar to SDS-PAGE. When a protein reaches the pH that matches its pI, it will assume a neutral net charge and cease migration. Thomassen *et al* published a novel method of focusing intact poliovirus particles by capillary isoelectric focusing with whole column imaging detection (CIEF-WCID), which involves focusing virus particles in a long capillary tube followed by imaging of the entire tube to prevent pI distortions from substrate mobilization[334]. By employing this method, the pI of multiple RV isolates can be determined, giving us further insight into the biochemistry of RV capsid disassembly and aid in the tailoring of future genotype-specific RV purification and storage protocols that will minimize aggregation and adhesion forces.

The effect of inhibitors of endosomal acidification on RV-C entry

As an increased sensitivity of the RV-C capsid to low pH was a secondary finding in Chapter 2 that did not play a role in loss of materials during purification, we did not pursue further studies down this route. However, this difference in pH sensitivity likely has large implications for viral entry mechanisms, tissue tropism, and even transmission. Many picornaviruses require endosomal acidification to promote the penetration of vRNA into the host cell cytoplasm, RV is no different[133]. The level of endosomal acidification that a viral capsid either requires or is able to withstand dictates at which compartment in the

cell the genomic payload is released[336–338]. Our results support the hypothesis that RV-C likely requires very minimal endosomal acidification prior to genomic penetration, because the viral capsid requires very little acid stimulus to form an unstable particle (Figure 2-4, 5). It would be interesting thus to answer this hypothesis by observing whether or not inhibition of endosomal acidification, perhaps by the experimental addition of lysosomotropic weak bases, carboxylic ionophores, or inhibitors of vacuolar H+-ATPases, would affect the compartment at which RV-C releases its genome *in vitro* (HeLa or HBEC-ALI cultures), and also to observe whether or not there is an effect on tissue tropism as well (*ex vivo* organ cultures)[339].

Any change in the RV life cycle or tropism following the inhibition of endosomal acidification would be valuable information, as inhibitors of endosomal acidification are being pursued for the treatment of other viral infections and may augment RV infections[339]. I hypothesize that we might see a change in cellular tropism because different cell types in the respiratory tract may have different rates and pH targets for endosomal acidification, which would implicate endosomal pH as a RV-C restriction factor[340]. I mention transmission as well, as virus particles that are highly sensitive to acid inactivation will require extra measures for protection when traveling through the gastrointestinal tract, such as a heavy coat of respiratory mucus, thus adding an extra level of complexity to the evolution of RV transmission.

Epithelial cell localization of CDHR3

In Chapter 3, we colocalized high levels of total CDHR3 staining to ciliated respiratory epithelial cells and thus concluded that the major reason why these are the cellular target for the RV-C is due to restriction of CDHR3 expression to the ciliated cell compartment. However, following high MOI infections, we also observed a subset of ciliated cells that expressed very high levels of CDHR3 but remained RV-C15-negative (Figure 3-7). The most likely explanation of this phenomenon is the

restriction of CDHR3 to cellular compartments that were not readily exposed to virus particles (e.g. cellular adherens junctions). Because the anti-CDHR3 antibody used in our experiments stained an intracellular epitope on CDHR3 and our staining procedure involved cell permeabilization, we measured total cellular CDHR3, regardless of cellular localization. An important follow up to our study would be to examine CDHR3 localization, ideally by utilizing an antibody that stains an extracellular epitope of CDHR3. These experiments could determine whether or not CDHR3 localization on the cell surface determines susceptibility to RV-C infection.

Furthermore, while CDHR3 surface staining should be quantified by flow cytometry, it needs to be examined in intact, respiratory epithelial cell sections. This is because CDHR3 is an intercellular cadherin, with the putative function of tethering adjacent cells together or to the basement membrane, and relaying signals to and from its derived cell. Conversion of intact epithelia to single-cell suspensions likely abolishes the physiologically relevant location of CDHR3 on the cellular surface, and may even result in its down-regulation. Analysis of thin, formalin-fixed, paraffin-embedded respiratory epithelial sections would preserve the structure and localization of CDHR3 well for the subsequent detection by the monoclonal anti-CDHR3 antibody used in our experiments, allowing us to answer the question of whether or not CDHR3 is more accessible to virus particles in some cell populations than others, or in diseases such as asthma with defective epithelial barrier function.

RV-C susceptible lower airway tissues and the effect of MCM on tissue susceptibility

The ultimate goal of the work from Chapter 3 was to determine not only the cellular target of the RV-C, but also the tissue tropism along the airways. Due to issues with sample acquisition, we were not able to analyze susceptible tissues in the lower respiratory tracts of humans, which would provide a very interesting insight into RV-C pathology. Our finding that ciliated cells are the main target of the RV-C suggests that susceptible airway tissues follow the spread of ciliated epithelium from the sinuses to the

respiratory bronchioles. However, the morphology of the ciliated cell progressively changes in more distal airways, which may affect virus-host cell interactions. To test these hypotheses, *ex vivo* organ cultures representative of different regions of the lower respiratory tract could be inoculated with RV-C15 and assessed by either qPCR for virus replication or immunohistochemistry to correlate cell morphology to infectivity, similar to our analysis of pharyngeal and palatine tonsils in Chapter 3 (Figure 3-8).

Furthermore, it would be interesting to compare the RV-C susceptibility of lower airway tissues that possess notable mucus cell metaplasia (MCM) with normal matched controls, as our studies indicate that epithelia with notable MCM should be less susceptible to infection by the RV-C, due to a decrease in the susceptible ciliated cell population. While examining the effect of MCM on RV-C infection in *ex vivo* organ cultures is desirable, it is a difficult experimental design. Not only are lower airway tissues difficult to acquire, they are also usually from healthy donor lungs that would not have any signs of MCM or other respiratory pathology. Thus, in order to test the hypothesis that MCM may protect against RV-C infection, one can culture airway epithelial cells exposed to IL-13 +/- IL-9 to induce MCM and the hypersecretion of mucins with donor matched control cultures[308,309]. Susceptibility to RV-C could then be measured as described in Chapter 2, or fluorescent microscopy and immunohistochemistry as described in Chapter 3. The results of these studies would provide insight into whether or not MCM plays a role in heightening or controlling the severity of RV-C infections in asthma.

The effect of RV species and genotype on infected cell shedding and bacterial transmigration

We observed that RV-C15 infection leads to infected cell shedding. This observation is notable, because previous studies have indicated that bacterial colonization of and transmigration through epithelia is related to disruption of epithelial barrier integrity[323]. For example, RV-39 infection breaks down the tight junctions between cells, allowing for increasing bacterial migration paracellularly, while influenza A virus destroys cells *in situ* and promotes rapid transmigration of cocultured bacteria[323]. RV infections

can promote bacterial superinfections[9,10,14,290]. Few studies in the literature have assessed RV cytopathogenic effects (CPE) *in vivo* or *in vitro* or observed significant shedding of infected cells[309,323,341]. Thus, our finding that RV-C15 leads to the shedding of intact, infected cells could contribute a mechanism for the initiation of bacterial superinfections, and perhaps affect the RV lifecycle as well. Based on published data of species effects on illness severity, I hypothesize that isolates of the RV-A and C are more likely to lead to infected cell shedding than those from the RV-B[41,46].

To test this hypothesis, one could inoculate *in vitro* airway cultures with isolates of the RV-A, B, and C that express GFP upon replication and perform time-lapse fluorescent imaging over the course of 18-24h in a humidified chamber. The data obtained can then be used to compare the kinetics, densities, and quantities of cell shedding between the RV isolates studied. Once this initial experiment is optimized, it can then be combined with apical bacterial co-culture techniques to examine the effect of bacterial colonization and transmigration following inoculation with different genotypes of RV[323]. Bacterial transmigration can then be measured by the serial, time-lapse inoculation of plates containing bacterial growth media with cell media from the basal chamber of the airway culture. I predict that airway cultures inoculated with the RV-A or C would have the quickest increase in bacterial contamination of the basal media chamber, than those inoculated with the RV-B, supporting the hypotheses that not only do the RV-A and C disrupt the epithelial barrier to a higher degree than do the RV-B, but also that a larger disruption promotes higher levels of bacterial colonization and transmigration.

The interaction of RV-C with cilia

While the conclusion of Chapter 3 is that ciliated cells are targeted by the RV-C due to high levels of expression in and the restriction of CDHR3 to this cell population, other properties of the ciliated cell could also promote RV binding and entry. This hypothesis is supported by our own data that not all

cell populations that express high levels of CDHR3 were infected by RV-C15, and data from a recent publication indicating that while ICAM-1 expression is not restricted to ciliated cells, RV-A16 still targets this cell population over all others (Figure 3-7)[309]. Conceptually, the large divergence in capsid evolution leading to a change in receptor specificity between the major group RVs and the RV-C could have just as easily retargeted RV isolates to non-ciliated cells, if cell tropism was solely a function of cell-entry receptor expression, and we know this is not the case[309]. Furthermore, studies of avian influenza virus infection of human airway cells indicate that the virus can be retargeted between secretory and ciliated cells with simple alterations in sialic acid receptor specificity, however only robust replication can occur following the infection of secretory cells, indicating a cellular preference unrelated to receptor expression[301,298,302]. Taken together, these findings indicate that the ciliated respiratory epithelial cell provides more than a cell entry receptor to promote progression of RV through its life cycle.

Recently, German investigators examined the interaction of virus-sized nanoparticles with motile respiratory cilia in the absence of mucus, and found that cilia have a propensity to non-specifically adhere to 40-nm particles[322]. They further noted that particle interaction resulted in an increased ciliary beat frequency, indicating a signaling mechanism that results in a highly responsive ciliary axoneme. Combining these findings with our own leads to the generation of the following hypothesis: the RV bind nonspecifically to host cell motile cilia prior to cell entry to increase the kinetics of cell entry. Virus "surfing" along the plasma membrane of host cells prior to cell entry has been documented previously[342]. These findings suggest that RV may bind motile cilia to quickly move through the secreted mucus barrier, down the ciliary axoneme, and reach plasma membrane locations that are conducive to the initiation of cell entry. Movement could easily be generated from the usurpation of intraflagellar transport (IFT) mechanisms that are normally used to carry IFT-particle cargos from the cytoplasm to the ciliary tips and back[343].

The first step to test this hypothesis is to determine whether or not RV will bind to motile cilia. The approach to test this hypothesis could center on a conserved endogenous mechanism of ciliary

autotomy. In brief, ciliary autotomy is the process by which incubation in the presence of high levels of calcium will promote the excision of motile cilia from the cell by the endogenous enzyme centrin[344]. The first experiment involves incubation of ciliated cells in suspension with buffers that promote deciliation, followed by inoculation with RV at room temperature, thus inhibiting any cell entry processes. In theory, this would provide a competitive environment for viral binding to either dissociated cilia or cells, which could then be easily separated by full-speed spinning on a benchtop centrifuge. The ciliary and cell fractions can then be analyzed for virus particle binding by either immunological or qPCR methods. An issue with this method would be normalizing fluid volumes and substrate surface areas, as the virus particles that are not binding substrate will remain in the fluid/cilia fraction, and cells have a substantially larger binding surface area than do cilia, respectively. Another method to test the role of cilia would be to use two intact airway epithelial cell cultures and incubate one in deciliation buffer. After waiting 24h to account for any off-target effects to diminish, inoculate each culture with RV and measure any alterations in virus binding, replication, or cellular target by PCR and immunological methods. This experiment is limited in that it cannot be easily used to determine whether or not RV directly binds motile cilia to promote cell entry, as the analysis is directed at viral replication, furthermore any decreases in viral replication in the deciliated cultures may be due to nonspecific effects of the treatment.

If in fact RV binds to cilia, the next step would be to determine whether or not virus particles can transit along the motile cilia prior to cell entry. This experiment is much more difficult to setup, but would likely involve the use of fluorescently-labeled virus particles and imaging of live-cells embedded in a viscous matrix to prevent ciliary movement. Indirect evidence of viral surfing down motile cilia could be achieved by selectively inhibiting components of IFT either with small molecule inhibitors or siRNA[344]. If these hypotheses are proven correct, and RV indeed binds to cilia prior to cell entry, we will have provided an extremely novel update to the mechanics of RV entry into its target host cell.

In conclusion, multiple questions were raised throughout the course of this work that could further our understanding of RV molecular biology and interactions with the host. The development of a

revised protocol allowing for the purification of all cloned RV-C isolates provides the tools needed for future studies of structural and replicative processes. The greater sensitivity of RV-C to low pH may indicate related alterations in cell entry and genome penetration processes. Finally, our finding that ciliated cells are the main target of the RV-C opened up a series of questions ranging from the function of MCM in the context of RV-C infection, to the role and localization of CDHR3 in respiratory epithelium, and to whether or not the RV utilize motile cilia adhesion to promote host cell targeting and entry. This work fills crucial knowledge gaps in our understanding of RV structural and anatomical biology, and provides the foundations for future studies that could eventually lead to the control of the most common human respiratory pathogen.

REFERENCES

1. Fokkens, W. J. *et al.* European Position Paper on Rhinosinusitis and Nasal Polyps 2012. *Rhinol. Suppl.* 3 p preceding table of contents, 1–298 (2012).
2. Johnston, S. L. *et al.* Community study of role of viral infections in exacerbations of asthma in 9-11 year old children. *BMJ* **310,** 1225–1229 (1995).
3. Friedlander, S. L. & Busse, W. W. The role of rhinovirus in asthma exacerbations. *J. Allergy Clin. Immunol.* **116,** 267–273 (2005).
4. Miller, E. K. *et al.* Rhinovirus-associated hospitalizations in young children. *J. Infect. Dis.* **195,** 773–781 (2007).
5. Brownlee, J. W. & Turner, R. B. New developments in the epidemiology and clinical spectrum of rhinovirus infections. *Curr. Opin. Pediatr.* **20,** 67–71 (2008).
6. Peltola, V. *et al.* Rhinovirus transmission within families with children: incidence of symptomatic and asymptomatic infections. *J. Infect. Dis.* **197,** 382–389 (2008).
7. Gern, J. E. The ABCs of rhinoviruses, wheezing, and asthma. *J. Virol.* **84,** 7418–7426 (2010).
8. Cox, D. W. *et al.* Human rhinovirus species C infection in young children with acute wheeze is associated with increased acute respiratory hospital admissions. *Am. J. Respir. Crit. Care Med.* **188,** 1358–1364 (2013).
9. Bosch, A. A. T. M., Biesbroek, G., Trzcinski, K., Sanders, E. A. M. & Bogaert, D. Viral and Bacterial Interactions in the Upper Respiratory Tract. *PLoS Pathog* **9,** e1003057 (2013).
10. Jakab, G. J. Mechanisms of bacterial superinfections in viral pneumonias. *Schweiz. Med. Wochenschr.* **115,** 75–86 (1985).
11. Heikkinen, T. & Järvinen, A. The common cold. *Lancet* **361,** 51–59 (2003).
12. Leder, K., Sinclair, M. I., Mitakakis, T. Z., Hellard, M. E. & Forbes, A. A community-based study of respiratory episodes in Melbourne, Australia. *Aust. N. Z. J. Public Health* **27,** 399–404 (2003).
13. Grüber, C. *et al.* History of respiratory infections in the first 12 yr among children from a birth cohort. *Pediatr. Allergy Immunol. Off. Publ. Eur. Soc. Pediatr. Allergy Immunol.* **19,** 505–512 (2008).
14. Mäkelä, M. J. *et al.* Viruses and bacteria in the etiology of the common cold. *J. Clin. Microbiol.* **36,** 539–542 (1998).
15. Monto, A. S. Epidemiology of viral respiratory infections. *Am. J. Med.* **112 Suppl 6A,** 4S–12S (2002).
16. Simmonds, P. *et al.* Proposals for the classification of human rhinovirus species C into genotypically assigned types. *J. Gen. Virol.* **91,** 2409–2419 (2010).
17. Gwaltney, J. M., Hendley, J. O., Simon, G. & Jordan, W. S. Rhinovirus infections in an industrial population. I. The occurrence of illness. *N. Engl. J. Med.* **275,** 1261–1268 (1966).
18. Passioti, M., Maggina, P., Megremis, S. & Papadopoulos, N. G. The common cold: potential for future prevention or cure. *Curr. Allergy Asthma Rep.* **14,** 413 (2014).
19. Jacobs, S. E., Lamson, D. M., St. George, K. & Walsh, T. J. Human Rhinoviruses. *Clin. Microbiol. Rev.* **26,** 135–162 (2013).
20. Products - Data Briefs - Number 94 - May 2012. at <http://www.cdc.gov/nchs/data/databriefs/db94.htm>
21. Corne, J. M. *et al.* Frequency, severity, and duration of rhinovirus infections in asthmatic and non-asthmatic individuals: a longitudinal cohort study. *Lancet* **359,** 831–834 (2002).
22. Jackson, D. J. *et al.* Wheezing rhinovirus illnesses in early life predict asthma development in high-risk children. *Am. J. Respir. Crit. Care Med.* **178,** 667–672 (2008).

23. Barrios, C. *et al.* Neonatal and early life immune responses to various forms of vaccine antigens qualitatively differ from adult responses: predominance of a Th2-biased pattern which persists after adult boosting. *Eur. J. Immunol.* **26,** 1489–1496 (1996).
24. Prescott, S. L. *et al.* Transplacental priming of the human immune system to environmental allergens: universal skewing of initial T cell responses toward the Th2 cytokine profile. *J. Immunol. Baltim. Md 1950* **160,** 4730–4737 (1998).
25. McManus, T. E. *et al.* Respiratory viral infection in exacerbations of COPD. *Respir. Med.* **102,** 1575–1580 (2008).
26. Rohde, G. *et al.* Respiratory viruses in exacerbations of chronic obstructive pulmonary disease requiring hospitalisation: a case-control study. *Thorax* **58,** 37–42 (2003).
27. Kherad, O. *et al.* Upper-respiratory viral infection, biomarkers, and COPD exacerbations. *Chest* **138,** 896–904 (2010).
28. Seemungal, T. *et al.* Respiratory viruses, symptoms, and inflammatory markers in acute exacerbations and stable chronic obstructive pulmonary disease. *Am. J. Respir. Crit. Care Med.* **164,** 1618–1623 (2001).
29. Smyth, A. R., Smyth, R. L., Tong, C. Y., Hart, C. A. & Heaf, D. P. Effect of respiratory virus infections including rhinovirus on clinical status in cystic fibrosis. *Arch. Dis. Child.* **73,** 117–120 (1995).
30. Olesen, H. V., Nielsen, L. P. & Schiotz, P. O. Viral and atypical bacterial infections in the outpatient pediatric cystic fibrosis clinic. *Pediatr. Pulmonol.* **41,** 1197–1204 (2006).
31. De Almeida, M. B. *et al.* Rhinovirus C and respiratory exacerbations in children with cystic fibrosis. *Emerg. Infect. Dis.* **16,** 996–999 (2010).
32. Kraft, C. S. *et al.* Severity of Human Rhinovirus Infection in Immunocompromised Adults Is Similar to That of 2009 H1N1 Influenza. *J. Clin. Microbiol.* **50,** 1061–1063 (2012).
33. Lau, S. K. P. *et al.* Clinical features and complete genome characterization of a distinct human rhinovirus (HRV) genetic cluster, probably representing a previously undetected HRV species, HRV-C, associated with acute respiratory illness in children. *J. Clin. Microbiol.* **45,** 3655–3664 (2007).
34. Dominguez, S. R. *et al.* Multiplex MassTag-PCR for respiratory pathogens in pediatric nasopharyngeal washes negative by conventional diagnostic testing shows a high prevalence of viruses belonging to a newly recognized rhinovirus clade. *J. Clin. Virol. Off. Publ. Pan Am. Soc. Clin. Virol.* **43,** 219–222 (2008).
35. Xiang, Z. *et al.* Human rhinovirus group C infection in children with lower respiratory tract infection. *Emerg. Infect. Dis.* **14,** 1665–1667 (2008).
36. Khetsuriani, N. *et al.* Novel human rhinoviruses and exacerbation of asthma in children. *Emerg. Infect. Dis.* **14,** 1793–1796 (2008).
37. Miller, E. K. *et al.* A novel group of rhinoviruses is associated with asthma hospitalizations. *J. Allergy Clin. Immunol.* **123,** 98–104.e1 (2009).
38. Han, T.-H., Chung, J.-Y., Hwang, E.-S. & Koo, J.-W. Detection of human rhinovirus C in children with acute lower respiratory tract infections in South Korea. *Arch. Virol.* **154,** 987–991 (2009).
39. Piralla, A. *et al.* Clinical severity and molecular typing of human rhinovirus C strains during a fall outbreak affecting hospitalized patients. *J. Clin. Virol. Off. Publ. Pan Am. Soc. Clin. Virol.* **45,** 311–317 (2009).
40. Linsuwanon, P. *et al.* High prevalence of human rhinovirus C infection in Thai children with acute lower respiratory tract disease. *J. Infect.* **59,** 115–121 (2009).
41. Lee, W.-M. *et al.* Human rhinovirus species and season of infection determine illness severity. *Am. J. Respir. Crit. Care Med.* **186,** 886–891 (2012).
42. Martin, E. K. *et al.* Molecular epidemiology of human rhinovirus infections in the pediatric emergency department. *J. Clin. Virol. Off. Publ. Pan Am. Soc. Clin. Virol.* **62,** 25–31 (2015).

43. Lu, Q.-B. *et al.* Molecular epidemiology of human rhinovirus in children with acute respiratory diseases in Chongqing, China. *Sci. Rep.* **4,** 6686 (2014).
44. Drysdale, S. B. *et al.* Respiratory outcome of prematurely born infants following human rhinovirus A and C infections. *Eur. J. Pediatr.* **173,** 913–919 (2014).
45. Bizzintino, J. *et al.* Association between human rhinovirus C and severity of acute asthma in children. *Eur. Respir. J.* **37,** 1037–1042 (2011).
46. Nakagome, K. *et al.* Effects of rhinovirus species on viral replication and cytokine production. *J. Allergy Clin. Immunol.* **134,** 332–341 (2014).
47. Lamphear, B. J., Kirchweger, R., Skern, T. & Rhoads, R. E. Mapping of functional domains in eukaryotic protein synthesis initiation factor 4G (eIF4G) with picornaviral proteases. Implications for cap-dependent and cap-independent translational initiation. *J. Biol. Chem.* **270,** 21975–21983 (1995).
48. Sommergruber, W. *et al.* 2A proteinases of coxsackie- and rhinovirus cleave peptides derived from eIF-4 gamma via a common recognition motif. *Virology* **198,** 741–745 (1994).
49. Park, N., Skern, T. & Gustin, K. E. Specific cleavage of the nuclear pore complex protein Nup62 by a viral protease. *J. Biol. Chem.* **285,** 28796–28805 (2010).
50. Park, N., Katikaneni, P., Skern, T. & Gustin, K. E. Differential targeting of nuclear pore complex proteins in poliovirus-infected cells. *J. Virol.* **82,** 1647–1655 (2008).
51. Gustin, K. E. & Sarnow, P. Inhibition of nuclear import and alteration of nuclear pore complex composition by rhinovirus. *J. Virol.* **76,** 8787–8796 (2002).
52. Watters, K. & Palmenberg, A. C. Differential processing of nuclear pore complex proteins by rhinovirus 2A proteases from different species and serotypes. *J. Virol.* **85,** 10874–10883 (2011).
53. Subauste, M. C., Choi, D. C. & Proud, D. Transient exposure of human bronchial epithelial cells to cytokines leads to persistent increased expression of ICAM-1. *Inflammation* **25,** 373–380 (2001).
54. Bochkov, Y. A. *et al.* Cadherin-related family member 3, a childhood asthma susceptibility gene product, mediates rhinovirus C binding and replication. *Proc. Natl. Acad. Sci. U. S. A.* (2015). doi:10.1073/pnas.1421178112
55. Hendley, J. O. & Gwaltney, J. M. Mechanisms of transmission of rhinovirus infections. *Epidemiol. Rev.* **10,** 243–258 (1988).
56. Dick, E. C., Jennings, L. C., Mink, K. A., Wartgow, C. D. & Inhorn, S. L. Aerosol transmission of rhinovirus colds. *J. Infect. Dis.* **156,** 442–448 (1987).
57. Gwaltney, J. M., Moskalski, P. B. & Hendley, J. O. Hand-to-hand transmission of rhinovirus colds. *Ann. Intern. Med.* **88,** 463–467 (1978).
58. Douglas, R. G., Cate, T. R., Gerone, P. J. & Couch, R. B. Quantitative rhinovirus shedding patterns in volunteers. *Am. Rev. Respir. Dis.* **94,** 159–167 (1966).
59. Gwaltney, J. M., Winther, B., Patrie, J. T. & Hendley, J. O. Combined antiviral-antimediator treatment for the common cold. *J. Infect. Dis.* **186,** 147–154 (2002).
60. Hendley, J. O. & Gwaltney, J. M. Viral titers in nasal lining fluid compared to viral titers in nasal washes during experimental rhinovirus infection. *J. Clin. Virol. Off. Publ. Pan Am. Soc. Clin. Virol.* **30,** 326–328 (2004).
61. Palmenberg, A. C. *et al.* Sequencing and analyses of all known human rhinovirus genomes reveal structure and evolution. *Science* **324,** 55–59 (2009).
62. Palmenberg, A. C., Rathe, J. A. & Liggett, S. B. Analysis of the complete genome sequences of human rhinovirus. *J. Allergy Clin. Immunol.* **125,** 1190–1199; quiz 1200–1201 (2010).
63. Hayden, F. G. *et al.* Efficacy and safety of oral pleconaril for treatment of colds due to picornaviruses in adults: results of 2 double-blind, randomized, placebo-controlled trials. *Clin. Infect. Dis. Off. Publ. Infect. Dis. Soc. Am.* **36,** 1523–1532 (2003).

64. Pevear, D. C. *et al.* Relationship of pleconaril susceptibility and clinical outcomes in treatment of common colds caused by rhinoviruses. *Antimicrob. Agents Chemother.* **49,** 4492–4499 (2005).
65. Webster, A. D. B. Pleconaril--an advance in the treatment of enteroviral infection in immuno-compromised patients. *J. Clin. Virol. Off. Publ. Pan Am. Soc. Clin. Virol.* **32,** 1–6 (2005).
66. Senior, K. FDA panel rejects common cold treatment. *Lancet Infect. Dis.* **2,** 264 (2002).
67. Feil, S. C. *et al.* An Orally Available 3-Ethoxybenzisoxazole Capsid Binder with Clinical Activity against Human Rhinovirus. *ACS Med. Chem. Lett.* **3,** 303–307 (2012).
68. Hayden, F. G. *et al.* Intranasal pirodavir (R77,975) treatment of rhinovirus colds. *Antimicrob. Agents Chemother.* **39,** 290–294 (1995).
69. Hayden, F. G., Andries, K. & Janssen, P. A. Safety and efficacy of intranasal pirodavir (R77975) in experimental rhinovirus infection. *Antimicrob. Agents Chemother.* **36,** 727–732 (1992).
70. Patick, A. K. Rhinovirus chemotherapy. *Antiviral Res.* **71,** 391–396 (2006).
71. Basta, H. A. *et al.* Modeling of the human rhinovirus C capsid suggests possible causes for antiviral drug resistance. *Virology* **448,** 82–90 (2014).
72. Bochkov, Y. A. *et al.* Molecular modeling, organ culture and reverse genetics for a newly identified human rhinovirus C. *Nat. Med.* **17,** 627–632 (2011).
73. Ashraf, S., Brockman-Schneider, R., Bochkov, Y. A., Pasic, T. R. & Gern, J. E. Biological characteristics and propagation of human rhinovirus-C in differentiated sinus epithelial cells. *Virology* **436,** 143–149 (2013).
74. Hao, W. *et al.* Infection and propagation of human rhinovirus C in human airway epithelial cells. *J. Virol.* **86,** 13524–13532 (2012).
75. Matthews, D. A. *et al.* Structure-assisted design of mechanism-based irreversible inhibitors of human rhinovirus 3C protease with potent antiviral activity against multiple rhinovirus serotypes. *Proc. Natl. Acad. Sci. U. S. A.* **96,** 11000–11007 (1999).
76. Binford, S. L. *et al.* Conservation of amino acids in human rhinovirus 3C protease correlates with broad-spectrum antiviral activity of rupintrivir, a novel human rhinovirus 3C protease inhibitor. *Antimicrob. Agents Chemother.* **49,** 619–626 (2005).
77. Hayden, F. G. *et al.* Phase II, randomized, double-blind, placebo-controlled studies of ruprintrivir nasal spray 2-percent suspension for prevention and treatment of experimentally induced rhinovirus colds in healthy volunteers. *Antimicrob. Agents Chemother.* **47,** 3907–3916 (2003).
78. Patick, A. K. *et al.* In vitro antiviral activity and single-dose pharmacokinetics in humans of a novel, orally bioavailable inhibitor of human rhinovirus 3C protease. *Antimicrob. Agents Chemother.* **49,** 2267–2275 (2005).
79. Mello, C. *et al.* Multiple Classes of Antiviral Agents Exhibit In Vitro Activity against Human Rhinovirus Type C. *Antimicrob. Agents Chemother.* **58,** 1546–1555 (2014).
80. Kuo, C.-J. *et al.* Design, synthesis, and evaluation of 3C protease inhibitors as anti-enterovirus 71 agents. *Bioorg. Med. Chem.* **16,** 7388–7398 (2008).
81. Turner, R. B. *et al.* Efficacy of tremacamra, a soluble intercellular adhesion molecule 1, for experimental rhinovirus infection: a randomized clinical trial. *JAMA* **281,** 1797–1804 (1999).
82. Brown-Augsburger, P. *et al.* Evidence that enviroxime targets multiple components of the rhinovirus 14 replication complex. *Arch. Virol.* **144,** 1569–1585 (1999).
83. Spickler, C. *et al.* Phosphatidylinositol 4-kinase III beta is essential for replication of human rhinovirus and its inhibition causes a lethal phenotype in vivo. *Antimicrob. Agents Chemother.* **57,** 3358–3368 (2013).
84. Hayden, F. G. & Gwaltney, J. M. Prophylactic activity of intranasal enviroxime against experimentally induced rhinovirus type 39 infection. *Antimicrob. Agents Chemother.* **21,** 892–897 (1982).
85. Levandowski, R. A., Pachucki, C. T., Rubenis, M. & Jackson, G. G. Topical enviroxime against rhinovirus infection. *Antimicrob. Agents Chemother.* **22,** 1004–1007 (1982).

86. Phillpotts, R. J., Wallace, J., Tyrrell, D. A. & Tagart, V. B. Therapeutic activity of enviroxime against rhinovirus infection in volunteers. *Antimicrob. Agents Chemother.* **23,** 671–675 (1983).
87. Miller, F. D. *et al.* Controlled trial of enviroxime against natural rhinovirus infections in a community. *Antimicrob. Agents Chemother.* **27,** 102–106 (1985).
88. Higgins, P. G. *et al.* Failure to demonstrate synergy between interferon-alpha and a synthetic antiviral, enviroxime, in rhinovirus infections in volunteers. *Antiviral Res.* **10,** 141–149 (1988).
89. Hayden, F. G., Albrecht, J. K., Kaiser, D. L. & Gwaltney, J. M. Prevention of natural colds by contact prophylaxis with intranasal alpha 2-interferon. *N. Engl. J. Med.* **314,** 71–75 (1986).
90. Hayden, F. G., Kaiser, D. L. & Albrecht, J. K. Intranasal recombinant alfa-2b interferon treatment of naturally occurring common colds. *Antimicrob. Agents Chemother.* **32,** 224–230 (1988).
91. Rotbart, H. A. Treatment of picornavirus infections. *Antiviral Res.* **53,** 83–98 (2002).
92. Sperber, S. J. & Hayden, F. G. Chemotherapy of rhinovirus colds. *Antimicrob. Agents Chemother.* **32,** 409–419 (1988).
93. Sperber, S. J., Levine, P. A., Innes, D. J., Mills, S. E. & Hayden, F. G. Tolerance and efficacy of intranasal administration of recombinant beta serine interferon in healthy adults. *J. Infect. Dis.* **158,** 166–175 (1988).
94. Sperber, S. J., Levine, P. A., Sorrentino, J. V., Riker, D. K. & Hayden, F. G. Ineffectiveness of recombinant interferon-beta serine nasal drops for prophylaxis of natural colds. *J. Infect. Dis.* **160,** 700–705 (1989).
95. Djukanović, R. *et al.* The effect of inhaled IFN-β on worsening of asthma symptoms caused by viral infections. A randomized trial. *Am. J. Respir. Crit. Care Med.* **190,** 145–154 (2014).
96. Butterworth, B. E. & Korant, B. D. Characterization of the large picornaviral polypeptides produced in the presence of zinc ion. *J. Virol.* **14,** 282–291 (1974).
97. Novick, S. G., Godfrey, J. C., Godfrey, N. J. & Wilder, H. R. How does zinc modify the common cold? Clinical observations and implications regarding mechanisms of action. *Med. Hypotheses* **46,** 295–302 (1996).
98. Korant, B. D. & Butterworth, B. E. Inhibition by zinc of rhinovirus protein cleavage: interaction of zinc with capsid polypeptides. *J. Virol.* **18,** 298–306 (1976).
99. Lee, W. *et al.* Solution structure of the 2A protease from a common cold agent, human rhinovirus C2, strain W12. *PloS One* **9,** e97198 (2014).
100. Harisch, G. & Kretschmer, M. Some aspects of a non-linear effect of zinc ions on the histamine release from rat peritoneal mast cells. *Res. Commun. Chem. Pathol. Pharmacol.* **55,** 39–48 (1987).
101. Singh, M. & Das, R. R. WITHDRAWN: Zinc for the common cold. *Cochrane Database Syst. Rev.* **4,** CD001364 (2015).
102. Science, M., Johnstone, J., Roth, D. E., Guyatt, G. & Loeb, M. Zinc for the treatment of the common cold: a systematic review and meta-analysis of randomized controlled trials. *CMAJ Can. Med. Assoc. J. J. Assoc. Medicale Can.* **184,** E551–561 (2012).
103. Das, R. R. & Singh, M. Oral zinc for the common cold. *JAMA* **311,** 1440–1441 (2014).
104. Jafek, B. W., Linschoten, M. R. & Murrow, B. W. Anosmia after intranasal zinc gluconate use. *Am. J. Rhinol.* **18,** 137–141 (2004).
105. Brinkeborn, R. M., Shah, D. V. & Degenring, F. H. Echinaforce and other Echinacea fresh plant preparations in the treatment of the common cold. A randomized, placebo controlled, double-blind clinical trial. *Phytomedicine Int. J. Phytother. Phytopharm.* **6,** 1–6 (1999).
106. Melchart, D., Linde, K., Worku, F., Bauer, R. & Wagner, H. Immunomodulation with echinacea - a systematic review of controlled clinical trials. *Phytomedicine Int. J. Phytother. Phytopharm.* **1,** 245–254 (1994).
107. Turner, R. B., Riker, D. K. & Gangemi, J. D. Ineffectiveness of Echinacea for Prevention of Experimental Rhinovirus Colds. *Antimicrob. Agents Chemother.* **44,** 1708–1709 (2000).

108. Sperber, S. J., Shah, L. P., Gilbert, R. D., Ritchey, T. W. & Monto, A. S. Echinacea purpurea for prevention of experimental rhinovirus colds. *Clin. Infect. Dis. Off. Publ. Infect. Dis. Soc. Am.* **38,** 1367–1371 (2004).
109. Turner, R. B., Bauer, R., Woelkart, K., Hulsey, T. C. & Gangemi, J. D. An evaluation of Echinacea angustifolia in experimental rhinovirus infections. *N. Engl. J. Med.* **353,** 341–348 (2005).
110. Linde, K., Barrett, B., Wölkart, K., Bauer, R. & Melchart, D. Echinacea for preventing and treating the common cold. *Cochrane Database Syst. Rev.* CD000530 (2006). doi:10.1002/14651858.CD000530.pub2
111. Karsch-Völk, M., Barrett, B. & Linde, K. Echinacea for preventing and treating the common cold. *JAMA* **313,** 618–619 (2015).
112. Hemilä, H. & Chalker, E. Vitamin C for preventing and treating the common cold. *Cochrane Database Syst. Rev.* **1,** CD000980 (2013).
113. Brockman-Schneider, R. A., Pickles, R. J. & Gern, J. E. Effects of vitamin D on airway epithelial cell morphology and rhinovirus replication. *PloS One* **9,** e86755 (2014).
114. Gwaltney, J. M. *et al.* Randomized controlled trial of clemastine fumarate for treatment of experimental rhinovirus colds. *Clin. Infect. Dis. Off. Publ. Infect. Dis. Soc. Am.* **22,** 656–662 (1996).
115. Gwaltney, J. M. & Druce, H. M. Efficacy of brompheniramine maleate for the treatment of rhinovirus colds. *Clin. Infect. Dis. Off. Publ. Infect. Dis. Soc. Am.* **25,** 1188–1194 (1997).
116. Sutter, A. I. M., Lemiengre, M., Campbell, H. & Mackinnon, H. F. Antihistamines for the common cold. *Cochrane Database Syst. Rev.* CD001267 (2003). doi:10.1002/14651858.CD001267
117. Herrmann, E. C. The usefullness of human fibroblast cell lines for the isolation of viruses. *Am. J. Epidemiol.* **85,** 200–206 (1967).
118. Stott, E. J. & Tyrrell, D. A. Some improved techniques for the study of rhinoviruses using HeLa cells. *Arch. Für Gesamte Virusforsch.* **23,** 236–244 (1968).
119. Arden, K. E., McErlean, P., Nissen, M. D., Sloots, T. P. & Mackay, I. M. Frequent detection of human rhinoviruses, paramyxoviruses, coronaviruses, and bocavirus during acute respiratory tract infections. *J. Med. Virol.* **78,** 1232–1240 (2006).
120. Freymuth, F. *et al.* Comparison of multiplex PCR assays and conventional techniques for the diagnostic of respiratory virus infections in children admitted to hospital with an acute respiratory illness. *J. Med. Virol.* **78,** 1498–1504 (2006).
121. Lamson, D. *et al.* MassTag polymerase-chain-reaction detection of respiratory pathogens, including a new rhinovirus genotype, that caused influenza-like illness in New York State during 2004-2005. *J. Infect. Dis.* **194,** 1398–1402 (2006).
122. McErlean, P. *et al.* Characterisation of a newly identified human rhinovirus, HRV-QPM, discovered in infants with bronchiolitis. *J. Clin. Virol. Off. Publ. Pan Am. Soc. Clin. Virol.* **39,** 67–75 (2007).
123. McErlean, P. *et al.* Distinguishing molecular features and clinical characteristics of a putative new rhinovirus species, human rhinovirus C (HRV C). *PloS One* **3,** e1847 (2008).
124. Tapparel, C. *et al.* Growth and characterization of different human rhinovirus C types in three-dimensional human airway epithelia reconstituted in vitro. *Virology* **446,** 1–8 (2013).
125. Basta, H. A., Sgro, J.-Y. & Palmenberg, A. C. Modeling of the human rhinovirus C capsid suggests a novel topography with insights on receptor preference and immunogenicity. *Virology* **448,** 176–184 (2014).
126. Bønnelykke, K. *et al.* A genome-wide association study identifies CDHR3 as a susceptibility locus for early childhood asthma with severe exacerbations. *Nat. Genet.* **46,** 51–55 (2014).
127. Rossmann, M. G. Structure of viruses: a short history. *Q. Rev. Biophys.* **46,** 133–180 (2013).
128. Rossmann, M. G. *et al.* Structure of a human common cold virus and functional relationship to other picornaviruses. *Nature* **317,** 145–153 (1985).

129. Olson, N. H. *et al.* Structure of a human rhinovirus complexed with its receptor molecule. *Proc. Natl. Acad. Sci. U. S. A.* **90,** 507–511 (1993).
130. Smith, T. J., Chase, E. S., Schmidt, T. J., Olson, N. H. & Baker, T. S. Neutralizing antibody to human rhinovirus 14 penetrates the receptor-binding canyon. *Nature* **383,** 350–354 (1996).
131. Domingo, E. *et al.* Viruses as quasispecies: biological implications. *Curr. Top. Microbiol. Immunol.* **299,** 51–82 (2006).
132. Kistler, A. L. *et al.* Genome-wide diversity and selective pressure in the human rhinovirus. *Virol. J.* **4,** 40 (2007).
133. Fuchs, R. & Blaas, D. Productive entry pathways of human rhinoviruses. *Adv. Virol.* **2012,** 826301 (2012).
134. Greve, J. M. *et al.* The major human rhinovirus receptor is ICAM-1. *Cell* **56,** 839–847 (1989).
135. Hofer, F. *et al.* Members of the low density lipoprotein receptor family mediate cell entry of a minor-group common cold virus. *Proc. Natl. Acad. Sci. U. S. A.* **91,** 1839–1842 (1994).
136. Garriga, D. *et al.* Insights into minor group rhinovirus uncoating: the X-ray structure of the HRV2 empty capsid. *PLoS Pathog.* **8,** e1002473 (2012).
137. Bostina, M., Levy, H., Filman, D. J. & Hogle, J. M. Poliovirus RNA is released from the capsid near a twofold symmetry axis. *J. Virol.* **85,** 776–783 (2011).
138. Brandenburg, B. *et al.* Imaging poliovirus entry in live cells. *PLoS Biol.* **5,** e183 (2007).
139. Bubeck, D. *et al.* The structure of the poliovirus 135S cell entry intermediate at 10-angstrom resolution reveals the location of an externalized polypeptide that binds to membranes. *J. Virol.* **79,** 7745–7755 (2005).
140. Bostina, M. *et al.* Single particle cryoelectron tomography characterization of the structure and structural variability of poliovirus-receptor-membrane complex at 30 A resolution. *J. Struct. Biol.* **160,** 200–210 (2007).
141. Fricks, C. E. & Hogle, J. M. Cell-induced conformational change in poliovirus: externalization of the amino terminus of VP1 is responsible for liposome binding. *J. Virol.* **64,** 1934–1945 (1990).
142. Xing, L. *et al.* Distinct cellular receptor interactions in poliovirus and rhinoviruses. *EMBO J.* **19,** 1207–1216 (2000).
143. Xing, L., Casasnovas, J. M. & Cheng, R. H. Structural analysis of human rhinovirus complexed with ICAM-1 reveals the dynamics of receptor-mediated virus uncoating. *J. Virol.* **77,** 6101–6107 (2003).
144. Pickl-Herk, A. *et al.* Uncoating of common cold virus is preceded by RNA switching as determined by X-ray and cryo-EM analyses of the subviral A-particle. *Proc. Natl. Acad. Sci. U. S. A.* **110,** 20063–20068 (2013).
145. Hogle, J. M. Poliovirus cell entry: common structural themes in viral cell entry pathways. *Annu. Rev. Microbiol.* **56,** 677–702 (2002).
146. Kolatkar, P. R. *et al.* Structural studies of two rhinovirus serotypes complexed with fragments of their cellular receptor. *EMBO J.* **18,** 6249–6259 (1999).
147. DeTulleo, L. & Kirchhausen, T. The clathrin endocytic pathway in viral infection. *EMBO J.* **17,** 4585–4593 (1998).
148. Danthi, P., Tosteson, M., Li, Q.-H. & Chow, M. Genome delivery and ion channel properties are altered in VP4 mutants of poliovirus. *J. Virol.* **77,** 5266–5274 (2003).
149. Harutyunyan, S., Kowalski, H. & Blaas, D. The Rhinovirus subviral a-particle exposes 3'-terminal sequences of its genomic RNA. *J. Virol.* **88,** 6307–6317 (2014).
150. Pfanzagl, B. *et al.* Entry of human rhinovirus 89 via ICAM-1 into HeLa epithelial cells is inhibited by actin skeleton disruption and by bafilomycin. *Arch. Virol.* **159,** 125–140 (2014).
151. Khan, A. G. *et al.* Entry of a heparan sulphate-binding HRV8 variant strictly depends on dynamin but not on clathrin, caveolin, and flotillin. *Virology* **412,** 55–67 (2011).

152. Fuchs, R. & Blaas, D. Uncoating of human rhinoviruses. *Rev. Med. Virol.* **20,** 281–297 (2010).
153. Khan, A. G. *et al.* Human rhinovirus 14 enters rhabdomyosarcoma cells expressing icam-1 by a clathrin-, caveolin-, and flotillin-independent pathway. *J. Virol.* **84,** 3984–3992 (2010).
154. Lau, C. *et al.* Syk associates with clathrin and mediates phosphatidylinositol 3-kinase activation during human rhinovirus internalization. *J. Immunol. Baltim. Md 1950* **180,** 870–880 (2008).
155. Snyers, L., Zwickl, H. & Blaas, D. Human rhinovirus type 2 is internalized by clathrin-mediated endocytosis. *J. Virol.* **77,** 5360–5369 (2003).
156. Huber, M., Brabec, M., Bayer, N., Blaas, D. & Fuchs, R. Elevated endosomal pH in HeLa cells overexpressing mutant dynamin can affect infection by pH-sensitive viruses. *Traffic Cph. Den.* **2,** 727–736 (2001).
157. Grunert, H. P. *et al.* Internalization of human rhinovirus 14 into HeLa and ICAM-1-transfected BHK cells. *Med. Microbiol. Immunol. (Berl.)* **186,** 1–9 (1997).
158. Harutyunyan, S. *et al.* Viral uncoating is directional: exit of the genomic RNA in a common cold virus starts with the poly-(A) tail at the 3'-end. *PLoS Pathog.* **9,** e1003270 (2013).
159. Flanegan, J. B., Petterson, R. F., Ambros, V., Hewlett, N. J. & Baltimore, D. Covalent linkage of a protein to a defined nucleotide sequence at the 5'-terminus of virion and replicative intermediate RNAs of poliovirus. *Proc. Natl. Acad. Sci. U. S. A.* **74,** 961–965 (1977).
160. Lee, Y. F., Nomoto, A., Detjen, B. M. & Wimmer, E. A protein covalently linked to poliovirus genome RNA. *Proc. Natl. Acad. Sci. U. S. A.* **74,** 59–63 (1977).
161. Nomoto, A., Detjen, B., Pozzatti, R. & Wimmer, E. The location of the polio genome protein in viral RNAs and its implication for RNA synthesis. *Nature* **268,** 208–213 (1977).
162. Yogo, Y. & Wimmer, E. Polyadenylic acid at the 3'-terminus of poliovirus RNA. *Proc. Natl. Acad. Sci. U. S. A.* **69,** 1877–1882 (1972).
163. Jang, S. K. *et al.* A segment of the 5' nontranslated region of encephalomyocarditis virus RNA directs internal entry of ribosomes during in vitro translation. *J. Virol.* **62,** 2636–2643 (1988).
164. Jang, S. K., Davies, M. V., Kaufman, R. J. & Wimmer, E. Initiation of protein synthesis by internal entry of ribosomes into the 5' nontranslated region of encephalomyocarditis virus RNA in vivo. *J. Virol.* **63,** 1651–1660 (1989).
165. Pelletier, J. & Sonenberg, N. Internal initiation of translation of eukaryotic mRNA directed by a sequence derived from poliovirus RNA. *Nature* **334,** 320–325 (1988).
166. Pelletier, J. & Sonenberg, N. Internal binding of eucaryotic ribosomes on poliovirus RNA: translation in HeLa cell extracts. *J. Virol.* **63,** 441–444 (1989).
167. Lin, J.-Y. *et al.* Viral and host proteins involved in picornavirus life cycle. *J. Biomed. Sci.* **16,** 103 (2009).
168. Arnold, E. *et al.* Implications of the picornavirus capsid structure for polyprotein processing. *Proc. Natl. Acad. Sci. U. S. A.* **84,** 21–25 (1987).
169. Harber, J. J., Bradley, J., Anderson, C. W. & Wimmer, E. Catalysis of poliovirus VP0 maturation cleavage is not mediated by serine 10 of VP2. *J. Virol.* **65,** 326–334 (1991).
170. Lee, W. M., Monroe, S. S. & Rueckert, R. R. Role of maturation cleavage in infectivity of picornaviruses: activation of an infectosome. *J. Virol.* **67,** 2110–2122 (1993).
171. Curry, S. *et al.* Dissecting the roles of VP0 cleavage and RNA packaging in picornavirus capsid stabilization: the structure of empty capsids of foot-and-mouth disease virus. *J. Virol.* **71,** 9743–9752 (1997).
172. Hindiyeh, M., Li, Q. H., Basavappa, R., Hogle, J. M. & Chow, M. Poliovirus mutants at histidine 195 of VP2 do not cleave VP0 into VP2 and VP4. *J. Virol.* **73,** 9072–9079 (1999).
173. Aldabe, R., Barco, A. & Carrasco, L. Membrane permeabilization by poliovirus proteins 2B and 2BC. *J. Biol. Chem.* **271,** 23134–23137 (1996).

174. Barco, A. & Carrasco, L. A human virus protein, poliovirus protein 2BC, induces membrane proliferation and blocks the exocytic pathway in the yeast Saccharomyces cerevisiae. *EMBO J.* **14,** 3349–3364 (1995).
175. Van Kuppeveld, F. J., Galama, J. M., Zoll, J., van den Hurk, P. J. & Melchers, W. J. Coxsackie B3 virus protein 2B contains cationic amphipathic helix that is required for viral RNA replication. *J. Virol.* **70,** 3876–3886 (1996).
176. Rust, R. C. *et al.* Cellular COPII proteins are involved in production of the vesicles that form the poliovirus replication complex. *J. Virol.* **75,** 9808–9818 (2001).
177. Jiang, P., Liu, Y., Ma, H.-C., Paul, A. V. & Wimmer, E. Picornavirus morphogenesis. *Microbiol. Mol. Biol. Rev. MMBR* **78,** 418–437 (2014).
178. Paul, A. V., van Boom, J. H., Filippov, D. & Wimmer, E. Protein-primed RNA synthesis by purified poliovirus RNA polymerase. *Nature* **393,** 280–284 (1998).
179. Pettersson, R. F., Ambros, V. & Baltimore, D. Identification of a protein linked to nascent poliovirus RNA and to the polyuridylic acid of negative-strand RNA. *J. Virol.* **27,** 357–365 (1978).
180. Kok, C. C. & McMinn, P. C. Picornavirus RNA-dependent RNA polymerase. *Int. J. Biochem. Cell Biol.* **41,** 498–502 (2009).
181. Barton, D. J., O'Donnell, B. J. & Flanegan, J. B. 5' cloverleaf in poliovirus RNA is a cis-acting replication element required for negative-strand synthesis. *EMBO J.* **20,** 1439–1448 (2001).
182. Jackson, W. T. *et al.* Subversion of cellular autophagosomal machinery by RNA viruses. *PLoS Biol.* **3,** e156 (2005).
183. Richards, A. L. & Jackson, W. T. How positive-strand RNA viruses benefit from autophagosome maturation. *J. Virol.* **87,** 9966–9972 (2013).
184. Gradi, A. *et al.* Human rhinovirus 2A proteinase cleavage sites in eukaryotic initiation factors (eIF) 4GI and eIF4GII are different. *J. Virol.* **77,** 5026–5029 (2003).
185. Lamphear, B. J. *et al.* Mapping the cleavage site in protein synthesis initiation factor eIF-4 gamma of the 2A proteases from human Coxsackievirus and rhinovirus. *J. Biol. Chem.* **268,** 19200–19203 (1993).
186. Castelló, A., Izquierdo, J. M., Welnowska, E. & Carrasco, L. RNA nuclear export is blocked by poliovirus 2A protease and is concomitant with nucleoporin cleavage. *J. Cell Sci.* **122,** 3799–3809 (2009).
187. Clark, M. E., Hämmerle, T., Wimmer, E. & Dasgupta, A. Poliovirus proteinase 3C converts an active form of transcription factor IIIC to an inactive form: a mechanism for inhibition of host cell polymerase III transcription by poliovirus. *EMBO J.* **10,** 2941–2947 (1991).
188. Clark, M. E., Lieberman, P. M., Berk, A. J. & Dasgupta, A. Direct cleavage of human TATA-binding protein by poliovirus protease 3C in vivo and in vitro. *Mol. Cell. Biol.* **13,** 1232–1237 (1993).
189. Yalamanchili, P., Datta, U. & Dasgupta, A. Inhibition of host cell transcription by poliovirus: cleavage of transcription factor CREB by poliovirus-encoded protease 3Cpro. *J. Virol.* **71,** 1220–1226 (1997).
190. Yalamanchili, P., Weidman, K. & Dasgupta, A. Cleavage of transcriptional activator Oct-1 by poliovirus encoded protease 3Cpro. *Virology* **239,** 176–185 (1997).
191. Campanella, M. *et al.* The coxsackievirus 2B protein suppresses apoptotic host cell responses by manipulating intracellular Ca2+ homeostasis. *J. Biol. Chem.* **279,** 18440–18450 (2004).
192. Doedens, J. R. & Kirkegaard, K. Inhibition of cellular protein secretion by poliovirus proteins 2B and 3A. *EMBO J.* **14,** 894–907 (1995).
193. Sandoval, I. V. & Carrasco, L. Poliovirus infection and expression of the poliovirus protein 2B provoke the disassembly of the Golgi complex, the organelle target for the antipoliovirus drug Ro-090179. *J. Virol.* **71,** 4679–4693 (1997).

194. Doedens, J. R., Giddings, T. H. & Kirkegaard, K. Inhibition of endoplasmic reticulum-to-Golgi traffic by poliovirus protein 3A: genetic and ultrastructural analysis. *J. Virol.* **71,** 9054–9064 (1997).
195. Blanco, J. C., Boukhvalova, M. S., Perez, D. R., Vogel, S. N. & Kajon, A. Modeling Human Respiratory Viral Infections in the Cotton Rat (Sigmodon hispidus). *J. Antivir. Antiretrovir.* **6,** 40–42 (2014).
196. Bartlett, N. W. *et al.* Mouse models of rhinovirus-induced disease and exacerbation of allergic airway inflammation. *Nat. Med.* **14,** 199–204 (2008).
197. Nagarkar, D. R. *et al.* Rhinovirus infection of allergen-sensitized and -challenged mice induces eotaxin release from functionally polarized macrophages. *J. Immunol. Baltim. Md 1950* **185,** 2525–2535 (2010).
198. Singanayagam, A. *et al.* A short-term mouse model that reproduces the immunopathological features of rhinovirus-induced exacerbation of COPD. *Clin. Sci. Lond. Engl. 1979* **129,** 245–258 (2015).
199. Price, W. H. THE ISOLATION OF A NEW VIRUS ASSOCIATED WITH RESPIRATORY CLINICAL DISEASE IN HUMANS. *Proc. Natl. Acad. Sci. U. S. A.* **42,** 892–896 (1956).
200. Krueger, A. P. & Tamada, H. T. THE PREPARATION OF RELATIVELY PURE BACTERIOPHAGE. *J. Gen. Physiol.* **13,** 145–151 (1929).
201. Stanley, N. F. Purification of Australian strains of Coxsackie virus. *Aust. J. Exp. Biol. Med. Sci.* **29,** 363–365 (1951).
202. Lin, W. *et al.* Purification, crystallization and X-ray analysis of swine vesicular disease virus. *Acta Crystallogr. D Biol. Crystallogr.* **58,** 1056–1058 (2002).
203. Lee, H. *et al.* A strain-specific epitope of enterovirus 71 identified by cryo-electron microscopy of the complex with fab from neutralizing antibody. *J. Virol.* **87,** 11363–11370 (2013).
204. Frommhagen, L. H. Level and specificity of antibodies evoked by crude and purified antigens of poliovirus I and echovirus 7. *Appl. Microbiol.* **13,** 895–898 (1965).
205. Sabin, A. B., Hennessen, W. A. & Winsser, J. Studies on variants of poliomyelitis virus. I. Experimental segregation and properties of avirulent variants of three immunologic types. *J. Exp. Med.* **99,** 551–576 (1954).
206. Hadfield, A. T., Diana, G. D. & Rossmann, M. G. Analysis of three structurally related antiviral compounds in complex with human rhinovirus 16. *Proc. Natl. Acad. Sci. U. S. A.* **96,** 14730–14735 (1999).
207. Rueckert, R. R. & Pallansch, M. A. Preparation and characterization of encephalomyocarditis (EMC) virus. *Methods Enzymol.* **78,** 315–325 (1981).
208. Lee, W. M., Wang, W. & Rueckert, R. R. Complete sequence of the RNA genome of human rhinovirus 16, a clinically useful common cold virus belonging to the ICAM-1 receptor group. *Virus Genes* **9,** 177–181 (1995).
209. Sherry, B., Mosser, A. G., Colonno, R. J. & Rueckert, R. R. Use of monoclonal antibodies to identify four neutralization immunogens on a common cold picornavirus, human rhinovirus 14. *J. Virol.* **57,** 246–257 (1986).
210. Wang, W., Lee, W. M., Mosser, A. G. & Rueckert, R. R. WIN 52035-dependent human rhinovirus 16: assembly deficiency caused by mutations near the canyon surface. *J. Virol.* **72,** 1210–1218 (1998).
211. Gerin, J. L., Richter, W. R., Fenters, J. D. & Holper, J. C. Use of zonal ultracentrifuge systems for biophysical studies of rhinoviruses. *J. Virol.* **2,** 937–943 (1968).
212. Griggs, T. F., Bochkov, Y. A., Nakagome, K., Palmenberg, A. C. & Gern, J. E. Production, purification, and capsid stability of rhinovirus C types. *J. Virol. Methods* **217,** 18–23 (2015).
213. Lynch, T. J. & Engelhardt, J. F. Progenitor cells in proximal airway epithelial development and regeneration. *J. Cell. Biochem.* **115,** 1637–1645 (2014).

214. Wadsworth, S. J., Freyer, A. M., Corteling, R. L. & Hall, I. P. Biosynthesized matrix provides a key role for survival signaling in bronchial epithelial cells. *Am. J. Physiol. Lung Cell. Mol. Physiol.* **286,** L596–603 (2004).
215. Boudreau, N., Werb, Z. & Bissell, M. J. Suppression of apoptosis by basement membrane requires three-dimensional tissue organization and withdrawal from the cell cycle. *Proc. Natl. Acad. Sci. U. S. A.* **93,** 3509–3513 (1996).
216. Terranova, V. P., Rohrbach, D. H. & Martin, G. R. Role of laminin in the attachment of PAM 212 (epithelial) cells to basement membrane collagen. *Cell* **22,** 719–726 (1980).
217. Evans, M. J., Van Winkle, L. S., Fanucchi, M. V. & Plopper, C. G. Cellular and molecular characteristics of basal cells in airway epithelium. *Exp. Lung Res.* **27,** 401–415 (2001).
218. Evans, M. J. & Plopper, C. G. The role of basal cells in adhesion of columnar epithelium to airway basement membrane. *Am. Rev. Respir. Dis.* **138,** 481–483 (1988).
219. Evans, M. J., Cox, R. A., Shami, S. G., Wilson, B. & Plopper, C. G. The role of basal cells in attachment of columnar cells to the basal lamina of the trachea. *Am. J. Respir. Cell Mol. Biol.* **1,** 463–469 (1989).
220. Hong, K. U., Reynolds, S. D., Watkins, S., Fuchs, E. & Stripp, B. R. In vivo differentiation potential of tracheal basal cells: evidence for multipotent and unipotent subpopulations. *Am. J. Physiol. Lung Cell. Mol. Physiol.* **286,** L643–649 (2004).
221. Knight, D. A. & Holgate, S. T. The airway epithelium: structural and functional properties in health and disease. *Respirol. Carlton Vic* **8,** 432–446 (2003).
222. Jeffery, P. K. Morphologic features of airway surface epithelial cells and glands. *Am. Rev. Respir. Dis.* **128,** S14–20 (1983).
223. Tam, A., Wadsworth, S., Dorscheid, D., Man, S. F. P. & Sin, D. D. The airway epithelium: more than just a structural barrier. *Ther. Adv. Respir. Dis.* **5,** 255–273 (2011).
224. Spina, D. Epithelium smooth muscle regulation and interactions. *Am. J. Respir. Crit. Care Med.* **158,** S141–145 (1998).
225. Yates, G. T., Wu, T. Y., Johnson, R. E., Cheung, A. T. & Frand, C. L. A theoretical and experimental study on tracheal muco-ciliary transport. *Biorheology* **17,** 151–162 (1980).
226. Tyner, J. W. *et al.* Blocking airway mucous cell metaplasia by inhibiting EGFR antiapoptosis and IL-13 transdifferentiation signals. *J. Clin. Invest.* **116,** 309–321 (2006).
227. Lumsden, A. B., McLean, A. & Lamb, D. Goblet and Clara cells of human distal airways: evidence for smoking induced changes in their numbers. *Thorax* **39,** 844–849 (1984).
228. Evans, C. M. & Koo, J. S. Airway mucus: the good, the bad, the sticky. *Pharmacol. Ther.* **121,** 332–348 (2009).
229. Hirota, N. & Martin, J. G. Mechanisms of airway remodeling. *Chest* **144,** 1026–1032 (2013).
230. Laoukili, J. *et al.* IL-13 alters mucociliary differentiation and ciliary beating of human respiratory epithelial cells. *J. Clin. Invest.* **108,** 1817–1824 (2001).
231. Vermeer, P. D., Harson, R., Einwalter, L. A., Moninger, T. & Zabner, J. Interleukin-9 induces goblet cell hyperplasia during repair of human airway epithelia. *Am. J. Respir. Cell Mol. Biol.* **28,** 286–295 (2003).
232. Mercer, R. R., Russell, M. L., Roggli, V. L. & Crapo, J. D. Cell number and distribution in human and rat airways. *Am. J. Respir. Cell Mol. Biol.* **10,** 613–624 (1994).
233. De Water, R. *et al.* Ultrastructural localization of bronchial antileukoprotease in central and peripheral human airways by a gold-labeling technique using monoclonal antibodies. *Am. Rev. Respir. Dis.* **133,** 882–890 (1986).
234. Sallenave, J. M., Shulmann, J., Crossley, J., Jordana, M. & Gauldie, J. Regulation of secretory leukocyte proteinase inhibitor (SLPI) and elastase-specific inhibitor (ESI/elafin) in human airway

epithelial cells by cytokines and neutrophilic enzymes. *Am. J. Respir. Cell Mol. Biol.* **11,** 733–741 (1994).

235. Hong, K. U., Reynolds, S. D., Giangreco, A., Hurley, C. M. & Stripp, B. R. Clara cell secretory protein-expressing cells of the airway neuroepithelial body microenvironment include a label-retaining subset and are critical for epithelial renewal after progenitor cell depletion. *Am. J. Respir. Cell Mol. Biol.* **24,** 671–681 (2001).
236. Wright, J. R. & Hawgood, S. Pulmonary surfactant metabolism. *Clin. Chest Med.* **10,** 83–93 (1989).
237. Wright, J. R. Immunoregulatory functions of surfactant proteins. *Nat. Rev. Immunol.* **5,** 58–68 (2005).
238. Dobbs, L. G. & Johnson, M. D. Alveolar epithelial transport in the adult lung. *Respir. Physiol. Neurobiol.* **159,** 283–300 (2007).
239. Chan, R. W. Y. *et al.* Tropism of and innate immune responses to the novel human betacoronavirus lineage C virus in human ex vivo respiratory organ cultures. *J. Virol.* **87,** 6604–6614 (2013).
240. Matsuyama, S. *et al.* Efficient Activation of the Severe Acute Respiratory Syndrome Coronavirus Spike Protein by the Transmembrane Protease TMPRSS2. *J. Virol.* **84,** 12658–12664 (2010).
241. To, K. F. *et al.* Tissue and cellular tropism of the coronavirus associated with severe acute respiratory syndrome: an in-situ hybridization study of fatal cases. *J. Pathol.* **202,** 157–163 (2004).
242. Parker, L. C., Stokes, C. A. & Sabroe, I. Rhinoviral infection and asthma: the detection and management of rhinoviruses by airway epithelial cells. *Clin. Exp. Allergy J. Br. Soc. Allergy Clin. Immunol.* **44,** 20–28 (2014).
243. Unger, B. L. *et al.* Rhinovirus attenuates non-typeable Hemophilus influenzae-stimulated IL-8 responses via TLR2-dependent degradation of IRAK-1. *PLoS Pathog.* **8,** e1002969 (2012).
244. Hewson, C. A., Jardine, A., Edwards, M. R., Laza-Stanca, V. & Johnston, S. L. Toll-like receptor 3 is induced by and mediates antiviral activity against rhinovirus infection of human bronchial epithelial cells. *J. Virol.* **79,** 12273–12279 (2005).
245. Slater, L. *et al.* Co-ordinated role of TLR3, RIG-I and MDA5 in the innate response to rhinovirus in bronchial epithelium. *PLoS Pathog.* **6,** e1001178 (2010).
246. Wang, Q. *et al.* Role of double-stranded RNA pattern recognition receptors in rhinovirus-induced airway epithelial cell responses. *J. Immunol. Baltim. Md 1950* **183,** 6989–6997 (2009).
247. Triantafilou, K. *et al.* Human rhinovirus recognition in non-immune cells is mediated by Toll-like receptors and MDA-5, which trigger a synergetic pro-inflammatory immune response. *Virulence* **2,** 22–29 (2011).
248. Parker, L. C. *et al.* A phosphatidylserine species inhibits a range of TLR- but not IL-1beta-induced inflammatory responses by disruption of membrane microdomains. *J. Immunol. Baltim. Md 1950* **181,** 5606–5617 (2008).
249. Morris, G. E. *et al.* Cooperative molecular and cellular networks regulate Toll-like receptor-dependent inflammatory responses. *FASEB J. Off. Publ. Fed. Am. Soc. Exp. Biol.* **20,** 2153–2155 (2006).
250. Kato, A., Favoreto, S., Avila, P. C. & Schleimer, R. P. TLR3- and Th2 cytokine-dependent production of thymic stromal lymphopoietin in human airway epithelial cells. *J. Immunol. Baltim. Md 1950* **179,** 1080–1087 (2007).
251. Sadik, C. D., Bachmann, M., Pfeilschifter, J. & Mühl, H. Activation of interferon regulatory factor-3 via toll-like receptor 3 and immunomodulatory functions detected in A549 lung epithelial cells exposed to misplaced U1-snRNA. *Nucleic Acids Res.* **37,** 5041–5056 (2009).
252. O'Neill, L. A. J., Golenbock, D. & Bowie, A. G. The history of Toll-like receptors - redefining innate immunity. *Nat. Rev. Immunol.* **13,** 453–460 (2013).

253. Brasier, A. R., Garcia-Sastre, A. & Lemon, S. M. *Cellular signaling and innate immune responses to RNA virus infections.* (2009).
254. Romani, N., Clausen, B. E. & Stoitzner, P. Langerhans cells and more: langerin-expressing dendritic cell subsets in the skin. *Immunol. Rev.* **234,** 120–141 (2010).
255. Hammad, H. & Lambrecht, B. N. Dendritic cells and epithelial cells: linking innate and adaptive immunity in asthma. *Nat. Rev. Immunol.* **8,** 193–204 (2008).
256. Nawijn, M. C., Hackett, T. L., Postma, D. S., van Oosterhout, A. J. M. & Heijink, I. H. E-cadherin: gatekeeper of airway mucosa and allergic sensitization. *Trends Immunol.* **32,** 248–255 (2011).
257. Rao, R. Occludin phosphorylation in regulation of epithelial tight junctions. *Ann. N. Y. Acad. Sci.* **1165,** 62–68 (2009).
258. Heijink, I. H. *et al.* Characterisation of cell adhesion in airway epithelial cell types using electric cell-substrate impedance sensing. *Eur. Respir. J.* **35,** 894–903 (2010).
259. Halbleib, J. M. & Nelson, W. J. Cadherins in development: cell adhesion, sorting, and tissue morphogenesis. *Genes Dev.* **20,** 3199–3214 (2006).
260. Leckband, D. & Prakasam, A. Mechanism and dynamics of cadherin adhesion. *Annu. Rev. Biomed. Eng.* **8,** 259–287 (2006).
261. Pokutta, S. & Weis, W. I. Structure and mechanism of cadherins and catenins in cell-cell contacts. *Annu. Rev. Cell Dev. Biol.* **23,** 237–261 (2007).
262. Cheng, D. *et al.* Airway epithelium controls lung inflammation and injury through the NF-kappa B pathway. *J. Immunol. Baltim. Md 1950* **178,** 6504–6513 (2007).
263. Pantano, C. *et al.* Nuclear factor-kappaB activation in airway epithelium induces inflammation and hyperresponsiveness. *Am. J. Respir. Crit. Care Med.* **177,** 959–969 (2008).
264. Solanas, G. *et al.* E-cadherin controls beta-catenin and NF-kappaB transcriptional activity in mesenchymal gene expression. *J. Cell Sci.* **121,** 2224–2234 (2008).
265. Cowell, C. F. *et al.* Loss of cell-cell contacts induces NF-kappaB via RhoA-mediated activation of protein kinase D1. *J. Cell. Biochem.* **106,** 714–728 (2009).
266. Heijink, I. H. *et al.* Down-regulation of E-cadherin in human bronchial epithelial cells leads to epidermal growth factor receptor-dependent Th2 cell-promoting activity. *J. Immunol. Baltim. Md 1950* **178,** 7678–7685 (2007).
267. Heijink, I. H. *et al.* Der p, IL-4, and TGF-beta cooperatively induce EGFR-dependent TARC expression in airway epithelium. *Am. J. Respir. Cell Mol. Biol.* **36,** 351–359 (2007).
268. Suffia, I., Reckling, S. K., Salay, G. & Belkaid, Y. A role for CD103 in the retention of CD4+CD25+ Treg and control of Leishmania major infection. *J. Immunol. Baltim. Md 1950* **174,** 5444–5455 (2005).
269. Smyth, L. J. C., Eustace, A., Kolsum, U., Blaikely, J. & Singh, D. Increased airway T regulatory cells in asthmatic subjects. *Chest* **138,** 905–912 (2010).
270. Banh, C., Fugère, C. & Brossay, L. Immunoregulatory functions of KLRG1 cadherin interactions are dependent on forward and reverse signaling. *Blood* **114,** 5299–5306 (2009).
271. Zemans, R. L., Colgan, S. P. & Downey, G. P. Transepithelial migration of neutrophils: mechanisms and implications for acute lung injury. *Am. J. Respir. Cell Mol. Biol.* **40,** 519–535 (2009).
272. Chun, J. & Prince, A. TLR2-induced calpain cleavage of epithelial junctional proteins facilitates leukocyte transmigration. *Cell Host Microbe* **5,** 47–58 (2009).
273. Kobayashi, N., Terada, N., Hamano, N., Numata, T. & Konno, A. Transepithelial migration of activated eosinophils induces a decrease of E-cadherin expression in cultured human nasal epithelial cells. *Clin. Exp. Allergy J. Br. Soc. Allergy Clin. Immunol.* **30,** 807–817 (2000).
274. Jacquet, A. Interactions of airway epithelium with protease allergens in the allergic response. *Clin. Exp. Allergy J. Br. Soc. Allergy Clin. Immunol.* **41,** 305–311 (2011).

275. Wills-Karp, M., Nathan, A., Page, K. & Karp, C. L. New insights into innate immune mechanisms underlying allergenicity. *Mucosal Immunol.* **3,** 104–110 (2010).
276. Winter, M. C., Shasby, S. S., Ries, D. R. & Shasby, D. M. PAR2 activation interrupts E-cadherin adhesion and compromises the airway epithelial barrier: protective effect of beta-agonists. *Am. J. Physiol. Lung Cell. Mol. Physiol.* **291,** L628–635 (2006).
277. Janssen-Heininger, Y. M. W. *et al.* Nuclear factor kappaB, airway epithelium, and asthma: avenues for redox control. *Proc. Am. Thorac. Soc.* **6,** 249–255 (2009).
278. McKerrow, J. H., Caffrey, C., Kelly, B., Loke, P. & Sajid, M. Proteases in parasitic diseases. *Annu. Rev. Pathol.* **1,** 497–536 (2006).
279. Pande, J., Szewczyk, M. M. & Grover, A. K. Phage display: concept, innovations, applications and future. *Biotechnol. Adv.* **28,** 849–858 (2010).
280. Savolainen-Kopra, C. *et al.* Single treatment with ethanol hand rub is ineffective against human rhinovirus--hand washing with soap and water removes the virus efficiently. *J. Med. Virol.* **84,** 543–547 (2012).
281. Behbehani, A. M. & Lee, L. H. Growth, plaque production, and cationic stabilization of rhinovirus type 1 (echovirus 28). *J. Bacteriol.* **88,** 1608–1611 (1964).
282. Milo, G. E. Thermal inactivation of poliovirus in the presence of selective organic molecules (cholesterol, lecithin, collagen, and beta-carotene). *Appl. Microbiol.* **21,** 198–202 (1971).
283. Rombaut, B., Vrijsen, R. & Boeyé, A. Stabilization by host cell components and Mg2+ of the neutralization epitopes of poliovirus. *J. Gen. Virol.* **66 (Pt 2),** 303–307 (1985).
284. Dorval, B. L., Chow, M. & Klibanov, A. M. Stabilization of poliovirus against heat inactivation. *Biochem. Biophys. Res. Commun.* **159,** 1177–1183 (1989).
285. Tomasula, P. M. *et al.* Thermal inactivation of foot-and-mouth disease virus in milk using high-temperature, short-time pasteurization. *J. Dairy Sci.* **90,** 3202–3211 (2007).
286. Sherry, B. & Rueckert, R. Evidence for at least two dominant neutralization antigens on human rhinovirus 14. *J. Virol.* **53,** 137–143 (1985).
287. Gassilloud, B. & Gantzer, C. Adhesion-aggregation and inactivation of poliovirus 1 in groundwater stored in a hydrophobic container. *Appl. Environ. Microbiol.* **71,** 912–920 (2005).
288. Fendrick, A. M., Monto, A. S., Nightengale, B. & Sarnes, M. The economic burden of non-influenza-related viral respiratory tract infection in the United States. *Arch. Intern. Med.* **163,** 487–494 (2003).
289. Monto, A. S., Bryan, E. R. & Ohmit, S. Rhinovirus infections in Tecumseh, Michigan: frequency of illness and number of serotypes. *J. Infect. Dis.* **156,** 43–49 (1987).
290. Hament, J.-M., Kimpen, J. L. ., Fleer, A. & Wolfs, T. F. . Respiratory viral infection predisposing for bacterial disease: a concise review. *FEMS Immunol. Med. Microbiol.* **26,** 189–195 (1999).
291. Ishizuka, S. *et al.* Effects of rhinovirus infection on the adherence of Streptococcus pneumoniae to cultured human airway epithelial cells. *J. Infect. Dis.* **188,** 1928–1939 (2003).
292. Monto, A. S. Epidemiology of viral respiratory infections. *Dis. Mon.* **49,** 160–174 (2003).
293. Gern, J. E. & Busse, W. W. Relationship of viral infections to wheezing illnesses and asthma. *Nat. Rev. Immunol.* **2,** 132–138 (2002).
294. Lemanske Jr., R. F. *et al.* Rhinovirus illnesses during infancy predict subsequent childhood wheezing. *J. Allergy Clin. Immunol.* **116,** 571–577 (2005).
295. Jackson, D. J. *et al.* Wheezing rhinovirus illnesses in early life predict asthma development in high-risk children. *Am. J. Respir. Crit. Care Med.* **178,** 667–672 (2008).
296. Walton, R. P. & Johnston, S. L. Role of respiratory viral infections in the development of atopic conditions. *Curr. Opin. Allergy Clin. Immunol.* **8,** 150–153 (2008).
297. Jackson, D. J. *et al.* Evidence for a Causal Relationship between Allergic Sensitization and Rhinovirus Wheezing in Early Life. *Am. J. Respir. Crit. Care Med.* **185,** 281–285 (2012).

298. Matrosovich, M. N., Matrosovich, T. Y., Gray, T., Roberts, N. A. & Klenk, H.-D. Human and avian influenza viruses target different cell types in cultures of human airway epithelium. *Proc. Natl. Acad. Sci. U. S. A.* **101,** 4620–4624 (2004).
299. Mounts, A. W. *et al.* Case-control study of risk factors for avian influenza A (H5N1) disease, Hong Kong, 1997. *J. Infect. Dis.* **180,** 505–508 (1999).
300. Centers for Disease Control and Prevention (CDC). Update: influenza activity--United States and worldwide, 2002-03 season, and composition of the 2003-04 influenza vaccine. *MMWR Morb. Mortal. Wkly. Rep.* **52,** 516–521 (2003).
301. Matrosovich, M. *et al.* Early alterations of the receptor-binding properties of H1, H2, and H3 avian influenza virus hemagglutinins after their introduction into mammals. *J. Virol.* **74,** 8502–8512 (2000).
302. Matrosovich, M., Matrosovich, T., Uhlendorff, J., Garten, W. & Klenk, H.-D. Avian-virus-like receptor specificity of the hemagglutinin impedes influenza virus replication in cultures of human airway epithelium. *Virology* **361,** 384–390 (2007).
303. Sims, A. C. *et al.* Severe acute respiratory syndrome coronavirus infection of human ciliated airway epithelia: role of ciliated cells in viral spread in the conducting airways of the lungs. *J. Virol.* **79,** 15511–15524 (2005).
304. Chan, R. W. Y. *et al.* Tropism of and innate immune responses to the novel human betacoronavirus lineage C virus in human ex vivo respiratory organ cultures. *J. Virol.* **87,** 6604–6614 (2013).
305. De Arruda, E., Mifflin, T. E., Gwaltney, J. M., Winther, B. & Hayden, F. G. Localization of rhinovirus replication in vitro with in situ hybridization. *J. Med. Virol.* **34,** 38–44 (1991).
306. Winther, B. *et al.* Surface expression of intercellular adhesion molecule 1 on epithelial cells in the human adenoid. *J. Infect. Dis.* **176,** 523–525 (1997).
307. Jakiela, B., Brockman-Schneider, R., Amineva, S., Lee, W.-M. & Gern, J. E. Basal cells of differentiated bronchial epithelium are more susceptible to rhinovirus infection. *Am. J. Respir. Cell Mol. Biol.* **38,** 517–523 (2008).
308. Lachowicz-Scroggins, M. E., Boushey, H. A., Finkbeiner, W. E. & Widdicombe, J. H. Interleukin-13-induced mucous metaplasia increases susceptibility of human airway epithelium to rhinovirus infection. *Am. J. Respir. Cell Mol. Biol.* **43,** 652–661 (2010).
309. Jakiela, B. *et al.* Th2-type cytokine-induced mucus metaplasia decreases susceptibility of human bronchial epithelium to rhinovirus infection. *Am. J. Respir. Cell Mol. Biol.* **51,** 229–241 (2014).
310. Zhu, J., Rogers, A. V., Burke-Gaffney, A., Hellewell, P. G. & Jeffery, P. K. Cytokine-induced airway epithelial ICAM-1 upregulation: quantification by high-resolution scanning and transmission electron microscopy. *Eur. Respir. J.* **13,** 1318–1328 (1999).
311. Bochkov, Y. A. & Gern, J. E. Clinical and molecular features of human rhinovirus C. *Microbes Infect. Inst. Pasteur* **14,** 485–494 (2012).
312. Wadsworth, S. J., Riedel, M., Afshari, A. E., Louis, S. & Dorscheid, D. PneumaCultTM-ALI: an improved media for mucociliary differentiation of primary human bronchial epithelial cells. *Am J Respir Crit Care Med* **185,** A6345 (2012).
313. Tesfaigzi, Y. Regulation of mucous cell metaplasia in bronchial asthma. *Curr. Mol. Med.* **8,** 408–415 (2008).
314. Villenave, R., Shields, M. D. & Power, U. F. Respiratory syncytial virus interaction with human airway epithelium. *Trends Microbiol.* **21,** 238–244 (2013).
315. Zhang, L., Peeples, M. E., Boucher, R. C., Collins, P. L. & Pickles, R. J. Respiratory syncytial virus infection of human airway epithelial cells is polarized, specific to ciliated cells, and without obvious cytopathology. *J. Virol.* **76,** 5654–5666 (2002).

316. Zhang, L., Collins, P. L., Lamb, R. A. & Pickles, R. J. Comparison of differing cytopathic effects in human airway epithelium of parainfluenza virus 5 (W3A), parainfluenza virus type 3, and respiratory syncytial virus. *Virology* **421,** 67–77 (2011).
317. Smith, C. M. *et al.* Ciliary dyskinesia is an early feature of respiratory syncytial virus infection. *Eur. Respir. J.* **43,** 485–496 (2014).
318. Mata, M. *et al.* Respiratory syncytial virus inhibits ciliagenesis in differentiated normal human bronchial epithelial cells: effectiveness of N-acetylcysteine. *PloS One* **7,** e48037 (2012).
319. Villenave, R. *et al.* In vitro modeling of respiratory syncytial virus infection of pediatric bronchial epithelium, the primary target of infection in vivo. *Proc. Natl. Acad. Sci. U. S. A.* **109,** 5040–5045 (2012).
320. Kuss, S. K. *et al.* Intestinal microbiota promote enteric virus replication and systemic pathogenesis. *Science* **334,** 249–252 (2011).
321. Robinson, C. M., Jesudhasan, P. R. & Pfeiffer, J. K. Bacterial lipopolysaccharide binding enhances virion stability and promotes environmental fitness of an enteric virus. *Cell Host Microbe* **15,** 36–46 (2014).
322. Bermbach, S. *et al.* Mechanisms of Cilia-Driven Transport in the Airways in the Absence of Mucus. *Am. J. Respir. Cell Mol. Biol.* **51,** 56–67 (2014).
323. Sajjan, U., Wang, Q., Zhao, Y., Gruenert, D. C. & Hershenson, M. B. Rhinovirus Disrupts the Barrier Function of Polarized Airway Epithelial Cells. *Am. J. Respir. Crit. Care Med.* **178,** 1271–1281 (2008).
324. Dezső, Z. *et al.* A comprehensive functional analysis of tissue specificity of human gene expression. *BMC Biol.* **6,** 49 (2008).
325. Proenca-Modena, J. L. *et al.* High rates of detection of respiratory viruses in tonsillar tissues from children with chronic adenotonsillar disease. *PloS One* **7,** e42136 (2012).
326. Ross, P. W., Chisty, S. M. & Knox, J. D. Sore throat in children: its causation and incidence. *Br. Med. J.* **2,** 624–626 (1971).
327. Suvilehto, J. *et al.* Rhinovirus/enterovirus RNA in tonsillar tissue of children with tonsillar disease. *J. Clin. Virol.* **35,** 292–297 (2006).
328. Geist, F. C. & Hayden, F. G. Comparative susceptibilities of strain MRC-5 human embryonic lung fibroblast cells and the Cooney strain of human fetal tonsil cells for isolation of rhinoviruses from clinical specimens. *J. Clin. Microbiol.* **22,** 455–456 (1985).
329. Ruco, L. P. *et al.* The lymphoepithelial organization of the tonsil: an immunohistochemical study in chronic recurrent tonsillitis. *J. Pathol.* **176,** 391–398 (1995).
330. Jartti, T. *et al.* Distinct regulation of tonsillar immune response in virus infection. *Allergy* **69,** 658–667 (2014).
331. Arruda, E. *et al.* Localization of human rhinovirus replication in the upper respiratory tract by in situ hybridization. *J. Infect. Dis.* **171,** 1329–1333 (1995).
332. Turner, R. B., Hendley, J. O. & Gwaltney, J. M. Shedding of infected ciliated epithelial cells in rhinovirus colds. *J. Infect. Dis.* **145,** 849–853 (1982).
333. Floyd, R. & Sharp, D. G. Viral aggregation: buffer effects in the aggregation of poliovirus and reovirus at low and high pH. *Appl. Environ. Microbiol.* **38,** 395–401 (1979).
334. Thomassen, Y. E., van Eikenhorst, G., van der Pol, L. A. & Bakker, W. A. M. Isoelectric point determination of live polioviruses by capillary isoelectric focusing with whole column imaging detection. *Anal. Chem.* **85,** 6089–6094 (2013).
335. Schnabel, U., Groiss, F., Blaas, D. & Kenndler, E. Determination of the pI of human rhinovirus serotype 2 by capillary isoelectric focusing. *Anal. Chem.* **68,** 4300–4303 (1996).
336. Cuesta-Geijo, M. A. *et al.* Endosomal maturation, Rab7 GTPase and phosphoinositides in African swine fever virus entry. *PloS One* **7,** e48853 (2012).

337. Zaitseva, E., Yang, S.-T., Melikov, K., Pourmal, S. & Chernomordik, L. V. Dengue virus ensures its fusion in late endosomes using compartment-specific lipids. *PLoS Pathog.* **6,** e1001131 (2010).
338. Diederich, S., Moll, M., Klenk, H.-D. & Maisner, A. The nipah virus fusion protein is cleaved within the endosomal compartment. *J. Biol. Chem.* **280,** 29899–29903 (2005).
339. Fredericksen, B. L., Wei, B. L., Yao, J., Luo, T. & Garcia, J. V. Inhibition of Endosomal/Lysosomal Degradation Increases the Infectivity of Human Immunodeficiency Virus. *J. Virol.* **76,** 11440–11446 (2002).
340. Scott, C. C., Vacca, F. & Gruenberg, J. Endosome maturation, transport and functions. *Semin. Cell Dev. Biol.* **31,** 2–10 (2014).
341. Gangl, K. *et al.* Infection with Rhinovirus Facilitates Allergen Penetration Across a Respiratory Epithelial Cell Layer. *Int. Arch. Allergy Immunol.* **166,** 291–296 (2015).
342. Sun, X. & Whittaker, G. R. Role of the actin cytoskeleton during influenza virus internalization into polarized epithelial cells. *Cell. Microbiol.* **9,** 1672–1682 (2007).
343. Blacque, O. E., Cevik, S. & Kaplan, O. I. Intraflagellar transport: from molecular characterisation to mechanism. *Front. Biosci. J. Virtual Libr.* **13,** 2633–2652 (2008).
344. Fliegauf, M. *et al.* Nephrocystin specifically localizes to the transition zone of renal and respiratory cilia and photoreceptor connecting cilia. *J. Am. Soc. Nephrol. JASN* **17,** 2424–2433 (2006).